SEPTEMBER 1961

experimental mechanics

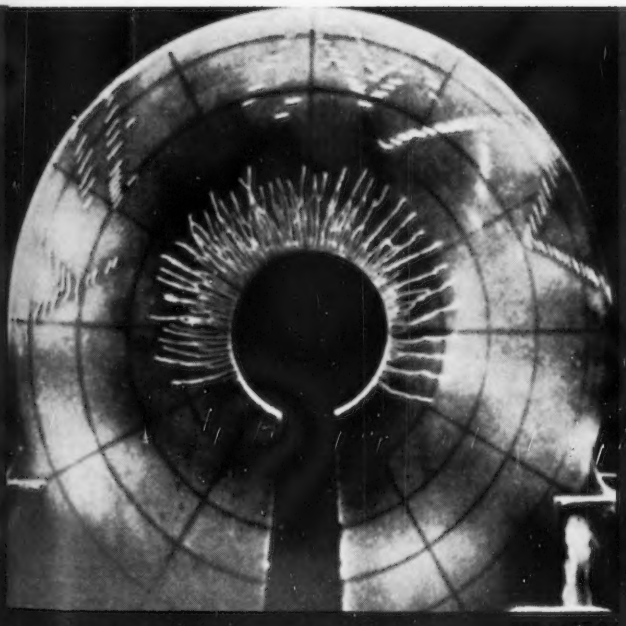

IN THIS ISSUE

PAGE

13A Shock Motions and Their Measurement

81 Stress and Deformation Analysis from Reduced-scale Plastic-model Testing

91 Lueders' Lines Detection by Means of Brittle Coatings

102 Beam Subjected to Eccentric Longitudinal Impact

105 Measurement of Surface Strain by Means of Bonded Birefringent Strips

113 Strain Field Associated with Brittle-fracture Propagation in Wide Steel Plates

SESA JOURNAL OF THE SOCIETY FOR EXPERIMENTAL STRESS ANALYSIS

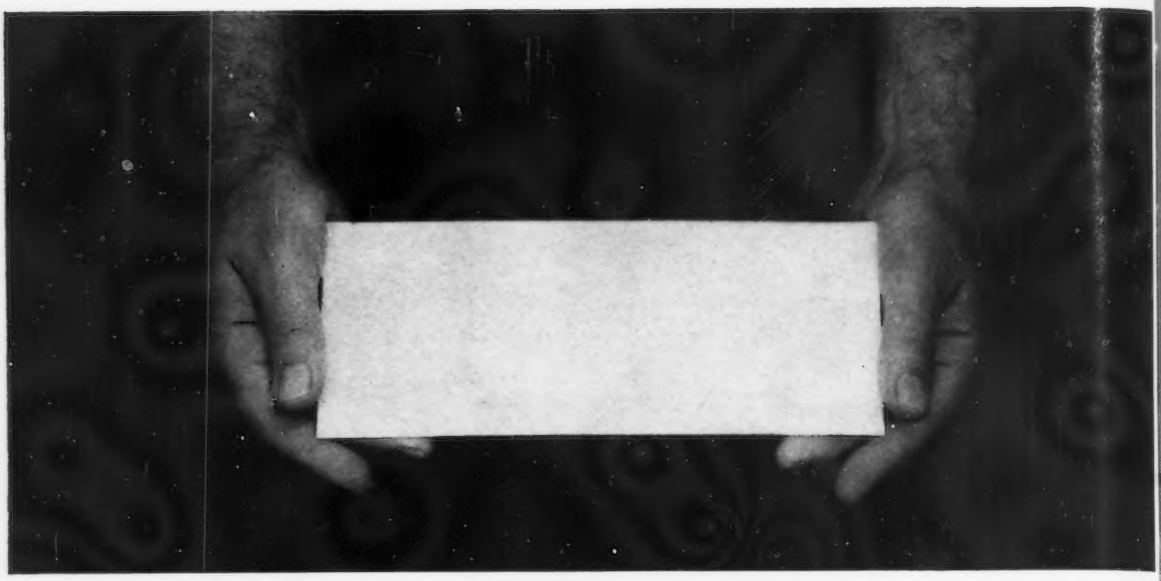

NEW! HIGH ELONGATION PhotoStress® PLASTIC

• 150% maximum elongation • Modulus of elasticity—350 psi • Maximum useable temperature—approx. 450°F. • Insignificant creep under load • K factor—0.0015 • Excellent linearity between strain and birefringence; good quantitative results • For use on any material having low modulus of elasticity and/or undergoing high elongation under load . . . such as solid rocket fuels, tires and other rubber products, plastics • Now available in 10″ x 10″ sheets, in thicknesses of 0.072″ and 0.120″; transparent or aluminum paint backed • *Write or call for full information or application assistance.*

THE BUDD COMPANY • **P.O. Box 245** • **Phoenixville, Pa.**
Consult your phone book for sales offices in:
Atlanta, Ga.; Chicago, Ill.; Detroit, Mich.; Seattle, Wash.; Dallas, Texas; Los Angeles, Calif.
In Canada: Budd Instruments, Ltd., 170 Donway West, Don Mills, Ont.
Other countries: Budd S.A., 10 Avenue de la Grande Armée, Paris 17e, France

INSTRUMENTS Budd DIVISION

For details, circle No. 1 on Reader Information Card

NAL OF THE SOCIETY FOR EXPERIMENTAL STRESS ANALYSIS

experimental mechanics

VOLUME 1 • NUMBER 9 • SEPTEMBER 1951

editor	**B. E. Rossi**
asst. editor	**C. H. Willer**
advertising	**D. L. Vidmark**
art	**Gil Miller**

OFFICERS AND EXECUTIVE COMMITTEE	JOURNAL ADVISORY COMMITTEE
D. C. Drucker *president*	**E. Wenk, Jr.** *chairman*
I. Vigness *vice-president*	**D. C. Drucker**
W. W. Soroka *vice-president*	**R. Guernsey, Jr.**
W. M. Murray *treasurer*	**B. J. Lazan**
B. E. Rossi *executive secretary*	**W. M. Murray**
F. C. Bailey	**C. C. Perry**
B. J. Lazan	**F. B. Stern, Jr.**
J. C. New	**I. Vigness**
C. E. Taylor	
E. Wenk, Jr.	

ublished monthly by the Society for Experimental Stress Analysis. ublication office, 20th and Northampton Streets, Easton, Pa. Editorial general offices, 21 Bridge Square, Westport, Conn. Subscription .00 per year in the United States and Canada; foreign countries .00. Single copies, nonmembers $1.50; members $1.00. Second-class ostage paid at Easton, Pa. Copyright 1961 by the Society for Experimental Stress Analysis. The Society is not responsible for any statement made or opinion expressed in its publications. Permission is given to reprint any article after its date of publication provided credit is given and provided the copies are not intended for sale.

this month

TABLE OF CONTENTS

page

13A Shock Motions and Their Measurement
by Irwin Vigness

81 Stress and Deformation Analysis from Reduced-scale Plastic-model Testing
by A. E. Johnson and R. H. Homewood

91 Lueders' Lines Detection by Means of Brittle Coatings
by A. J. Durelli, A. Kobayashi and K. Hofer

102 Beam Subjected to Eccentric Longitudinal Impact
by S. S. Kuo

109 Measurement of Surface Strain by Means of Bonded Birefringent Strips
by J. Duffy and T. C. Lee

113 Strain Field Associated with Brittle-fracture Propagation in Wide Steel Plates
by S. T. Rolfe and W. J. Wall

119 On Saint Venant's Principle Under Dynamic Conditions
Discussion
by S. F. Borg

3A Experimentally Speaking

4A Tracking Station

6A Personnel in the News

7A New Products

11A New Literature

12A Book Review

13A E/M Field Report

17A Reader Information Card

18A Index to Advertisers

19A SESA News

21A Program for Congress

25A Section Reports

26A From the Campus

1961 SESA EXPOSITION

in conjunction with

FIRST INTERNATIONAL CONGRESS ON EXPERIMENTAL MECHANICS

Hotel New Yorker • November 1–3

All on one floor . . . at New York's famous and popular hotel . . . lively exhibits of what's what in experimental mechanics . . . by the who's who in the industry.

Manufacturers of all types of engineering and scientific equipment used in this field are invited to exhibit.

Hundreds of engineers and scientists involved in instrumentation, measuring such mechanical quantities as stress, strain, load, displacement, acceleration, pressure, and vibration, will attend. These men are most directly concerned with specifying, buying and using equipment.

Some choice booths still available—
First come, first served.

For prompt action, phone collect: Capitol 7-0829 (Westport).

FOR FURTHER INFORMATION WRITE:

SESA HEADQUARTERS
21 BRIDGE SQUARE
WESTPORT, CONNECTICUT

or circle No. 20 on Readers Information Card

Experimentally Speaking

MATERIALS SCIENCE AND THE SESA

In recent years, the complete understanding of the behavior of materials under a variety of environmental conditions has become one of the most important aspects of technology and science. References are frequently made to the "material barrier" and the limitations of materials in meeting the demands of certain operational conditions. Conditions of high temperatures—in missiles, space vehicles, nuclear energy equipment, high-speed aircraft and many other applications—is an example of one area where research is greatly needed.

There are a number of developments indicating that engineers and scientists are aware that greater efforts need to be made in this important field of materials science. Last year the Federal government, through such agencies as Advanced Research Projects Agency, recognized the need by establishing large long-range grants for materials research in selected universities. National societies have recognized the importance of the field in various ways. For example, the American Society for Testing Materials recently established a Materials Science Division. Educational institutions throughout the country are establishing undergraduate and graduate degree programs covering all aspects of this science.

The future place of the Society for Experimental Stress Analysis in the important area of materials science can be a significant one. For it seems to me that various societies interested in materials have not fully developed the aspect that deals with the evaluation and interpretation of mechanical or stress-strain properties of materials and the utilization of these properties in design. Such investigations logically fall within the interests of the SESA, and, in the past, the Society has published some papers in this area. The broadening of the scope of our Society, as reflected by the establishment of the new journal on experimental mechanics, provides a framework for a valuable engineering contribution. Of course, your submission of papers on engineering aspects of materials science is necessary for success in this activity.

Joseph Marin
PAST PRESIDENT, SESA

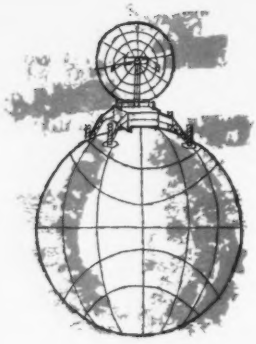

tracking station

the industry in focus

ASTM Elects National Officers

The new national officers of the American Society for Testing Materials were named during the 64th Annual Meeting in Atlantic City, N. J.

Miles N. Clair was elected president to serve a one-year term.

Alfred C. Webber was elected vice-president. R. Wade Seniff will continue as senior vice-president.

Ground Breaking for NBS Laboratories

Ground has been broken for the new National Bureau of Standards laboratories at Gaithersburg, Md. With the initial construction phase underway for a 20-building, $104-million research facility, present plans will permit complete relocation of the Bureau from Northwest Washington to the 555-acre site in Montgomery County in the period between 1963–65. First priority has been given to the Engineering Mechanics Laboratory.

Navy Develops Shock Recorders

Several peak shock-recording devices, described as having "discriminating minds of their own," have been developed to isolate and record specific shocks received by air-dropped weapons, whether they be from hitting the water, a whale or the ocean floor.

The devices are attached on prototype weapons to determine the magnitude of shocks received when the weapons are dropped during ruggedness tests. Covering a shock range from 30 to 20,000 times the pull of gravity, the devices are accurate in excess of 80% for simple shock pulses.

G. E. Builds Space Simulator

For approximating the conditions beyond the earth's atmosphere, this space simulator is shown under construction at General Electric Co.'s multimillion dollar Valley Forge Space Technology Center. The Center will be devoted entirely to space research and the design and production of space vehicles.

To test actual manned space vehicles in the chamber, a near vacuum of one billionth of a billionth of the earth's atmosphere, temperatures lower than minus 300° F and the effects of solar energy in space will be created.

Conical Shocktube Constructed by Navy

The Navy has constructed a 180-ft conical shocktube in which 5-lb explosive charges have produced blastwaves as powerful as those generated by simultaneously firing six World War II blockbusters.

Installed at the Naval Ordnance Laboratory in Silver Spring, Md., the device was conceived and developed by physicist W. S. Filler of NOL's Explosions Research Department. It is a scale-model designed to predict the performance and to aid in the design of a 2000-ft shocktube in which a blastwave from a 1000-lb charge can be effectively amplified to correspond to that from a nuclear explosion of many kilotons. Such a nuclear-blast simulator will give the Navy a facility capable of economically creating "inside the laboratory" repeated radiation-free blastwaves of nuclear size at relatively short intervals.

Microdot Adds New Plant

Microdot Inc. has started construction on a 38,000-sq- ft building in South Pasadena to house their Connector Division, and to provide new executive offices and other facilities.

The two-story structure, cited for good design, is to align with the existing Microdot plant and will combine a lower-floor long-span shop area and engineering offices with top-floor executive offices, cafeteria and roof-top parking.

Kemp Engineering to Represent B & F Instruments

B & F Instruments, Inc., of Philadelphia, Pa., has selected Kemp Engineering Co., Dallas, Tex., to represent them in the Texas-Oklahoma area.

Kemp will handle B & F's strain-gage and transducer-input conditioning equipment, plotting and logging systems, and torquemeter systems.

FUTURE MEETINGS

SESA

NOVEMBER 1–3. First International Congress on Experimental Mechanics. Hotel New Yorker, New York, N. Y.

MAY 16–18, 1962. Spring Meeting. Sheraton-Dallas Hotel, Dallas, Texas.

OCTOBER 24–26, 1962. Annual Meeting. Hotel Schroeder, Milwaukee, Wis.

● Related Conference:

OCTOBER 29–31. International Symposium on Photoelasticity. Illinois Institute of Technology, Chicago, Ill.

ASA

NOVEMBER 9–11. Meeting of the Acoustical Society of America. Cincinnati and Dayton, Ohio

IAS

OCTOBER 23–24. Institute of the Aerospace Sciences. Joint meeting with Canadian Aeronautical Institute. Quebec, Que., Can.

NRL

OCTOBER 10–12. The 30th Symposium on Shock, Vibration and Associated Environments. Detroit, Mich. Classified. Address: Code 4021 U. S. Naval Research Laboratory, Washington, 25, D. C.

SAE

SEPTEMBER 11–15. Society of Automotive Engineers. National Farm, Construction and Industrial Machinery Meeting. Milwaukee Auditorium, Milwaukee, Wis.

OCTOBER 9–13. National Aeronautic Meeting. Ambassador Hotel, Los Angeles, Calif.

personnel

in the news

WENK ACCEPTS BID TO FEDERAL SCIENCE COUNCIL

Edward Wenk, Jr., former scientific consultant to Congress, has been appointed technical assistant to Jerome B. Wiesner, special assistant to the President for science and technology. In his new capacity, Dr. Wenk will also serve as executive secretary of the Federal Council for Science and Technology of which Dr. Wiesner is chairman.

The Federal Council was established by executive order in 1959 and has broad functions affecting the over-all national scientific effort. Membership includes representatives of policy rank, from the Departments of Defense, Interior, Argiculture, Commerce, and Health, Education and Welfare; also the chiefs of the NSF, NASA, AEC, as well as observers from the State Department and Bureau of the Budget. Increased activity in the Council is in line with the Government's growing multibillion dollar research and development programs.

Highlights in Dr. Wenk's extensive background include his graduation with honors in civil engineering from The Johns Hopkins University where he later earned his Ph.D. in engineering. He received his M.S. in applied mechanics from Harvard University and also studied at the Harvard Graduate School of Design.

Dr. Wenk began his career at the Navy's David Taylor Model Basin, becoming a specialist in the field of structural mechanics and an international authority on design of submarines. He then successively served as a government research administrator, as an executive in an industrial research laboratory, as a private engineering consultant, and since 1959, as the first science consultant to members and committees of the U. S. Congress. During this most recent association as senior specialist in science and technology at the Legislative Reference Service of the Library of Congress, he prepared a number of major congressional studies relating science to public policy.

Past president of the Society for Experimental Stress Analysis and present chairman of the Journal Advisory Committee, Dr. Wenk is also active with the ASCE, ASME, ARS, NAS, AAAS, as well as other professional and honorary groups.

Edward Wenk, Jr.

EXECUTIVE POST FOR FELIX

Harold E. Felix has been appointed vice president and director of engineering at Midwestern Instruments, Inc. Mr. Felix joined the Tulsa organization after twenty-one years of design engineering experience with Douglas Aircraft Co.

As director of engineering at Midwestern, his responsibilities will cover the entire field of electronic instruments manufactured by the company.

CUNNIEN MADE DIRECTOR OF ENGINEERING

The appointment of James M. Cunnien as director of engineering for Minneapolis-Honeywell's Precision Meter Division, Manchester, N. H., has been announced. Mr. Cunnien has served as a project engineer with the division since 1959. He succeeds E. S. Maury, who has resigned.

Mr. Cunnien joined Honeywell in Minneapolis in 1950 as a design engineer and worked there until 1959 on a number of product development projects. He holds patents on a number of devices.

BETZ APPOINTED MANAGER

Minneapolis-Honeywell's Precision Meter division has announced the appointment of William J. Betz as sales manager for aviation products. He was formerly New York branch sales manager for their Micro Switch division.

Mr. Betz joined Micro Switch in 1953 as a field sales engineer in the New York office, and later held several sales assignments there until he was named branch manager in 1959. Prior to joining Honeywell he worked for Moore Business Forms, Inc., and American Hard Rubber Co.

RYDEN, NUNAN ELECTED TO BOARD

Arnold J. Ryden, president of Midwest Technical Development Corp., and James K. Nunan, president of Electra Scientific Corp., have been elected to the board of directors of Midwestern Instruments, Inc., Tulsa, Okla.

Mr. Ryden helped establish Control Data Corporation in Minneapolis and had previously held financial executive positions at Engineering Research Associates (now Remington Rand Univac) and Minneapolis-Honeywell Aeronautical Division.

Mr. Nunan, a prominent engineering executive, formerly headed the Electronics Engineering Department at the University of Southern California, and was a wartime associate director of the Navy's Underwater Sound Laboratory.

WITZKE APPOINTED VICE PRESIDENT

F. W. Witzke has been appointed vice president and chief administrative officer of the Cleveland Instrument Co., a subsidiary of The Bendix Corp., according to an announcement by Charles E. Heitman, vice president and group executive of Bendix. The position was held by John O. Nagle who has resigned to accept another position.

Mr. Witzke, previously manager of sales engineering, joined the company in 1956. He has been active in the design and marketing of new gage designs, and has several patents pending in this field.

Previous to World War II he worked for the P. A. Geier Co., Weatherhead Co., and Jack and Heintz, Inc.

KLEES HEADS NEW UNIT

Beckman Instruments, Inc., announced the consolidation of its corporate and division advertising functions within a Corporate Marketing Services group and the appointment of Robert E. Klees as manager of the new unit.

Mr. Klees was formerly manager of advertising and sales promotion for the company's Scientific and Process Instruments Division at Fullerton, Calif.

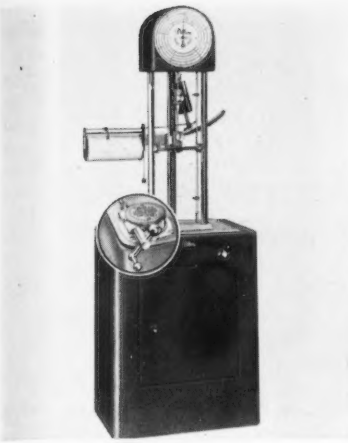

SPEED CONTROL FOR TESTER

A remote speed control is said to permit greatly increased precision in pre-setting their low-range tester to ASTM and Federal specifications according to W. C. Dillon & Co., Inc., 14620 Keswick St., Van Nuys, Calif. A 360-deg segmented dial selects infinite variable crosshead speeds from 0-20 ipm.

Remote speed controls are now supplied for all Dillon low-range testers in the following 5 ranges: 0–10, 0–25, 0-50, 0–100 and 0–300 lb. They are available also with a wide variety of gripping fixtures and accessories for testing materials for tensile, compression, transverse and shear. **53**

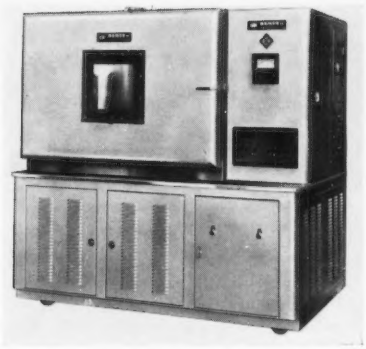

HIGH-LOW TEMPERATURE CHAMBERS

A series of high-low temperature chambers featuring cascade refrigeration systems is announced by Bemco Inc., 9908 San Fernando Rd., Pacoima, Calif. Chambers use non-explosive freon as coolant, and electric resistance type units for heating.

Stabilized glass-fiber insulation is used between steel outer and stainless-steel inner walls, welded to prevent condensation from forming on the insulation. Fan is corrosion-resistant, with the motor mounted externally the manufacturer relates.

Models in this "F" series are available in five test-space sizes—2, 3, 8, 27 and 64 cu ft. Temperature ranges are −100 to +350° F and −100 to +500° F. All units are mounted on casters for easy portability. **55**

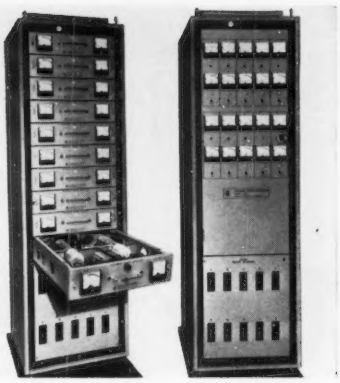

MULTICHANNEL POWER REGULATORS

Research, Inc., Box 6164, Minneapolis 24, Minn., announces two a-c power-regulator systems for use where space is limited and multichannel control is needed. Their chief function is the regulation of power applied to ovens, furnaces and similar devices in direct proportion to control signals from set point meters, temperature controllers, programmers, etc. As many as ten channels may be installed in a single rack.

Model Y4079 is a single channel, plug-in module using two C16J thyratrons for a rated capacity of 40 amp in each channel. Overloads up to 200% of rating reportedly can be tolerated for periods up to 5 min. Cooling fans and mating connector plugs are contained in the rack which is prewired for either single or 3-phase operation.

Higher capacities are available in the model G 4078 which uses ignitrons rated at 100 amp per channel. **59**

new products

For more details regarding these products, circle item number on Reader Information Card

PORTABLE CALIBRATION INDICATOR

A portable instrument for calibration service with either tension or compression loads has been introduced by Electronics & Instrumentation Division, Waltham 54, Mass., of Baldwin-Lima-Hamilton Corp. Designated the Type 65 automatic null-balance calibration indicator, the company states that the unit also can be used to indicate weight, force and thrust.

When used with a Baldwin-Lima-Hamilton calibration load cell, the calibration indicator readings are compared against those of the working system to provide for rapid calibration. Digital readout in pounds eliminates any chance of reading errors which could be caused by bad parallax and incorrect interpolation of readings on instruments equipped with meters and dials. **51**

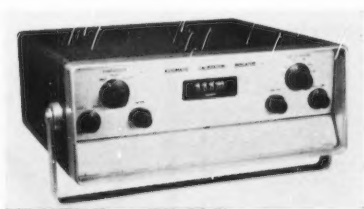

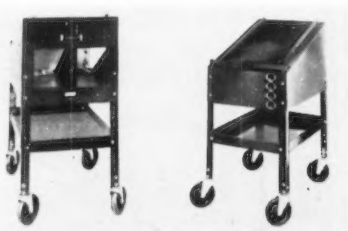

OSCILLOSCOPE DOLLY

Produced by Metal Dynamics Corp., 9430 State Rd., Philadelphia 14, Pa., model No. 61056 Scope Dolly features 3 convenient power outlets and one input. In addition, the manufacturer points out that a storage area is provided for spare preamplifiers plus a storage pan for accessories.

Design includes a 20 deg viewing angle to accommodate any popular type laboratory scope. Casters are 5 in. diam ball-bearing swivel type with semihard rubber wheels. A protective rubber gasket prevents damage to the scope while installing or removing. **60**

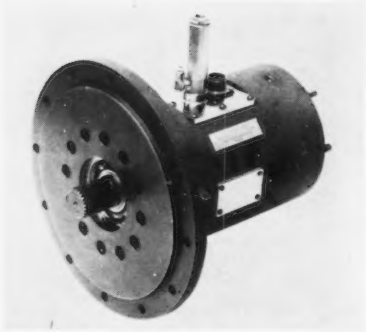

TORQUE TRANSDUCERS

A series of torquemeters, constructed with inherent strength to support a large load, is reported by B & F Instruments, Inc., 3644 N. Lawrence St., Philadelphia 40, Pa. The 10 in. bolt circle conforms to AND standard specifications. This type of construction is described as often being used to mate with hydraulic pumps, generators and starters. The torquemeter supports itself and its load in cantilever fashion. It is said to be especially useful on test stand applications for rapidly changing the device under test. With regard to special applications, B & F states that it has constructed the 10-in. bolt circle on both the load and drive end. **61**

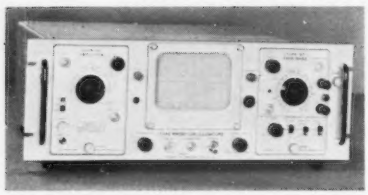

OSCILLOSCOPE

A rack-mount oscilloscope that accepts a wide range of plug-in units in both channels, the Type RM561, is offered by Tektronix, Inc., P.O. box 500, Beaverton, Ore.

Characteristics are said to include: a 5-in. rectangular crt, 3.5 kv accelerating potential, 8 x 10 centimeter viewing area, z-axis input, amplitude calibrator, regulated d-c heater voltage, and regulated d-c supply—that operates between 105 to 125 v or 210 to 250 v, 50 to 800 cycles to provide 90 w of power for the plug-in units. **65**

HYDRAULIC LOAD SIMULATOR

A 10-channel hydraulic load simulator, said to be capable of accurately delivering up to 500,000 lb per channel, has been announced by Gilmore Industries, Inc., 13015 Woodland Ave., Cleveland 20, Ohio.

The simulator control console contains all the measuring and control components for ten independent channels of hydraulic force control. Each channel uses a load-cell transducer coupled to a hydraulic cylinder. A force on any cell will cause an unbalance of the strain-gage bridge within the cell resulting in a voltage signal proportional to the force. The control console receives this signal and compares it to a "command" signal, that is controlled by the operator. Any difference in signal is detected by the servo amplifier and a correction signal is sent to the four-way servo valve which will vary the hydraulic pressure at the cylinder. **67**

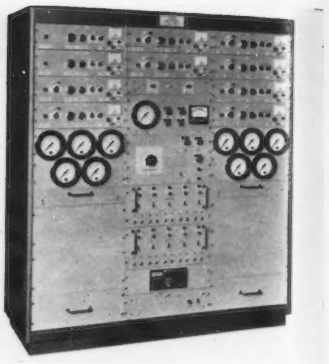

PHOTOELASTIC STRESS ANALYSIS WITH POLAROID* FILTERS

Standard Equipment or Special
Complete Apparatus or Components

Point Light Sources
White Light and Monochromatic (546 or 589 line)

Matched Quarter Wave Plates to 17″ diameter

Polaroid Polarizers to 17″ diameter
Cemented Glass Laminations #6/006

Straining Frames

Recording Cameras

* T. M. Reg. U. S. Pat. Off. by Polaroid Corporation

THE POLARIZING INSTRUMENT COMPANY, Inc.
IRVINGTON-ON-HUDSON, NEW YORK

For details, circle No. 5 on Reader Information Card

STRESS ENGINEERS for KAMAN AIRCRAFT

The nation's largest independent producer of Rotary Wing Aircraft located in Bloomfield, Conn. (6 miles from Hartford, Conn.)

Will perform Stress Analysis of mechanical assemblies, assume responsibility for structural integrity of portions of aircraft including complete major sub-assemblies. Specify and witness tests designed to determine structural adequacy of components.

Requires 2–10 years experience plus a degree in Mechanical, Aeronautical or Chemical engrg.

Send complete resume & salary required

V. C. REPKEWICH
Technical Personnel
Industrial Relations Department
KAMAN AIRCRAFT CORP.
BLOOMFIELD, CONN.

An Equal Opportunity Employer

PRESSURE CELL

A general-purpose pressure cell, designed for precisely measuring fluid pressures in a wide range of applications, has been introduced by Electronics & Instrumentation Division, Waltham 54, Mass., of Baldwin-Lima-Hamilton Corp.

Said to provide a combination of inherent high-accuracy, rugged construction, long-term stability, infinite resolution, and high output signal the pressure transducer reportedly was developed for use in such fields as aircraft and missiles, process-control systems, automotive, chemical, petrochemical, hydraulic and pneumatic systems, food processing and for general precise laboratory work. **75**

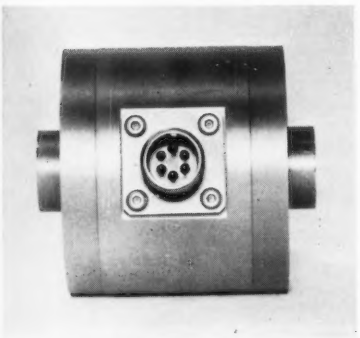

DIFFERENTIAL PRESSURE TRANSDUCER

The first of a line of strain-gage pressure transducers for high-line, low-differential service has been introduced by the Transducer Division of Consolidated Electrodynamics Corp., 360 Sierra Madre Villa, Pasadena, Calif.

The new Type 4 351 is said to combine high performance characteristics with small size, measuring only $2^{3}/_{4}$ in. diam and $2^{3}/_{8}$ in. long. The unit also is said to feature a line pressure rating of 5000 lb with less than 1% full range shift from zero to 5000 psi and will withstand 8000 psi without damage. The differential pressure range is from ±15 to ±100 psid. **77**

NEW BLH-BUILT INSTRUMENTATION INSURES MORE ACCURATE, VERSATILE STRAIN GAGE TRANSDUCER READOUT

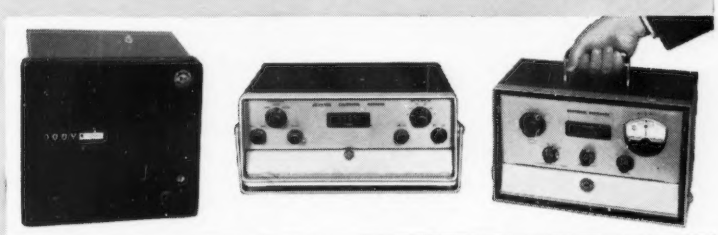

The complete line of mv/v instrumentation designed and built entirely by BLH now includes these new indicators for use with any strain gage transducer system.

Type 30 Digital Indicator, shown at left above, is particularly suited to load, pressure and torque systems. It provides system accuracy to ±0.25%—higher accuracies on special order. Designed for panel mounting or bench operation, it is available for fast delivery at a very reasonable cost. With the addition of this instrument, BLH now offers you a full choice of digital, disc or pointer indicators for industrial and laboratory applications.

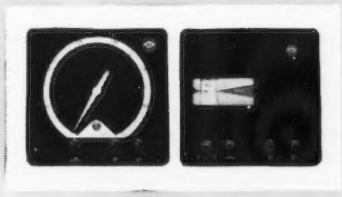

Type 65 Automatic Calibration Indicator, middle above, is among the most accurate of all BLH instruments. This portable unit automatically reads out in pounds—is used to calibrate a variety of load measurement systems and features automatic null balance, digital readout, plus a built-in check calibrate circuit. Instrument accuracy ±0.05% of interval is standard.

Type 25 Universal Indicator can be used with any BLH load, pressure or torque transducer by simply setting a gage resistance and mv/v output dial on the front of the instrument. Manually null balanced—digital indication—transistorized, lightweight and portable. Instrument accuracy is ±0.1% of full scale. Durable Formica case.

Write for data sheets or contact your nearest BLH sales engineering representative for information and a demonstration.

BALDWIN • LIMA • HAMILTON
Electronics & Instrumentation Division
Waltham 54, Mass.

FIRST in force measurement

SR-4® Strain Gages • Transducers • Temperature Sensors • Systems

For details, circle No. 2 on Reader Information Card

new

SOLID STATE TRANSDUCERS

PRESSURE

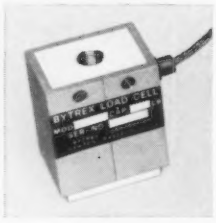

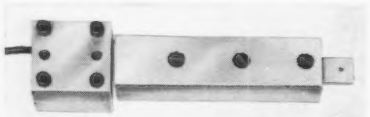

LOAD

ACCELERATION

Piezoresistive semiconductor strain gages and transducers with exceptional combinations of performance characteristics . . .

- *High Output (volts)*
- *High Accuracy (0.1%)*
- *High Frequency (KC)*
- *Low Deflection*
- *Reliability*
- *Small Size*
- *AC or DC Power*
- *Static or Dynamic*

Write for further details and for information on gaging services and engineered systems.

KULITE-BYTREX CORPORATION

50 HUNT ST. • NEWTON 58, MASS.

Semiconductor Strain Gages
Semiconductor Strain Gage Devices

For details, circle No. 3 on Reader Information Card

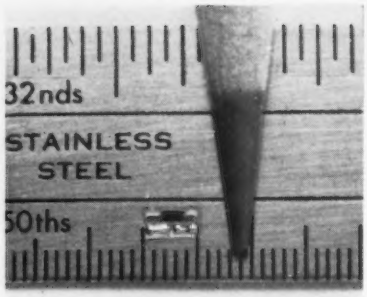

SEMICONDUCTOR STRAIN GAGES

A microminiature silicon strain gage measuring only 0.05 in. active length, and said to be especially suited for biomedical instrumentation, transducer applications, and experimental stress analysis, is manufactured and marketed by Micro Systems, Inc., 319 Agostino Rd., San Gabriel, Calif., a subsidiary of Electro-Optical Systems, Inc.

With a gage factor of 110 and resistance of 120 ohms, the MS301-120 is the smallest of 29 new types of semiconductor strain gages now being marketed by Micro Systems. Gage lengths run from the miniature 0.05 in. size to 0.5 in. length, with resistance ranging from 120 to 1000 ohms, and gage factors from +120 to −100.

Temperature range of the expanded line is from −320 to +650° F Gages are available with or without adhesive backings. **89**

PUNCHED FOIL GAGES

A precision process, developed for accurately punching out strain gages from thin metal foil, has led to the marketing of punched foil gages by Dentronics Inc., 16 Bland Ave., Emerson, N. J.

The metal thickness covers a range from about 0.0005 to 0.0001 in. The clean cut edges are said to permit very accurate control of resistance so that closely matched batches can readily be produced.

The manufacturer points out that there is no border on the two outside strands; the outside edges are cut accurately with a die so that a border is not necessary for insulation. There is about 0.0015 in. between the edge and the lower surface of the insulating base.

There is said to be no limit to the range of metals that can be processed. Series 200 strain gages are made of "Advance" metal (45% Ni; 55% Cu approx.) with epoxy and fiber backing. The backing consists of several very thin layers of epoxy and pure cellulose fibers of a special high-dielectric grade with a very high bond strength between individual grid filaments of the gage and the backing, the manufacturer relates. **91**

VIBRATION-MEASURING SYSTEM

Chadwick-Helmuth Co., 472 E. Duarte Rd., Monrovia, Calif., announces a new vibration-measuring system for use in sinusoidal laboratory vibration testing. This system permits continuous automatic recording of complete data from accelerometer signals, including phase, distortion and amplitude, the manufacturer states. This sampling technique is particularly useful with "hi-fi" accelerometers, where phase and distortion information cannot be recorded by conventional techniques.

Designated "VMS," unit creates exact slow-motion replica of accelerometer signals while accelerometer signal sweeps from 10 cps to 10 kc. Any slow motion from $^1/_3$ to 3 cps can be chosen. **92**

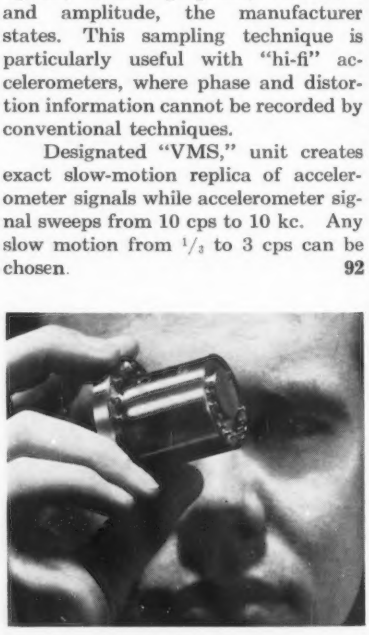

MINIATURE SLIP RING

The availability of a sealed 10-circuit miniature slip-ring for general purpose work has been announced by Michigan Scientific Co., 730 Bellevue, Milford, Mich. It features a manually operated brush lifter to extend brush life. Applications include strain gage, thermocouple and vibration measurements on automotive and aircraft engines, wheels and similar rotating parts. The unit, Model SR10M, is only 2-OD by $1^5/_8$ in. long.

It is sealed for operation in presence of oil, water, dust and other contaminants. Manual rotation of the brush lifter about 90 deg raises the brushes from the slip rings when measurements are not being made. **93**

To obtain free literature, circle item number on Reader Information

Polariscopes for PhotoStress Technique

The Budd Co., P.O. Box 245, Phoenixville, Pa., has recently released Catalog PS 2062 "PhotoStress—Large Field Meter Type LF/2," and Catalog PS 2063 "PhotoStress—Small Field Meter Type SF/Z."

The "large field meter" is described as being a special reflection-type polariscope. The "SF/Z meter" is said to be a small-field reflection-type polariscope in the form of a special-type microscope with incorporated light source. Both polariscopes are used principally to perform photoelastic stress analysis on actual parts by the PhotoStress technique. They also have additional applications. The LF/Z meter can be used for conventional stress analysis in photoelastic models. The SF/Z meter can be employed for conventional two- or three-dimensional model photoelasticity. The main feature claimed for the latter polariscope is excellent accuracy in areas of high strain gradients. **109**

Miniaturized Pressure Potentiometers

A complete line of new miniaturized pressure potentiometers is described in Technical Bulletin 1045 recently released by Trans-Sonics, Inc., P.O. Box 328, Lexington 73, Mass.

Available in ranges from 0–10 to 0–5000 psia in one basic miniaturized configuration, the units will withstand 35 g to 2000 cps without fluid damping. Having a temperature sensitivity of less than 0.008%/°F and a 1 in. diam, the units are particularly suited for providing high-level signal outputs for missile telemetry or control systems, according to manufacturer.

Also available in gage or differential models, and with corrosion-resistant sensing elements. **111**

Angular-position Transducer

The "Angulator"—a device which measures limited angular displacements—is described in a new data sheet, No. 4353, published by Baldwin-Lima-Hamilton Corp., Electronics & Instrumentation Division, 42 Fourth Ave., Waltham 54, Mass.

The data sheet furnishes application information, features dimensions, a complete summary of specifications and illustrates the Model 236 angular-position transducer.

Weighing 2 oz., and with no wearing parts, the angular-position transducer permits continuous measurement and remote indication of the angular position of such rotary mechanical elements as those for aircraft control surfaces, machine tools, industrial process controls and radar scanner of limited travel, the manufacturer reports.

The transducers operate on ac or dc, and are protected, by overload stops, against damage from excessive angular rotation. Standard capacities available offer useful measuring ranges of ±20, 30 and 60 deg. **117**

Semiconductor Strain Gages

A new catalog on 29 new Micro-Sensor semiconductor strain gages is now available from Micro Systems, Inc., 319 Agostino Rd., San Gabriel, Calif.

The four-page catalog lists the entire gage line, indicating resistance, lengths, gage factors, curvature radii, temperature range, dimensions and price.

The brochure also describes special gaging facilities available at Micro Systems, Inc. **119**

Weldable Strain Gages

Microdot Inc., 220 Pasadena Ave., South Pasadena, Calif. now has available a bulletin (SG-1) which describes in full their weldable strain gage, said to be capable of continuous operation at 750° F and dynamic test to 1500° F. Designed for applications in missile, space and atomic projects, this gage has been applied to atomic reactors, submarine hulls, the inside walls of chemical vats and underwater pilings, according to manufacturer. **121**

Current Probe Systems

A spec sheet describing the P6016 high-frequency current probe systems is available from Tektronix. Inc., P.O. Box 500, Beaverton, Ore. This two-page specification sheet details characteristics of two systems for observation and measurement of current waveforms.

The P6016 a-c current probe and type 131 amplifier constitute a current-detecting system for use with a wide-band oscilloscope. This system provides accurate displays for observation and measurement of current waveforms of low amplitude and fast risetime, the manufacturer states. Current range is 1 ma to 10 amp. Passband, with a 30-mc oscilloscope, is 50 cps to 17 mc.

The P6016 a-c current probe with a passive termination provides for observation and measurement of current waveforms at frequencies to 20 mc (with 30-mc oscilloscope) and sensitivity of either 2 or 10 ma/mv (of oscilloscope sensitivity). **127**

Electrical-contacts Guide

A "Basic Guide to Electrical Contacts" has just been published by Tricon Manufacturing Co., 8010 S. Wallace, Chicago, Ill. The two-color, eight-page bulletin includes charts covering applications and technical data for the various contact alloys and specifications of the most commonly employed stock contacts. Other sections of the guide discuss points to be considered in the design, specification and purchase of rivet contacts, laminated contacts, spring and blade components and complete assemblies. **133**

D-C Amplifier

A small (4.75 cu in.), solid-state, direct-coupled differential input d-c amplifier, said to be designed for extremely rugged operational environments, is described in Bulletin DCA-1 now available from Microdot Inc., 220 Pasadena Ave., South Pasadena, Calif. The manufacturer states that extended frequency response, freedom from hash and rapid recovery from overloads are made possible by the absence of any form of chopper.

Header arrangements, can configurations and full specifications are included in this bulletin. **135**

Metal Quality Control

A new 4-page folder titled "Automatic X-ray Spectrograph Speeds Analyzing of Metals," reprint of an article describing Westinghouse foundry operations, is available gratis from Philips Electronic Instruments, 750 S. Fulton Ave., Mount Vernon, N. Y.

The folder covers X-ray quality control of raw materials and finished products involving copper, manganese-bronzes, tin-bronzes, aluminum-bronzes, tin-base and lead-base materials. **129**

Pressure Cell

A differential pressure cell, said to provide exceptionally high linearity, is described in a data sheet published

BARRY
CONTROLS
VARIPULSE®
SHOCK TESTING MACHINES
• ECONOMICAL • PRECISE
• REPEATABLE • SIMPLE • SAFE

TYPE 16750 ▸
Maximum Capacity: 35 lbs.
8½"x 10" x 10" high

TYPE 15000 ▾
Maximum Capacity: 600 lbs.
30" x 30" x 67" high

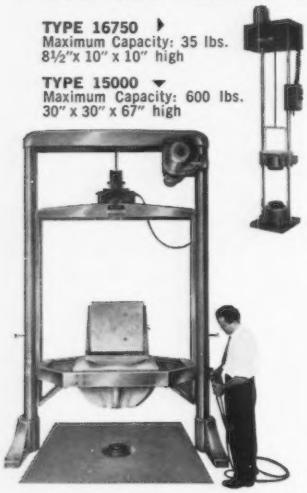

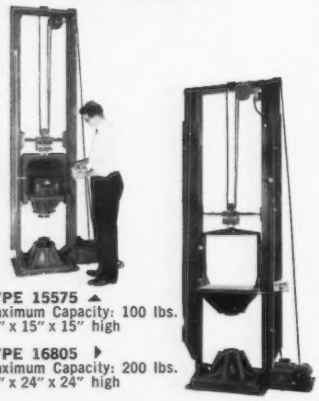

TYPE 15575 ▴
Maximum Capacity: 100 lbs.
15" x 15" x 15" high

TYPE 16805 ▸
Maximum Capacity: 200 lbs.
24" x 24" x 24" high

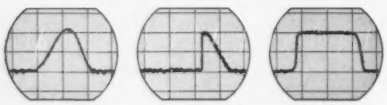

Typical half-sine saw-tooth, and square wave pulses produced by Barry Varipulse® machines.

Barry Varipulse® machines are designed to accommodate a broad range of test requirements in accordance with numerous specifications. For more information on your specific problem write:

BARRY CONTROLS
Division of Barry Wright Corp. BW
700 PLEASANT ST., WATERTOWN 72, MASS.
1400 NO. FLOWER ST., GLENDALE, CALIFORNIA

LEADERS IN SHOCK SIMULATION
For details, circle No. 6 on Reader Information Card

by Electronics & Instrumentation Division, Baldwin - Lima - Hamilton Corp., 42 Fourth Ave., Waltham 54, Mass.

The data sheet covers the Type MM SR-4 pressure cell, and furnishes general application information, specifications, features and dimensions with an illustration of the pressure cell.

A high-accuracy cell, the Type MM is available in capacities of plus or minus 15, 30 and 60 lb per sq in. and is suitable for a wide range of military, industrial and laboratory applications to measure static and low-frequency differential, absolute or gage pressures, the manufacturer explains.

143

Reviews...

BRIEF BUT CRITICAL EVALUATIONS OF CURRENT BOOKS BY AUTHORITIES IN THEIR FIELDS

FRAME ANALYSIS

A. S. Hall and R. W. Woodhead. John Wiley & Sons, New York, 1961. Cloth, 6 x 9¼ in., 115 Figs., 27 tables, 247 pages, $8.50

REVIEWED BY R. O. BELSHEIM, HEAD, STRUCTURES BRANCH, MECHANICS DIVISION, U. S. NAVAL RESEARCH LABORATORY, WASHINGTON, D. C.

The modern engineer in any field today must learn to use the computational tools now available. One of these tools is the computer, which makes feasible the solution of problems using procedures long known, but requiring much arithmetic. This book on frame analysis gives the competent structures man, or the student who has had the usual undergraduate courses in structures, the insight needed so he can use modern computational procedures. It is written concisely and clearly. It has adequate examples. It does presume the reader is familiar with usual structures theory, although useful references are included. It does not tell the reader how to utilize a computer, but its usefulness is emphasized, and the methods are formulated in a general way so that computer usage is obviously desirable. It uses matrices liberally, and has an appendix which contains the essentials of matrix algebra.

Since the authors assume reader familiarity with basic structural theory, their main objective is to use this theory to solve general structural problems. Two basic approaches are used, the flexibility method, e.g., using influence coefficients, and the stiffness method, e.g., using slope-deflection techniques. The first half of the book develops the flexibility matrix approach, beginning with the fundamental equations of equilibrium, and compatibility. These are used first to study elementary members and then to study progressively more complex structures, with general matrix usage always adhered to. Special problems, such as transformation of axes, scale factors, changes or choice of releases, etc., are described in some detail.

The alternative method, where stiffness instead of flexibilities are computed, is next described in a similar fashion. Here the particular solution is obtained with all connections rigid and the complementary solutions result when artificial "fixities" are released appropriately. As the authors point out, the two approaches are related and each has its advantages and its disadvantages; the problem itself often suggests which is the more suitable method.

The final two chapters discuss briefly the special analysis procedures of relaxation and coefficient of restraint. Since each of these procedures has numerous variations, the treatment can only be indicative of the possibilities.

The writer believes this book fills a void in the literature on structural analysis. The emphasis on the application of basic analysis procedures to general structures is needed, and this lucid presentation should be of considerable assistance to structural engineers. Because of its nature, it is not directly comparable either with the many texts containing basic structural theory or with the specialized books treating a particular procedure in a comprehensive manner. Several universities now offer courses with comparable coverage, and recent literature, e.g., "Matrix Analysis of Structures Curved in Space," by F. Baron in the March 1961 *Journal of Structural Division*, ASCE, has contained several articles on this subject.

E/M Field Report

Periodic reviews of the state of the art—techniques, instrumentation, theory—in areas of experimental mechanics.
Report No. 1:

Shock Motions and Their Measurement

by Irwin Vigness

Introduction

A review in expanded outline form is presented, wherein shock motions and means of their measurement are described. Because of their present popularity, more detailed considerations are given to piezoelectric accelerometers. References to recent literature are included which contain detailed considerations of these subjects. The first three references are regularly issued publications. References 4 through 13 are handbooks and texts. The remaining refer to individual papers.

Shock Motions, Shock Spectra, Simple Shock Pulses

A *shock motion* is defined[14] as a transient disturbance that involves a significant change in position in a relatively short time. Shock motions normally encountered in field work involve translations and rotations in all directions. In addition there are distortions and relative motions which may cause damage to items having several attachment points. Consideration is given here, as usual, to only the translational component of motion in a uniaxial direction.

Recordings of shock motions as normally obtained from field measurements are too complex to be of direct use to the engineer. They must be expressed in some simplified manner which includes their most significant components of *damage potential*. What constitutes damage potential is complicated and controversial, but, roughly, the probability of damage to an item can be taken as proportional to the magnitude of response of the item to a shock motion. Fatigue is important if the shocks involve many cycles of stress.

Shock Spectra[15] constitute one such way of expressing the damage potentials of shock motions. Consider a series of mass-spring systems (single-degee-of-freedom systems) having a range of natural frequencies and attached to a common rigid base. The base is then subjected to a shock motion. The *shock spectrum* of that motion is a curve representing the maximum responses of each of these systems plotted as a function of their natural frequencies. Shock spectra can be expressed in terms of (absolute) accelerations, velocities or (relative) displacements.

If the duration of a shock transient is very short, such as may be caused by an impact when an item is dropped, then it may be permissible to approximate the shock motion by merely expressing it as a sudden velocity change. This is called *velocity shock* (see Ref. 3, page 89) and its magnitude is equal to the step-change in velocity. If the duration of the impact time is appreciable, then the shock may be approximated by a simple pulse. A *half-period sine pulse* (of acceleration) is frequently used because it is easy to generate; a rigid mass dropped against a linear spring experiences a half-period sine pulse. However a *sawtooth pulse*[16] is generally considered to be better for test purposes as its shock spectra has equal positive and negative values with no periodically varying small values. The *maximum value* of acceleration is significant only if its duration (time spent near the maximum value) is long compared with periods of fundamental modes of vibration of an item subjected to the acceleration. This statement is generally true relative to structural damage;

Irwin Vigness is head of the Shock and Vibration branch of the U. S. Naval Research Laboratory, Washington 25, D. C.

however, exceptions occur for conditions such as relay chatter and microphonics. When the waveform of the shock motion is complex in a significant manner, then it may be analyzed in terms of a continuous Fourier spectrum (Fourier integral techniques), or its damage potential can be expressed in terms of a shock spectrum.

Although shock motions are not usually analyzed in terms of their frequency components, it is useful, from the viewpoint of their measurement, to think of the frequency-amplitude range associated with their Fourier spectra. The shock motions can be measured in terms of acceleration, velocity or displacement. As the ranges of amplitudes involved in the three cases are greatly different, there are advantages in selecting a unit which provides the most convenient range for measurement. If the shocks are caused by an impact, it can be taken as a rule-of-thumb that the range of maximum probable velocity amplitudes will be small and independent of frequency. The maximum probable amplitude values of accelerations will increase directly with frequency, and the maximum probable amplitude values of displacements will decrease inversely with frequency. (The rule is, of course, applicable only within a limited frequency range.) This makes the measurement of shock motions in terms of velocity much easier than in terms of displacement or acceleration because of the smaller range of values encountered for an extended frequency coverage. However, if high frequencies are of most importance, then acceleration measurements are indicated, and if low frequencies are of most importance, then displacement records may be obtained. These can, of course, be obtained by integrating the output of an accelerometer.

Transducers or Pickups

A *transducer*, or *pickup*, is a device that converts a quantity to be measured into a signal that is more easily recorded. Pickups that provide output signals proportional respectively to displacement, velocity, or acceleration, are called displacement, velocity, or acceleration pickups, although the latter is usually misnamed by calling it an accelerometer.

All pickups are limited as to the *amplitude and frequency range* over which they will perform with acceptable accuracy. These ranges must be specified.[17, 18] The pickup specification should state (Ref. 6, chapter 15) upper and lower frequency limits and upper and lower amplitude limits within which it will perform within specified accuracy. Calibrations[18] are required to establish the specifications and to check the sensitivity of the pickup. The *sensitivity* is defined as the ratio between the output and input of the pickup. As phase and amplitude are both involved, this ratio is a complex number.

Pickups of all types have been extensively discussed in recent literature.[7, 9, 11] Because of this, consideration will be limited to piezoelectric type accelerometers (acceleration pickups) which have undergone considerable improvements in the last few years.

Mechanical Considerations

An accelerometer consists essentially of a mass supported by a sensing element which, in the case considered, is a piezoelectric material. In order for the mass to experience the same acceleration as the accelerometer case, and consequently exert an inertial force on the sensor which is proportional to the acceleration, the support must be relatively rigid. This condition exists for all frequencies less than about $^1/_4$ the natural frequency of the system. The accelerometer should therefore have a natural frequency as high as possible, and at least 4 times as high as any measured frequency component. The pickup should be as small and light as possible so that its weight will not influence the shock motions. However, as the pickup is made smaller and of higher natural frequency, its sensitivity decreases, and suitable compromises must be made to obtain optimum values.

Sensing Elements

A general consideration of sensing elements is given in Ref. 9, chapter 15. Discussion will be limited here to ceramic piezoelectric materials[12, 13] of the barium titanate class. The electrical properties of these materials are analogous to the magnetic properties of iron, so they are sometimes called "ferroelectric" materials. The ceramics can have their sensitive piezoelectric axis established in any direction by applying a suitable polarizing voltage under proper temperature conditions. The piezoelectric properties can be improved by adding suitable "impurities." Nonlinearities and relaxation effects become important if pressures or voltages of excessive values are applied; or if lesser values are applied for long times. These effects would be functions of temperature. At a certain upper temperature limit, called the *Curie Point*, the thermal energy is sufficient to destroy the polarization, and the material ceases to be piezoelectric. Low-temperature Curie Points (transition temperatures) may also exist below which the piezoelectric effect be-

comes small. Devices employing these materials should operate within these temperature limits.

Zero Shifts and Spurious Outputs

Fortunately, zero shifts and output distortions of an accelerometer and associated equipment can usually be recognized from the appearance of the record. In addition, the integration of the record should give values that check with final values of velocity and displacement involved. The latter are usually known. Causes of distorted outputs will now be considered.

If an accelerometer is operated within limits established by the manufacturer, most causes of zero shifts are faults of the associated electrical equipment. These faults are:

1. Inadequate Time Constant. The piezoelectric sensor generates a given charge (quantity of electricity) in response to a given acceleration (force). This charge will gradually leak through any resistance across the sensor. This will make it appear as though the acceleration were decreasing. If the acceleration should become zero, the sensor will absorb the charge it had previously developed. If this charge has leaked away, a signal will be generated which appears like an acceleration of opposite sign. To eliminate this effect, the "RC" time constant must be made large compared to periods of acceleration pulses. R is the leakage resistance and C is the capacitance of, and in parallel with, the sensor.

2. Nonlinear Amplification. If a low-pass filter is used to eliminate an upper frequency range of accelerations, and if an amplifier provides less amplification for, say, negative signals than for positive signals in this upper frequency range, then a "rectified" signal will result which will be passed by the filter and appears as a zero shift. To reduce this effect, place more capacity across the accelerometer so as to reduce its voltage output, or use preamplifiers capable of handling greater swings of input voltage.

3. Cable Signals. The cable connecting the accelerometer to the preamplifier is subjected to severe shock motions that may cause it to develop electrical signals. Tests for this effect can be made by subjecting the cable to the shock motion while it is disconnected from the accelerometer. To reduce this effect, use specially prepared low-noise cable and higher output accelerometers.

4. Ringing Frequencies. Characteristic frequencies, in particular, cut-off frequencies of filters, may be shock-excited and appear in the record. These can be eliminated by introducing resistance in the electrical circuits in which the ringing occurs.

Occasionally spurious signals are the fault of the accelerometer. Frequency-dependent amplitude and phase distortions are functions of the natural frequencies and damping of the pickup. The frequency range where these are important is above that which should be specified for their proper operation.[17] Spurious signals may occasionally be introduced by the sensor. It is not surprising that this is so. The piezoelectric material consists of electric domains whose change-of-alignment cause changes of the dimensions of the material. A load applied to the material will cause some domains to change direction. This is accompanied by internal stresses and mechanical relaxations. Removal of the load will permit internal stresses and electrical forces to eventually bring about the original condition. For relatively small loads applied for relatively short times, the magnitudes of these effects are negligible. However when the loads become excessive and when they are applied for an appreciable time, a significant amount of internal inelastic motion may take place. When the load is removed, an appreciable time is required for the internal elastic stresses to re-establish the original condition. During this time the signal will slowly drift back to zero. To eliminate this effect requires either that a better sensor material be used or that the sensor be subjected to less load.

References

1. "Shock and Vibration Bulletins," Secretary of Defense Research and Development, Washington 25, D. C.; (W. W. Mutch, Code 4021, U. S. Naval Research Laboratory, Washington 25, D. C., editor.) 29 sets of bulletins have been published which contain much of the important literature in this field.

2. "Environmental Effects on Materials and Equipment, Abstracts," Prevention of Deterioration Center, National Academy of Sciences, Washington 25, D. C. This is a new abstracting journal.

3. "Journal of Environmental Sciences," and "Proceedings of the IES," Institute of Environmental Sciences, P.O. Box 191, Mt. Prospect, Ill.

4. "Mechanical Vibrations," J. P. Den Hartog, McGraw-Hill Book Co. (4th ed., 1956).

5. Jacobsen, L. S., and Ayre, R. S., "Engineering Vibrations," McGraw-Hill Book Co. (1958).

6. Crede, C. E., "Vibration and Shock Isolation," John Wiley and Sons, New York (1951).

7. "Random Vibration," edited by S. H. Crandall, Mass. Inst. of Tech., (1958). (See especially chapter 7).

8. MacDuff, J. N., and Curreri, J. R., "Vibration Control," McGraw-Hill Book Co. (1958).

9. "Handbook of Noise Control," edited by C. M. Harris, McGraw-Hill Book Co. (1957). (See especially chapter 15).

10. "Shock and Vibration Control," edited by C. M. Harris and C. E. Crede, McGraw-Hill Book Co. (1961).

11. "Handbook for Experimental Stress Analysis," edited by M. Hetenyi, John Wiley and Sons (1950).

12. "Proceedings of Symposium on Barium Titanate Accelerometers," edited by T. A. Perls, National Bureau of Standards Report 2654 of 1953.

13. Mason, W. P., "Piezoelectric Crystals and Their Application to Ultrasonics," D. VanNostrand Co. (1950). (See especially pages 304–309).

14. "Acoustical Terminology (Including Mechanical Shock and Vibration)," Standard Sl. 1-1960, Am. Stds. Assoc., 10 E. 40th St., New York 16, N. Y.

15. Vigness, Irwin, "The Fundamental Nature of Shock and Vibration," Electrical Mfg., 89–108 (June 1959).

16. Morrow, C. T., and Sargeant, H. I., "Sawtooth Shock as a Component Test," Jnl. Acoustic. Soc. Am., 28, 959 (1956).

17. "Specifying the Characteristics of Pickups for Shock and Vibration Measurements," Standard Z24.21-1957, Am. Stds. Assoc., New York 16, N. Y.

18. "Methods of Calibration of Shock and Vibration Pickups," Standard S2.2-1960, Am. Stds. Assoc., New York 16, N. Y.

dynamic instrumentation Σ

HANDY REFERENCE MATERIAL ON SHOCK MEASUREMENT

IS YOURS FOR THE ASKING: If you use accelerometers, amplifiers or complete systems—tear out this page, check off the literature you want, mail it to us and we will send it to you by return mail. No obligation whatsoever.

☐ **Model 2225 Accelerometer Data Sheet** describes a unique piezoelectric accelerometer specially designed for shock and impact testing. High mounted resonance frequency 80 Kcps nominal. Frequency response ±10% from below 2 cps to 15 Kcps. Design utilizes very low crystal loadings for maximum stability during severe impacts.

☐ **Model 2614B Amplifier Data Sheet** describes a versatile amplifier with frequency response from below 2 cps to 20 Kcps. Adjustable capacitive attenuator for transducer standardization. Up to 14 volts peak output.

☐ **Endevco Calibration Service for Piezoelectric Accelerometers** is a description of the calibration services offered by Endevco, including shock calibration at levels up to 15000g.

☐ **Endevco Tech Data 922** includes a complete discussion of system frequency response requirements for accurate measurement of various transients.

☐ **Endevco Tech Data 1110** recommends the Endevco systems for measuring shock motions of various categories.

☐ **Endevco Tech Data 213** is an illustration of the continuous spectrum nature of transients.

☐ **Endevco Tech Data 111** is a description of Endevco Model 2880 Shock Measuring System packaged for use as a laboratory working standard.

☐ **The Absolute Calibration of Pickups on a Drop-Ball Shock Machine for the Ballistic Type** is a technical paper prepared by R. R. Bouche, Endevco Corporation.

☐ **Electronic & Dynamic Formula** is a handy pocket guide of commonly used conversion factors, formula and other data useful to the environmental engineer for measuring vibration, shock, pressure and other dynamic phenomena.

FILL OUT BELOW AND MAIL TO

ENDEVCO CORPORATION,

161 E. California Boulevard, Pasadena, California

Name _____

Company _____

Address _____

City & Zone _____ State _____

A Note to AUTHORS

- All papers and technical notes should conform to style requirements set forth in the manual "An SESA Paper" and the "Authors' Check List." Obtain your copies from SESA Headquarters, 21 Bridge Square, Westport, Conn.

- All papers and technical notes must be reviewed and accepted by the Papers and Proceedings Committee in order to qualify for publication.

- Authors must provide a statement that their articles have not been previously published nor submitted for publication elsewhere.

- One original and two copies of the manuscript, complete and carefully typed with double spacing and wide margins, are to be sent to: Roscoe Guernsey, Chairman, Papers and Proceedings Committee, Space Technology Laboratories, Inc., P. O. Box 95001, Los Angeles 45, Calif.

- Authors should state their affiliation, title or position and mailing address.

- All papers, but not necessarily technical notes, must be presented at a Society Meeting either orally or by title.

- If at all possible, length of text should not exceed 4000 words; a technical note should not contain more than 750 words.

- Illustrations must be clearly drawn in ink and should not be larger than $8\frac{1}{2}$ x 11 in. "Guided" lettering should be used at all times and should be large enough to be legible when reduced. Photographs must be sharp, glossy prints. A separate list of captions for all figures must be typed with double spacing. The figure number and author's name should appear on the back of each illustration.

- Reprints may be ordered from SESA Headquarters.

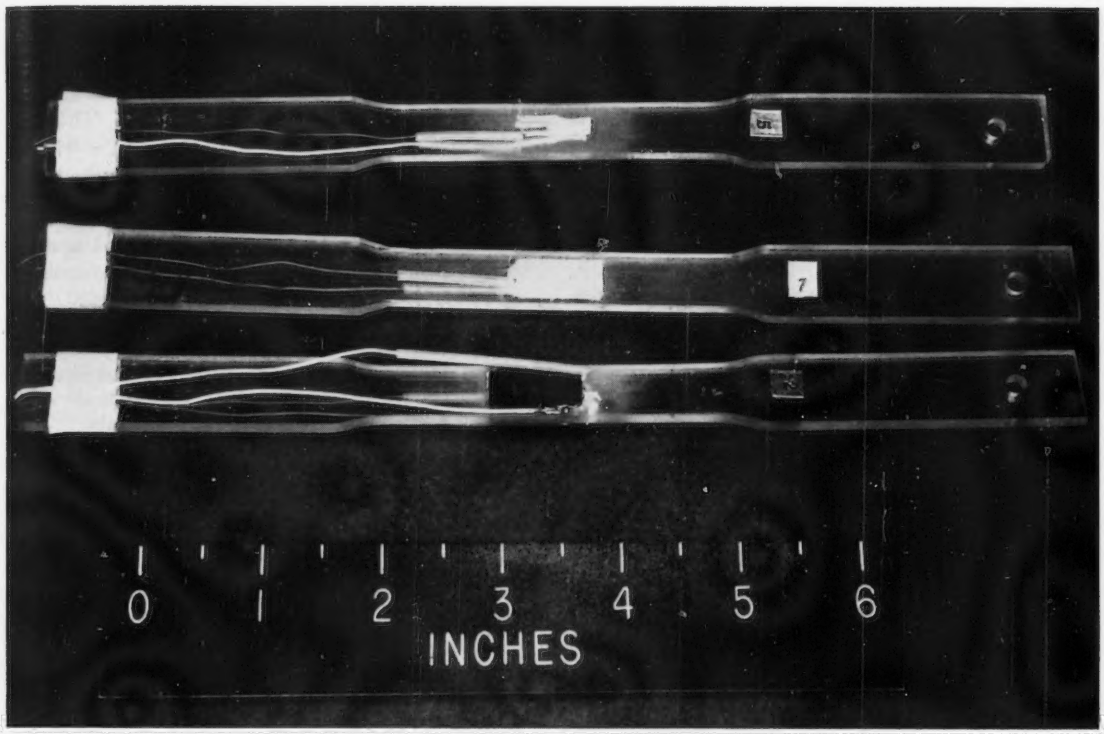

Fig. 1—Plastic tensile specimens

Stress and Deformation Analysis from Reduced-scale Plastic-model Testing

Guides to successful use of plastic-model testing and some limitations of the method are presented. Also, the special strain-gage application and testing techniques required are detailed.

by Aldie E. Johnson, Jr., and R. H. Homewood

ABSTRACT—The use of scale models, which are made from plastic material, for stress and deformation analysis of missile nose-cone structures is discussed. The special strain-gage application and testing techniques, which are required because of the use of plastic materials, are detailed.

The utilization of relatively inexpensive simplified models for the investigation of two specific design conditions is cited. The first case is a stress and deformation study of a thin, constant-thickness, shallow spherical shell which is supported by a circumferential line reaction and subjected to uniform external pressure. Comparisons are made with a recently published theoretical analysis of the problem.

The second case is a particular design problem which is concerned with the determination of the stress and deformation in a variable-thickness, shallow spherical shell with several various-size cutouts. The shell is loaded with a varying external-pressure load which is reacted by a circumferential line load at the periphery. Influence curves for both stress and deformation are given.

Some limitations of plastic-model testing are reviewed, and guides to successful use of the method are given.

Aldie E. Johnson, Jr., and R. H. Homewood are associated with Research and Advanced Development Division, Avco Corp. Wilmington, Mass.

Paper was presented at 1959 SESA Spring Meeting held in Washington, D. C. on May 20–22.

Introduction

There are many advantages to be obtained by studying stresses and deformations in structures experimentally through the use of scale models. This

is particularly true with structures that are so complex that a complete mathematical analysis is virtually impossible or, where, in the course of attempting a mathematical analysis, simplifying assumptions are made that require verification. The use of scale models provides an understanding of the structural action and, intrinsically, includes many considerations that cannot be covered in a theoretical analysis. The time which is required for an experimental structural analysis of a complex structure (including the time for making the model) is usually no greater, and often is much less, than that required for a theoretical analysis.

To perform structural-model analyses, it is necessary to have a model which is representative of the structure to be analyzed. The model should be reasonably priced, easy to fabricate and machine, impose no restriction on the structural action, be capable of being as simple or as complex as required for the application (i.e., welded, bolted or essentially integral construction), be reasonably simple to load, test, and analyze, and should not require expensive tools, equipment or methods for testing.

For many applications, the use of plastic scale models satisfies most of the above requirements; however, the shortcomings of plastics restrict or prohibit their use in fields such as dynamics, fatigue, time-temperature-dependent loads, thermal stress, etc. Thus, the general field of static stress and deformation studies appears to be the area of greatest usefulness.

The intention of this paper is not to picture plastic models as a cure-all but, rather, to indicate areas in which they can be used to advantage, and to describe methods and procedures which have been utilized by the Applied Mechanics Laboratory of the Avco Corp., Research and Advanced Development Division, to obtain useful results. This work includes the results of considerable previous effort by others[1–7] which have been correlated with supplementary studies by Avco to provide a usable procedure for plastic-model investigations.

Background

To assess the merits of plastic models for static stress and deformation testing, a review of some background material may be helpful. In subsequent sections are given the advantages of using plastics, the disadvantages, limitations and precautions necessary to their use, and a brief review of some previous work from which pertinent data have been obtained. In addition, a detailed procedure for the application of strain gages, testing procedures and corrections for data analyses which have been used for the present study are given.

Advantages

A review of the literature (for example, references 1, 2 and 8) indicated several advantages and reasons for using plastics in structural-model analysis. The more important advantages are summarized in brief review in subsequent paragraphs.

Generally speaking, the modulus of elasticity is 500,000 psi or lower at room temperature. Because of the low modulus of elasticity, small loads will produce large and easily measured strains. This fact is particularly desirable where space, equipment or facilities for testing are limited inasmuch as the fabrication of end fixtures, loading fixtures, etc., can be relatively simple, lightweight and inexpensive.

Plastics are relatively easy to fabricate and are inexpensive. Most of them are thermoplastic (i.e., they become soft when they are heated) and, thus, are easily molded when hot; and the heating and cooling cycle can be repeated any number of times. They can be easily sawed, drilled and machined. Another important factor is that many plastics can be cemented together with solvent-type cements to form cohesive joints which are strong and reliable.

With the proper selection of plastic material, essentially homogeneous, isotropic materials can be obtained which are consistent with most structural materials or the usual assumption of material properties.

Thus, plastic models have the advantage of low fabrication cost, they are homogeneous and isotropic and they can be constructed quickly and easily and tested with relatively simple experimental equipment.

Disadvantages

Unfortunately, plastics have some serious disadvantages when they are used in structural models. Plastics (to a varying degree) creep under load. That is, when a plastic model is stressed (even well below the yield point), a deformation occurs and continues at a decreasing rate when the load is held constant.

Most plastics are extremely sensitive to temperature changes. That is, they have a high coefficient of thermal expansion and the modulus of elasticity changes with temperature. The softening of plastics at temperatures not too much above room temperature is desirable for forming and fabrication, but is undesirable during testing, particularly during warmer months of the year where air conditioning is not available.

The mechanical properties of some plastics are sensitive to humidity. This has been reported elsewhere[9] for cellulose acetate and cellulose nitrate, and may also be true for the methacrylate family. The literature[1–4, 6, 8, 9] shows that no systematic work has been done on the effect of humidity on the modulus of elasticity of plastics, which is the important material property in structural-model analysis.

Solvent-type cements, which are used to bond plastics, soften the area where they are applied and cause a local lowering of the modulus of elasticity. Caution must be exercised when using solvent-type cement to insure that the cement does not touch areas

that are not being bonded. In addition, it has been recommended[3] that when many cemented joints are made, the model should be allowed to cure for an appropriate length of time before using.

Limitations

There are, of course, some additional limitations in the use of plastics. The physical size of commercially available sheet materials, thickness, flatness and thickness tolerances may influence the model size or the type of fabrication. For example, methyl methacrylate is a commonly used model material, but it cannot be obtained in thin sheets (minimum sheet thickness is 0.040 in.). The variation of thickness within the sheet is generally large whereas other plastics, such as cellulose nitrate and polyvinyl chloride, can be obtained in very thin sheets (0.010 in. and less) and have excellent sheet-thickness tolerance. Mylar has a relatively low coefficient of thermal expansion but, at the present time, it is available in only thin sheets (0.010 in. maximum) and structurally satisfactory bonds are difficult (if not impossible) to achieve.

Previous Areas of Usefulness

Despite the adverse properties, plastics have been used by many persons for structural-model analysis.

Boulton Paul Aircraft Ltd., has constructed and tested several structural models which have been made from cellulose nitrate. Redshaw and Palmer[8] have described the construction and testing of a cellulose nitrate model of delta aircraft to investigate wing stiffness, stress distributions, ground resonance and wind-tunnel flutter characteristics. In their model, many of the parts were formed by pressing pieces of the plastics at room temperature with tools which had been preheated in a water bath to a temperature of 212° F. Individual parts were then cemented together with a solution of 60% acetone and 40% amyl acetate.

At the Watertown Arsenal, a study of the buckling characteristics of bulkheads was made with structural scale models which had been made from rigid sheets of vinyl chloride deacetate resin, a thermoplastic material, commercially known as vinylite.[10] The material was formed by placing the sheet of vinylite on the surface of boiling water until the material could be readily formed. A male form was placed in the center of the sheet and allowed to become heated while partially forming the plastic sheet. After the form had become heated, it was removed with the sheet of plastic and inserted into a female mold and pressure was applied to complete the forming.

Cellulose acetate models (which were originally made as visualization models) of a gun turret and a low-pressure steam-turbine casing were used in an experimental deflection analysis by Meadows.[3] [It was noted by Redshaw and Palmer[8] that cellulose acetate materials were inferior (for use in structural models) to materials with a cellulose-nitrate base because of dimensional instability.] Also, Meadows[3] reported on a study of the effect of age on cemented models. The variation of modulus of elasticity with time for cemented box-girder models of methyl methacrylate and cellulose acetate was determined experimentally. It was found that the variation was very high at first but leveled off to 330 psi per day for methyl methacrylate and 800 psi per day for cellulose acetate after 15 days. Even after 3 months, the variation was over 100 psi per day for both materials. Meadows indicated that the variation in modulus might have been less severe if the box girder models had been cured at an elevated temperature.

Structural scale models (which were made from methyl methacrylate plastic) of statically indeterminate frames and of the vertical control shaft of a dam were used to determine influence lines of stress.[1] Stresses were determined by use of bonded wire strain gages which had been cemented to the models at the points of interest.

Methyl methacrylate plastics were also used to determine stress and deflection experimentally in aircraft wing and fuselage models.[2, 4] The particular methacrylate in these tests was Plexiglas I-A. Zender[4] indicated that maximum model stresses should be in the range from 500 to 600 psi to avoid difficulty from the effects of creep. Tests by Avco on Plexiglas II-UVA indicated that model stresses between 1500 and 2000 psi could be tolerated without excessive difficulties from creep.

Avco Procedures

It was necessary to determine stress and deflection distributions and influence lines for both stress and deflection. Deflections could be measured readily with dial-indicator-type gages, and stresses could be determined most conveniently from bonded wire strain gages. However, there were disagreements in the literature[1,5] on the suitability of adhesives for cementing strain gages to Plexiglas (which was the material selected for the models).

Thus, an investigation was required to determine a suitable method of bonding strain gages (SR-4 type gages) to Plexiglas and; also, to establish test procedures for using Plexiglas for stress and deformation studies. The use of nitrocellulose cement (Duco) was recommended for SR-4 gage applications, but the literature [for example, Reference 5] indicated that Duco cement was generally unsuitable for cementing strain gages to Plexiglas. Landdeck,[1] however, indicated that "SR-4 gages may be bonded to either methyl methacrylate or polystyrene plastics without difficulty using Duco cement."

Bonding Procedure

Standard bonding procedures were used to apply the gages,[11] except that the gage area was lightly but thoroughly sanded with No. 600 grit paper. Trichlorethylene was used as the cleaning agent. A minimum amount of cement was spread on the back of the gage, so that there was little excess cement under and around the gage when applied.

Test Procedure

To determine a suitable means of bonding strain gages, the following standard procedure was used throughout this investigation. A standard tensile-test specimen was cut and numbered; the specimens were loaded in a tensile-testing machine, and load-strain data for each specimen were obtained autographically from an inductance-type 2-in. gage length averaging extensometer. The material was never stressed to the yield stress. After the initial loading, a pair of bonded wire strain gages was applied back-to-back on the specimen with standard application procedure (see Bonding Procedure), and the gages were dried at room temperature for 24 hr.

The specimen was retested, and load-strain data were obtained from the averaging extensometer and from the strain gages. The individual strain-gage readings were averaged to eliminate bending strains. Temperature was recorded during each test. From each of the three sets of load-strain data, a modulus of elasticity was computed and corrected (by means of the procedures which will be described in subsequent paragraphs) for the added stiffness of the specimen, due to the strain gages, and the effect of temperature on the modulus.

Results

The data from all tests are shown in Table 1 where the moduli of elasticity have been computed from the load-strain data and corrected to a reference temperature of the test before wire gages have been applied to the specimen. Several tests (specimens 1 to 10) were run on tensile specimens which had Duco-bonded A5 and A7 strain gages. In addition, one specimen each was tested with A5 gages which had been bonded with SR-4 precoat and cement and a white resin glue (specimens 11 and 12, respectively). Specimens 1 to 3 had A5 gages which had been trimmed to the felt width; specimens 4 and 5 had A7 gages which had been trimmed to a width of $^3/_{16}$ in. and a length of $^3/_8$ in.; specimens 6 to 9 had untrimmed A7 gages; and specimens 10 to 12 had A5 gages which had been trimmed to the felt width. A photograph of representative gage installations on the tensile specimens is shown in Fig. 1.

The temperature correction is based on information from the Plexiglas Handbook[6] which shows that the value of the modulus is reduced by approximately 2780 psi for each degree Fahrenheit rise in temperature.

The correction for the stiffening effect of the wire gages has been determined by Brock of the David Taylor Model Basin. Brock[7] "has found it takes about 3.9 lb to elongate a pair of A5 gages trimmed to the $^9/_{32}$ felt width approximately 1000 microinches per inch." Although the paper in the gage accounts for only approximately 90% of the stiffness and there is approximately a 50% increase in paper thickness for the A7 gages (with respect to A5 gages), a factor of 1.5 on the A5 stiffness has been used for the A7 gages.

From the results in Table 1, two conclusions are evident: (1) a satisfactory bonding of SR-4 gages to Plexiglas II can be achieved with Duco cement without appreciably affecting the properties of the material, and (2) the large scatter of values of modulus of elasticity indicates that the modulus is affected by some factor, or factors, other than temperature.

TABLE 1—DATA FROM PLASTIC TENSILE SPECIMENS

Specimen No.	SR-4 gages	Extensometer, No SR-4 gages		Extensometer data, SR-4 gages applied					SR-4 indicator data					Bonding agent
		Temp. °F	E × 10^{-3}	Temp. °F	E_{nc}[a] × 10^{-3}	C_G × 10^{-3}	C_T × 10^{-3}	E_C × 10^{-3}	Temp. °F	E_{nc} × 10^{-3}	C_G × 10^{-3}	C_T × 10^{-3}	E_C × 10^{-3}	
1	A5	76	374	84.5	384	−17.4	+23.6	390.2	84.5	413	−55.5	+23.6	381.1	Duco cement
2	A5	84	386	78	415	−17.8	−16.7	380.5	78	447	−56.8	−16.7	373.5	Duco cement
3	A5	86	374	79.5	390.5	−15.9	−18.1	356.5	79.5	435.5	−50.7	−18.1	366.7	Duco cement
4	A7	78	434	81	414	−14.3	+8.3	408.0	81	485	−76.3	+8.3	417.0	Duco cement
5	A7	78	401	82	374	−16.1	+11.1	369.0	82	460	−85.7	+11.1	385.4	Duco cement
6	A7	78	405	79.5	389	−25.9	+4.2	367.3	79.5	444.5	−82.8	+4.2	365.9	Duco cement
7a	A7	78	397	74	397	−24.6	−11.1	361.3	74	479.5	−78.7	−11.1	389.7	Duco cement
7b	A7	74.5	386	...	...	...	...	...	...	...	...	...	...	Duco cement
7c	A7	82.0	389	...	...	...	...	...	...	...	...	...	...	Duco cement
7d	A7	74.0	400	...	...	...	...	...	...	...	...	...	...	Duco cement
8	A7	76.5	385.5	79.5	386.5	−24.1	+8.3	370.7	79.5	461	−77.0	+8.3	392.3	Duco cement
9	A7	75.5	404	81.5	395.5	−26.2	+16.7	386.0	81.5	433	−83.7	+16.7	366.0	Duco cement
10	A5	73	386	69	396	−8.7	−11.1	376.2	69	429	−27.8	−11.1	390.1	Duco cement
11	A5	73	386	73.5	386	−8.4	+1.4	379.0	73.5	409	−26.9	+1.4	383.5	SR-4 precoat and cement
12	A5	73	396	70	386	−8.7	−8.3	369.0	70	429	−27.8	−8.3	392.9	White resin glue

[a] E_{nc} = apparent modulus before correcting for temperature and gage stiffness; C_G = correction of apparent modulus due to gage stiffness; C_T = correction of modulus back to temperature given in column 3; E_C = modulus after correcting for temperature and gage stiffness.

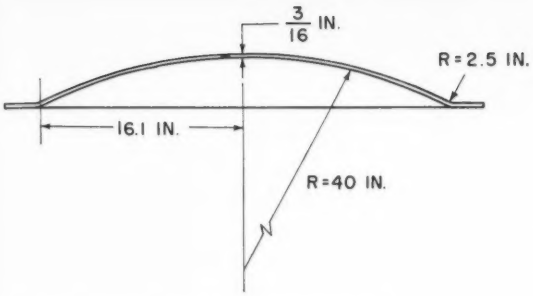

Fig. 2—Cross section of plastic spherical shell

These differences cannot be attributed to a variation of material properties from sheet to sheet because specimens 1 to 9 were cut from the sheet of material from which the models were subsequently fabricated, and specimens 10 to 12 were cut from a second sheet of material. In addition, the second conclusion was further substantiated by a series of tests on a single specimen (No. 7), on different days at different temperatures, using only an extensometer to measure strain. These data are included in Table 1. The differences cannot be attributed solely to temperature effects.

Material Creep

Creep characteristics of methyl methacrylate were noted elsewhere,[7] in which it was recommended that a 6-min period elapse between the application of the load and taking of the strain data. This recommendation was substantiated by data which were taken during tensile loading of the strain-gage specimens. The rate of creep, as it was observed on the SR-4 strain indicator, was negligible 5 min after an increment of load was applied, and the recommended 6-min period was used for all tests.

Zero Drift

In addition, it was found that when the gages were initially energized, an appreciable drift in zero reading took place. This was attributable to the heating of the material under the gage which was caused by the current (although extremely low values of current were present, the wire size was also very small) flowing through the gage. To eliminate the zero drift of the gage, all gages were powered at all times by a constant-voltage source during a test. Although it had been suggested[7] that humidity might have an effect on material properties, no humidity control was used for day-by-day variations, and the change in humidity within the test duration was believed to be negligible.

Investigation of Shallow Spherical Shell

An experimental stress and deformation analysis was required to substantiate an existing theoretical solution of a thin, constant-thickness, shallow spherical shell which was subjected to a uniform pressure on the convex side and supported by a circumferential line reaction. As a consequence of the information which was described in preceding sections, the use of a reduced-scale plastic model appeared to be desirable. The results given herein are from a recently published report.[12]

Fabrication of Specimen

A shell was formed to a spherical shape from a single flat sheet of plastic by the vacuum-snapback method. A cross section through the axial centerline of the shell is shown in Fig. 2. A methyl methacrylate, Plexiglas II-UVA, was selected as the plastic.

Although the sheet of plastic had been carefully selected for uniformity of thickness, there were considerable variations in thickness in both meridional and circumferential directions due to the manufacturing process. These variations were noted particularly in the regions of a deep draw around the mold. The thicknesses were measured after forming and are shown in Fig. 3.

Loading Conditions

Uniform air pressure was applied to the convex surface of the model, which was reacted by a circumferential axial line load. The circumferential line load was applied at three different diameters (16, 18 and 20 in.) to evaluate the effect of line-reaction location. The shell was supported in a test fixture which provided the seal and reaction to the pressure load. This fixture (shown schematically in Fig. 4) consisted of a straight-flanged pressure head which had been adapted to clamp the edge of the shell. A four-legged steel loading frame was bolted to the pressure head to provide a reaction for the line load.

The circumferential line load was applied through a loading cylinder. The cylinder acted directly on the shell for the 18-in. diam, and through a wooden ring for the 16- and 20-in. diam lines. Thus, there was actually a finite width of "line" ($^1/_4$ in. wide for the 16- and 20-in. diam loadings and $^1/_2$ in. wide for the 18-in. diam loading).

Instrumentation

Inasmuch as the shell and loading conditions were rotationally symmetric about the axial centerline, the principal strains and stresses theoretically would be meridional and circumferential. Strains were measured by use of bonded wire strain gages located at close intervals along a meridional line. At each location, gages were applied to both surfaces of the shell in both principal directions. In addition, gages were applied along other meridional lines as a check on symmetry of loading.

A switching and balancing unit was used in conjunction with a SR-4 strain indicator for multigage reading. However, with this system, voltage is applied only to the gage in the reading circuit. As a consequence of this, and to eliminate the zero-shift error in each successive gage as it was switched into the reading circuit, a constant voltage, which is

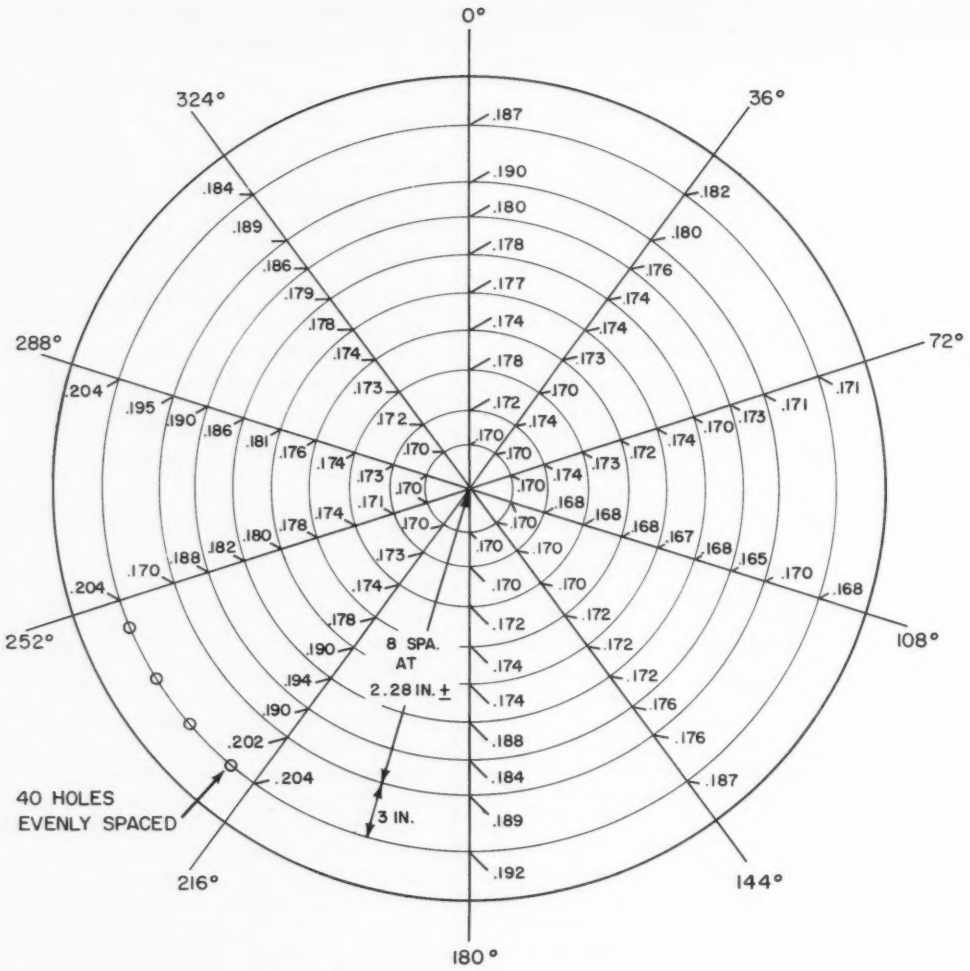
0°
36°
72°
108°
144°
180°
216°
252°
288°
324°
.187
.190
.180
.178
.177
.174
.178
.172
.170
.170
.174
.173
.170
.170
.174
.173
.172
.174
.170
.173
.171
.171
.170
.173
.174
.172
.173
.170
.174
.168
.168
.168
.167
.168
.165
.170
.168
.172
.172
.172
.174
.174
.176
.176
.188
.184
.187
.189
.192
.194
.190
.202
.204
.204
.170
.188
.182
.180
.178
.174
.173
.171
.170
.174
.173
.170
.174
.173
.172

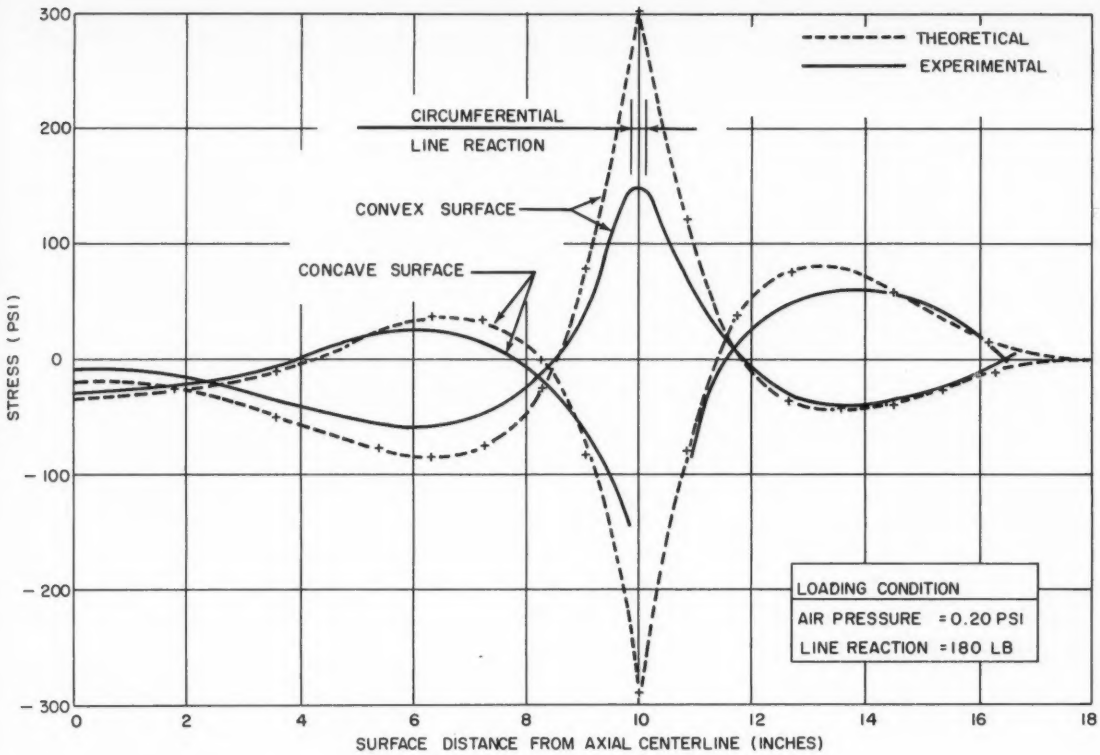

Fig. 5—Typical Plexiglas spherical-shell meridional stresses

tain the air pressure loading on the convex surface. Clamping of the edges induced self-equilibrating bending moments and forces normal to the axes of the shell during loading.

Tests were run in accordance with the procedures previously discussed; i.e., tests were run in an insulated room with care taken to prevent air transients, a 6-min wait period was allowed after applying load before taking data, etc.

Analysis of Data

The strain-gage readings were averaged to obtain average strains per increment of load. Although the variation in strain increments was fairly high in some cases, all increments were averaged to obtain the average strain increments. The modulus of elasticity which was used to compute the stresses corresponded to the modulus at the average temperature during the test. A value of 0.35 was used for Poisson's ratio.[6]

The stress-strain relationship of the material was determined from tests on the tensile specimens which were discussed in previous sections. In determining strains, the same procedure was used for the tensile specimens as was used for the test models. For the test model, strains were restricted to values well within the apparent elastic limit of the material.

Dial-gage readings (which were taken normal to the surface) were corrected to axial deflections and, then, averaged to obtain deflection per increment of load.

Results

The experimentally determined meridional and circumferential stresses for the convex and concave surfaces and for the three loading diameters were plotted and compared with the theoretical stress curves. Figure 5 shows theoretical and experimental curves of stress for a typical loading condition. The experimental curves of stress on the concave surface are discontinuous at the line load because no strain gages were placed directly under the load. The deflections (which are plotted as axial displacements with the apex of the shell as a zero reference displacement) for a typical case are compared with theoretical displacements in Fig. 6. The experimental and theoretical deflection curves show excellent agreement, except at the periphery of the shell where the curves diverge. This is attributable to the difference in edge conditions. The experimental shell has been fixed at the periphery whereas a free periphery is assumed in the theoretical analysis. This difference of theoretical and experimental boundary condition is also somewhat evident in the stress curves. Inasmuch as the edge conditions do not influence the action of shells be-

yond a nominal distance inboard, no difference in stress or deflection due to edge conditions should be discernible except near the edges.

The experimental and theoretical stress curves (Fig. 5) show good qualitative agreement throughout and fairly good quantitative agreement, except in the vicinity of the line load. Some discrepancy is to be expected in this area because an assumption of an infinitesimal "line" has been made in the theoretical analysis whereas the experiments require a "line" of finite width.

An indication of the effect of the finite width of the "line" was observed from the tests. It was expected (from the theoretical analysis which showed that in this region there should be a monotonic variation in stress under the point of loading) that the values of stress and deflection at the line for the

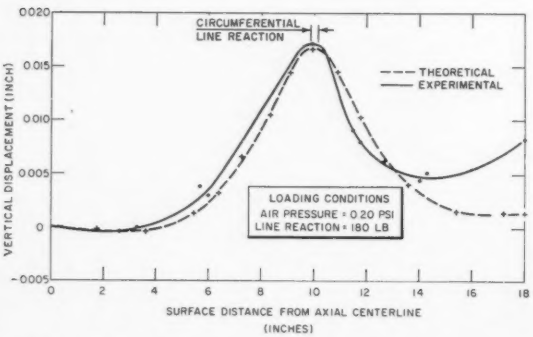

Fig. 6—Typical Plexiglas spherical-shell vertical displacements

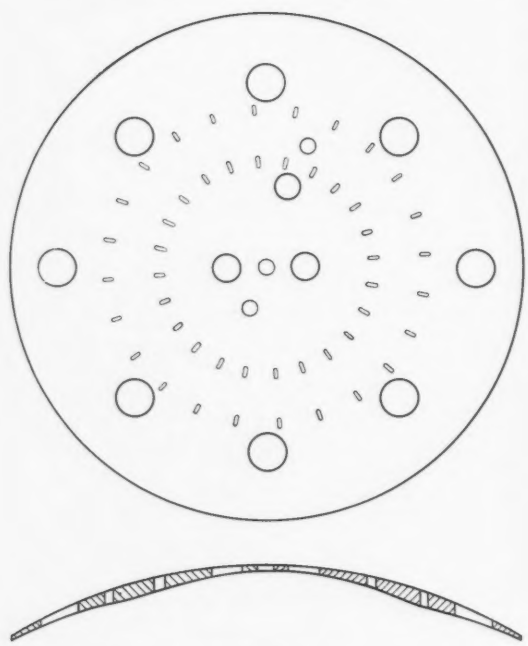

Fig. 7—Schematic of shallow spherical shell with cutouts

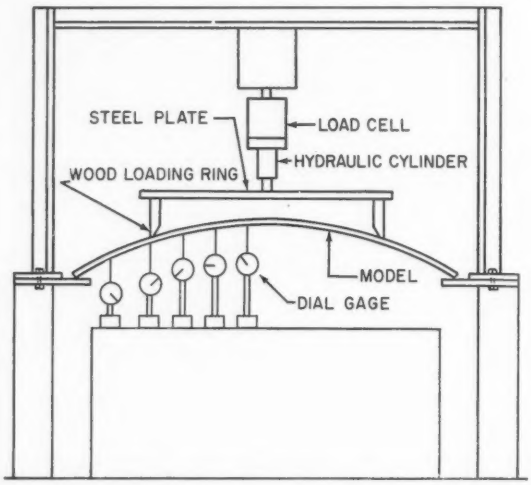

a.—Schematic

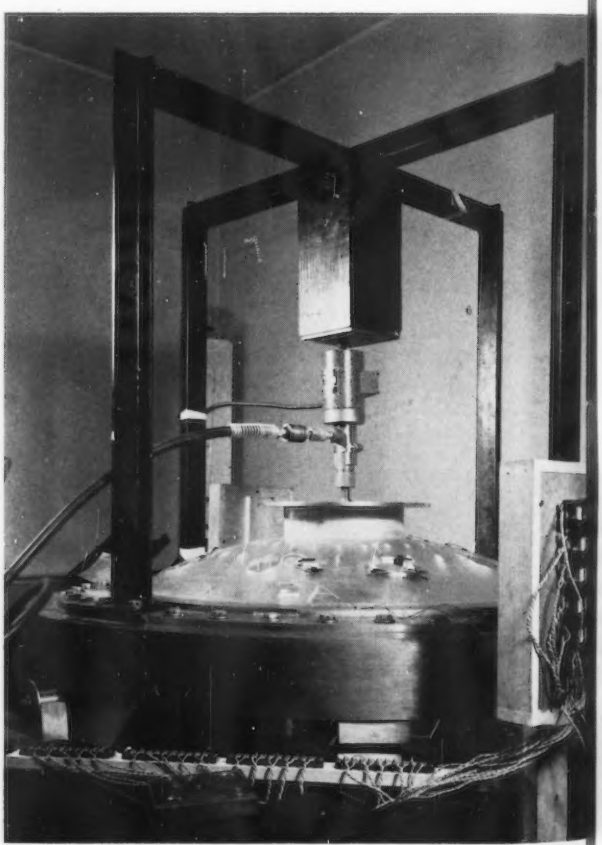

b.—Actual

Fig. 8—Test facility for shallow spherical shell with cutouts

18-in. diam loading condition would be between the values for the 16-and 20-in. diam loading conditions. However, the values of stress for the 18-in. diam loading "line" were lower than the values of stress for either the 16- or 20-in. diam loading because of the difference in width of loading "line."

These results are tabulated below for increments of 0.20 psi air pressure and 180-lb "line" load:

Loading diameter, in.	20	18	16
Width of loading "line," in.	0.25	0.50	0.25
Meridional stress, psi	150	130	230
Circumferential stress, psi	125	110	120
Vertical displacement, in.	0.0170	0.0165	0.0230

Investigation of Design of Shallow Spherical Shell with Cutouts

Another instance where a plastic structural scale model was used in design of a complex structure involved the stresses and deformation in a variable-thickness, shallow spherical shell with several various-size cutouts. The shell is loaded with a varying external load which is reacted by a circumferential line load.

The shell structure nested inside another shell structure and, therefore, to evaluate the magnitude of the interaction loads and determine the influence coefficients, it was necessary to determine the deflected shape of the structure under various loading conditions. Because of the nonuniform nature of the structure which had variously sized holes throughout, and was of varying thickness in the meridional direction, the theoretical deformation analysis contained many unevaluated assumptions.

In addition to the influence coefficients, it was also desirable to determine the effect of geometry on the stress distributions especially in the vicinity of the larger holes.

Fabrication of Specimen

A one-half scale model was fabricated from a single sheet of Plexiglas II-UVA by molding the sheet to the general shape, and then machining to proper thickness and contour. The holes which were expected to have a significant effect on the influence coefficients were machined in the shell. A schematic of the test model is shown in Fig. 7.

Loading Conditions

The model was supported at the periphery by a circumferential line reaction. Loading was applied through wooden rings which had been placed on the convex surface. Six separate tests were made with the applied line load at a different diameter for each test. The wooden rings were $^1/_8$-in. thick at the point of contact with the model. Figure 8a shows a schematic of the test setup, and Fig. 8b is a photograph of the test facility. The load was applied by the hydraulic cylinder through the steel plate to the

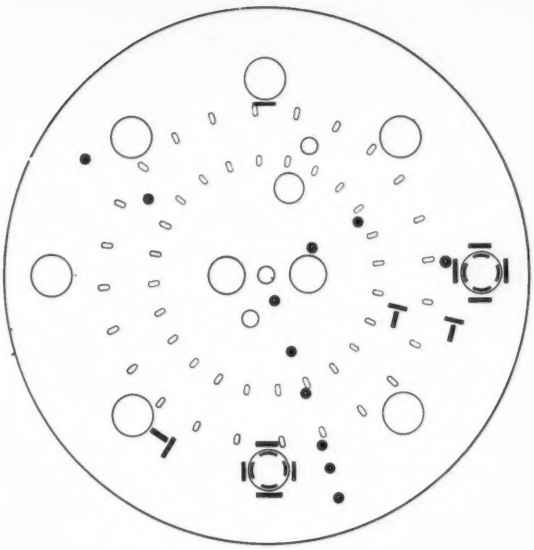

Fig. 9—Instrumentation on shallow spherical shell with cutouts

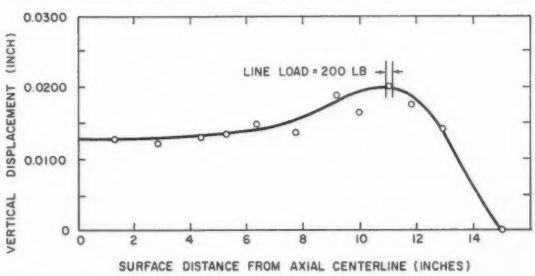

Fig. 10—Typical vertical displacements for shallow spherical shell with cutouts

wooden rings. The cylinder was reacted by a four-legged steel loading frame which was bolted to the model reaction support. The load was measured by a load cell which was located between the hydraulic cylinder and the loading frame.

Deflections were measured with six dial-indicator gages which were located along a meridian (one gage at each loading diameter). In addition, five other gages were located at intermediate distances to check uniformity of deflections in the circumferential direction.

Bonded wire strain gages were applied to both sides of the model at several locations (see Fig. 9) in both meridional and circumferential directions. In addition, in two of the larger holes, strain gages were bonded at the median surface at four locations.

Test Procedures

For each test, loads were applied in 200-lb increments to a maximum of 1000 lb. Strain and dial-gage measurements were taken after each loading increment.

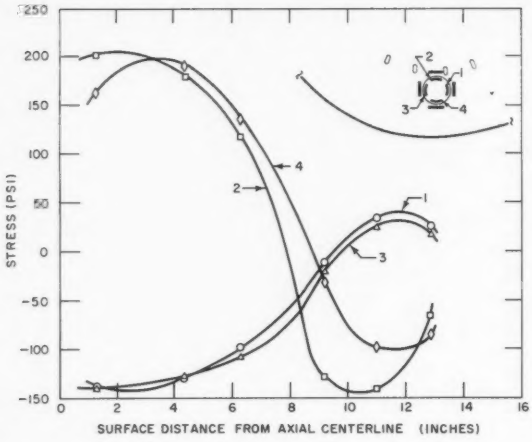

Fig. 11—Typical influence curves for stresses in shallow spherical shell with cutouts (200-lb line load)

Results

The strain and dial-gage readings were reduced to strain and deflection increments per increment of load. Stresses were computed from the strain data using the formula for stress in biaxial-strain field. The modulus of elasticity which was used to compute stresses corresponded to the modulus at the average temperature during the test. A value of 0.35 was used for Poisson's ratio.[6]

A typical curve of deflection as a function of surface distance from axial centerline is shown in Fig. 10. From the stress data, influence lines for stress were drawn for each strain-gage location. A typical curve is shown in Fig. 11.

The relation of stresses in the prototype to stresses in the model can be obtained from the standard scaling relationship:

$$\sigma_p = \frac{P_p}{P_m}\,\sigma_m S^2 \qquad (1)$$

where P is load, S is the scale (model to prototype) and the subscripts p and m refer to the prototype and model, respectively.

In a similar manner, the relationship of deflections in the prototype to deflections in the model can be obtained from:

$$\delta_p = \frac{P_p}{P_m}\,\frac{E_m}{E_p}\,S\delta_m \qquad (2)$$

Stresses at any location can be determined by interpolation between influence curves for any loading condition and by superposition of stress values from the influence curves. By combining the results of several conditions, stresses for any distributed loading can be determined.

Deflections at any location and for any loading condition can be determined in a similar manner from the deflection curves.

Concluding Remarks

To predict prototype stresses and deformations from an experimental plastic-model analysis, the modulus of elasticity of the model must be known accurately. Inasmuch as deflections are inversely proportional to the modulus and, in the case of stresses, the measured strains are used with the modulus to determine stress, the requirement of knowing accurately the modulus of the model material imposes one of the greatest difficulties in plastic-model testing for stress and deformation data.

The modulus of elasticity of plastics is affected by creep, temperature and, possibly, humidity. These conditions can be controlled or compensated for and, therefore, the accuracy of an analysis depends to a large extent on the amount of effort that is expended in controlling these items. The effect of creep on modulus of elasticity can be minimized by the determination of modulus (on a tensile specimen cut from the model material) for a specified elapsed time between loading and strain measurement, and maintaining this time interval between loading and strain or deformation measurement while testing the model.

It is desirable to make plastic-model tests in temperature- and humidity-controlled rooms (if possible) with special care taken to eliminate air currents, and thus, the effect of these variables on the modulus of elasticity. The model should never be exposed to direct sunlight. Bonded wire strain gages, if used, should be continuously connected to a voltage source which is equal to the voltage of the reading instrument to prevent thermal strains (zero drift) due to the heating of the strain gage.

The modulus of elasticity of most plastics varies from sheet to sheet and, therefore, the model should be constructed from a single sheet of material if possible. Tensile specimens should be cut from more than one area in the sheet, and used to determine an average value of modulus of elasticity for the sheet.

References

1. *Landdeck, N. E., "A Direct Method for Model Analysis," Jnl. Structural Div., Proc. ASCE, 82, ST1 (January 1956).*
2. *Zender, G. W., "Comparison of the Theoretical Stresses and Deflections of Multi-Cell Wings with Experimental Results Obtained from Plastic Models," National Advisory Committee for Aeronautics Technical Note 3813 (November 1956).*
3. *Meadows, R., "Deflection Tests of Plastics Models," Proc. Soc. Exper. Stress Anal., Vol. VIII, No. 2 (1951).*
4. *Zender, G. W., "Experimental Analysis of Aircraft Structures by Means of Plastic Models," Ibid., XIV, No. 1 (1956).*
5. *Dietz, A. G. H., and Campbell, W. H., "Bonded-Wire Resistance Strain Gage Techniques for Polymethyl Methacrylate Plastics," Ibid., V, No. 1 (1947).*
6. *Rohm and Haas Co., "Plexiglas Handbook for Aircraft Engineers," Second Edition (1952).*
7. *Eney, W. J., "Discussion of Paper Entitled Bonded Wire Strain Gage Techniques for Polymethyl Methacrylate Plastics," Proc. Soc. Exper. Stress Anal., V, No. 1 (1947).*
8. *Redshaw, S. C., and Palmer, P. J., "The Construction and Testing of a Xylonite Model of a Delta Aircraft," The Aero. Quart., III (September 1951).*
9. *Lawton, T. S., and Carswell, T. S., "Effect of Some Environmental Conditions of the Mechanical Properties of Cellulose Acetate and Cellulose Nitrate Plastic Sheets," Trans. ASME, 67, 1 (1945).*
10. *Radkowski, P., "The Stability of Truncated Cones," Proc. Second Conference on the Mechanics of Elasticity and Plasticity, Washington, D. C. (1957).*
11. *Baldwin-Lima-Hamilton Corp., How to Apply SR-4 Strain Gages, Bulletin 4453 (1951).*
12. *Homewood, R. H., "Experimental Analysis of Thin Shallow Shells Supported by a Circumferential Line Reaction and Subjected to Uniform External Pressure as Determined from Plastic Model Tests," Avco Corp., RAD Div. TR-9-59-11 (March 1959).*

Lueders' Lines Detection by Means of Brittle Coatings

Some of the techniques employed to detect Lueders' lines are compared and the results of a more extensive study using the brittle-coating method are presented

by A. J. Durelli, A. Kobayashi and K. Hofer

ABSTRACT—The objective of this paper is to compare some of the techniques used to detect Lueders' lines and present the results of a more extensive study using the brittle-coating method. A hot-rolled steel tensile specimen was yielded plastically under successively higher amounts of load and the resulting Lueders' lines were recorded using oblique-incident light, etching, photoelastic coatings and brittle coatings. When the results from the various methods were compared, the authors found some advantages in the use of brittle coatings. This method was then used to record the Lueder's lines in beams under pure bending and simple bending, and in plates with notches and holes.

Introduction

When a mild-steel bar is uniformly loaded in tension or compression beyond the yield limit of the material, isolated plastic regions appear interspersed among regions which remain elastic. With a further increase in load, these isolated plastic regions spread out, merge with each other and propagate along the specimen until the entire gage length of the specimen has been covered by these bands. These isolated narrow plastic regions were first described by Lueders in 1854 and are called Lueders' lines. The observation of the initiation and subsequent spread of these lines gives important information on the phenomenon of plastic yielding in mild steel; therefore, they have been investigated by many people[1] for over a century.

Half a dozen experimental methods of detecting Lueders' lines in mild-steel specimens have been used in the past, more or less successfully, depending on the problem to which they were applied. The purpose of this paper is to compare some of these methods and apply one of them, the brittle-coating method, to beams and plates.

Description of the Detection Methods

The following is a short description of some of the techniques used to detect Lueders' lines.

Oblique-incident Light

Lueders' lines appear as fine dull bands of depressions and ridges on the polished surfaces of mild steel specimens. These lines on the specimen may be observed and photographed with oblique-incident light if the proper angle of illumination is used. Furthermore, such processes as metal rolling and other continuous plastic-flow processes may be observed by means of motion pictures taken during the plastic flow provided the illumination is always favorable.

A variation of the oblique-incident light method is the "Schlierenmethode,"[1] which uses parallel light (by means of an optical system). Another extension of this method is described by MacGregor[2] for the purpose of studying continuous flow processes such as occur during metal forming. An advantage of MacGregor's "Plasticscope" is that the equipment can be easily moved and the plastic flow can be revealed on a ground-glass screen without the necessity of darkening the room.

Interferometry

If the surface of the specimen is originally optically flat, light-wave interference can be used to detect the hills and valleys on the deformed surface. A ray of light is partially reflected from and partially transmitted through a medium (generally a half mirror) before impinging upon the surface of the yielded specimen. The ray reflected from the surface of the specimen may interfere with the incoming ray depending on the length of the air gap between mirror and specimens. If the retardation of the second ray is an odd multiple of half wave lengths of the light, an interference band will appear. In Reference 3, a method of detecting Lueders' lines by an interferometry method which employs mirrors with different specific interferences is described.

Etching

Normalized mild steel at room temperature may be considered as a supersaturated solid solution of nitrogen. During plastic flow this nitrogen is precipitated in the regions where flow takes place. Some chemicals react particularly well with the precipitated nitrogen after the steel has been heated at 100° C for a short time. Plastically yielded regions will appear dark against the light background of the unyielded regions. This method is particularly

A. J. Durelli, A. Kobayashi and K. Hofer were associated with Armour Research Foundation at the time paper was prepared.

Paper was presented at 1959 SESA Annual Meeting held in Detroit, Mich., on October 21–23.

suited for studying Lueders' lines in the interior of mild-steel specimens, which are dissected after unloading and etched. The most commonly used etchant for this purpose is Fry's etchant which is a solution of concentrated hydrochloric acid and anhydrous cupric chloride.* The plastically yielded specimen is first heated at 440° F for about 30 min, cooled to room temperature and then etched with Fry's etchant for about three hours. The specimen is then dipped in concentrated hydrochloric acid for about ten seconds, rinsed with tap water and polished.

The procedure of obtaining consistently satisfactory results using Fry's etchant is not well established at the present time. Some references in the literature[3] indicate that low-carbon steel with high nitrogen content etches successfully. In the present series of tests, a commercial grade of low-carbon steel (SAE 1018) was used.

A point to be remembered when using this technique is that machining stresses should be as small as possible when the specimens are prepared. The specimens used in this investigation were machined without the necessary precautions and were found to have excessive machining stresses which obscured the etched patterns of plastically yielded regions. Details of the results will be discussed later in this paper.

Brittle Coatings

The earliest application of the brittle-coating technique for detecting Lueders' lines was the flaking of the oxidized mill scale on hot-rolled mild steel. This technique was later improved by painting white wash on the specimen and observing the flaking of the white wash when the Lueders' lines propagate. More than a decade ago, Miklowitz[4] used a brittle coating of very low sensitivity to detect plastic strains of the order of 0.01 to 0.05 in./in. A preliminary investigation conducted by the authors showed that a coating of very low sensitivity was not very suitable for the detection of Lueders' lines. Subsequent investigations showed that brittle coatings can be more efficiently used provided the following conditions are met: (1) the strain sensitivity of the coating at the beginning of the test is approximately equal to the strain value at the yield point of the material; (2) the total duration of the loading procedure is not of such length as to decrease the sensitivity of the coating (by the creep of the coating) below the sensitivity necessary to detect Lueders' lines.†

The brittle coating used in the investigation was Stresscoat‡ with a strain sensitivity which is approximately equal to the yield-strain value of the material or about 0.0011 in./in. for hot-rolled mild-steel specimens. The specimens were coated with Stresscoat, ST1200, cured at 90° F for 12 hr and subsequently at room temperature for 12 hr. The specimens were then loaded by increments in a constant-deflection-type testing machine. The crack patterns which represent the Lueders' lines were developed by the Statiflux technique after each increment of load and photographed. This procedure was repeated until the major portion of the specimen yielded plastically.

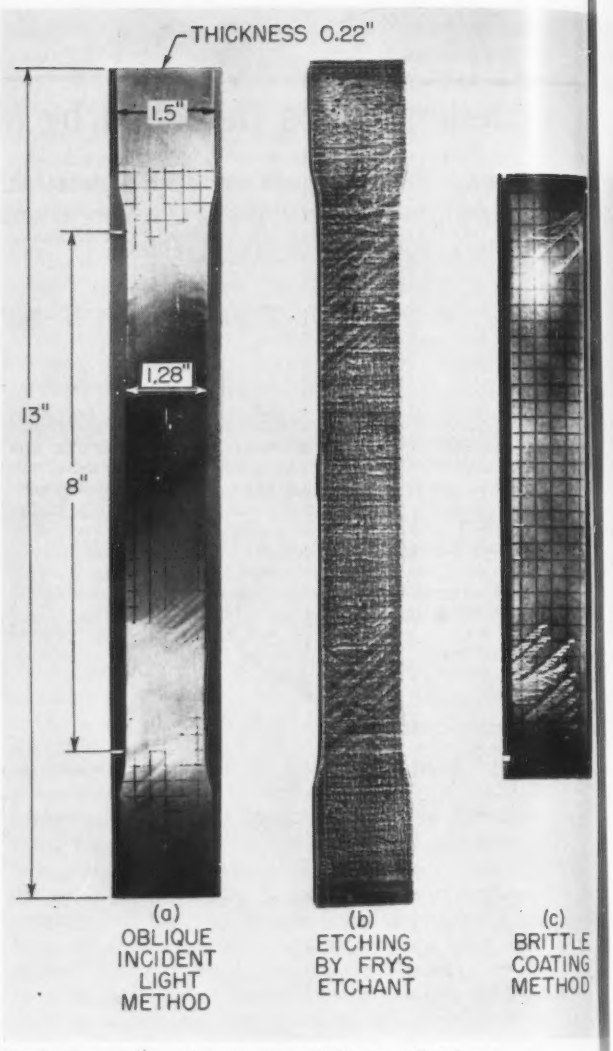

Fig. 1—Comparison of three methods for recording Lueders' lines. The tensile specimen is made of a hot-rolled mild steel. The brittle-coating crack pattern was developed by Statiflux penetrant

Photoelastic Coating

Photoelastic coatings for Lueders' line detection were used by Zandman[5] among others. The authors followed Zandman's method in this investigation

* *The composition of Fry's etchant used here was taken from Reference 3. It consists of 60 g of anhydrous cupric chloride, 120 cc of concentrated hydrochloric acid and 120 cc of tap water.*

† *Contrary to the conventional brittle-coating test procedure for an elastic analysis, the specimen cannot be unloaded after each load increment. The load level must be maintained between each load increment.*

‡ *A commercial product marketed by Magnaflux Corp., Chicago, Ill.*

and applied a liquid plastic§ to the specimen to be analyzed. The coating surface was then machined with a router in order to obtain a uniform thickness of coating of about 0.015 in. The reasons for using such thin coating are: (1) to establish with some precision the boundaries between the plastically yielded Lueders' lines, and (2) to obtain photoelastic fringe patterns of the Lueders' lines with fringe orders which are not so high that evaluation becomes difficult.

The coated specimen was loaded by increments in a constant-deflection-type testing machine and the photoelastic patterns due to Lueders' lines were observed with a diffused-light circular polariscope.

X-rays

Grains are the structural units of which metals are constituted. The grains are composed of atoms which are arranged in a well-ordered array or lattice. The grain boundaries are not always well defined but probably represent transitional zones between grains of different lattice orientation. The behavior of the individual grains, oriented in a multidirectioned manner, modified by the mutual interaction through the grain boundary, is responsible for the nonhomogeneous inelastic phenomenom which is detected on the macroscopic scale as Lueders' lines.

§ *Type A, Photostress, a commercial product marketed by the Budd Co., Instruments Division, Phoenixville, Pa.*

An X-ray upon penetrating the surface of a specimen encounters these ordered lattices in the form of planes-of-atoms which reflect the incident ray at an angle depending upon its relative orientation in the grain aggregate. If a photographic film is placed parallel to the surface of the specimen, the reflected rays impinge upon the film and form a concentric circular ring composed of fine spots.

For elastic deformation, the planes of atoms are merely moved parallel to one another within a grain and merely cause an increase or decrease in diameter of the observed circular rings. For plastic deformation, however, the atomic planes are warped and bent so that a blurring or distortion of the individual spots in the circular ring takes place.

The methods of X-ray analysis are not used to detect Lueders' lines as such but are rather a valuable tool for studying stress distributions in or near a Lueders' line.

Comparison of the Detection Methods

The test specimens used to compare four of the above-mentioned methods were tensile specimens with the dimensions shown in Fig. 1. The specimens were machined out of $^1/_4$-in. hot-rolled mild-steel plates and the two flat surfaces were finished by grinding to a thickness of 0.223 ± 0.015 in.

The yield stress of this material is about 35,000

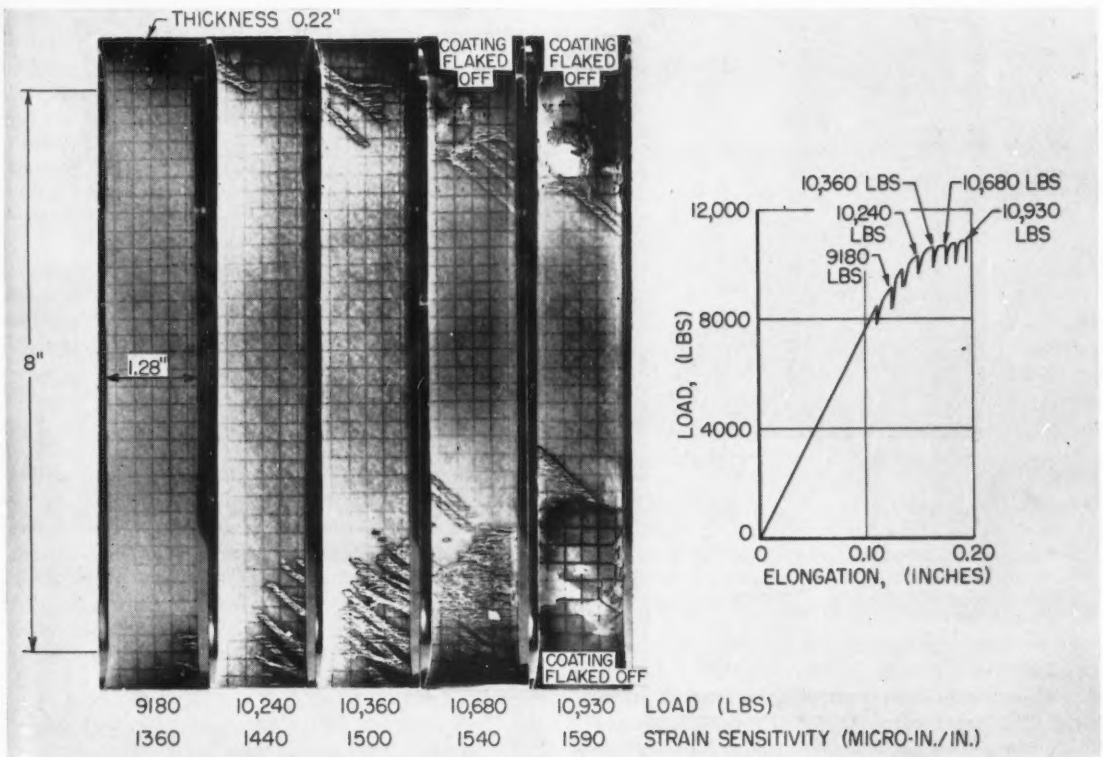

Fig. 2—Propagation of Lueders' lines with increasing loads on a hot-rolled mild-steel tensile specimen (brittle-coating pattern). The brittle-coating crack pattern was developed by using Statiflux penetrant. The five photographs were taken from a series of nine. The corresponding load and the strain sensitivity of the coating are marked under each photograph

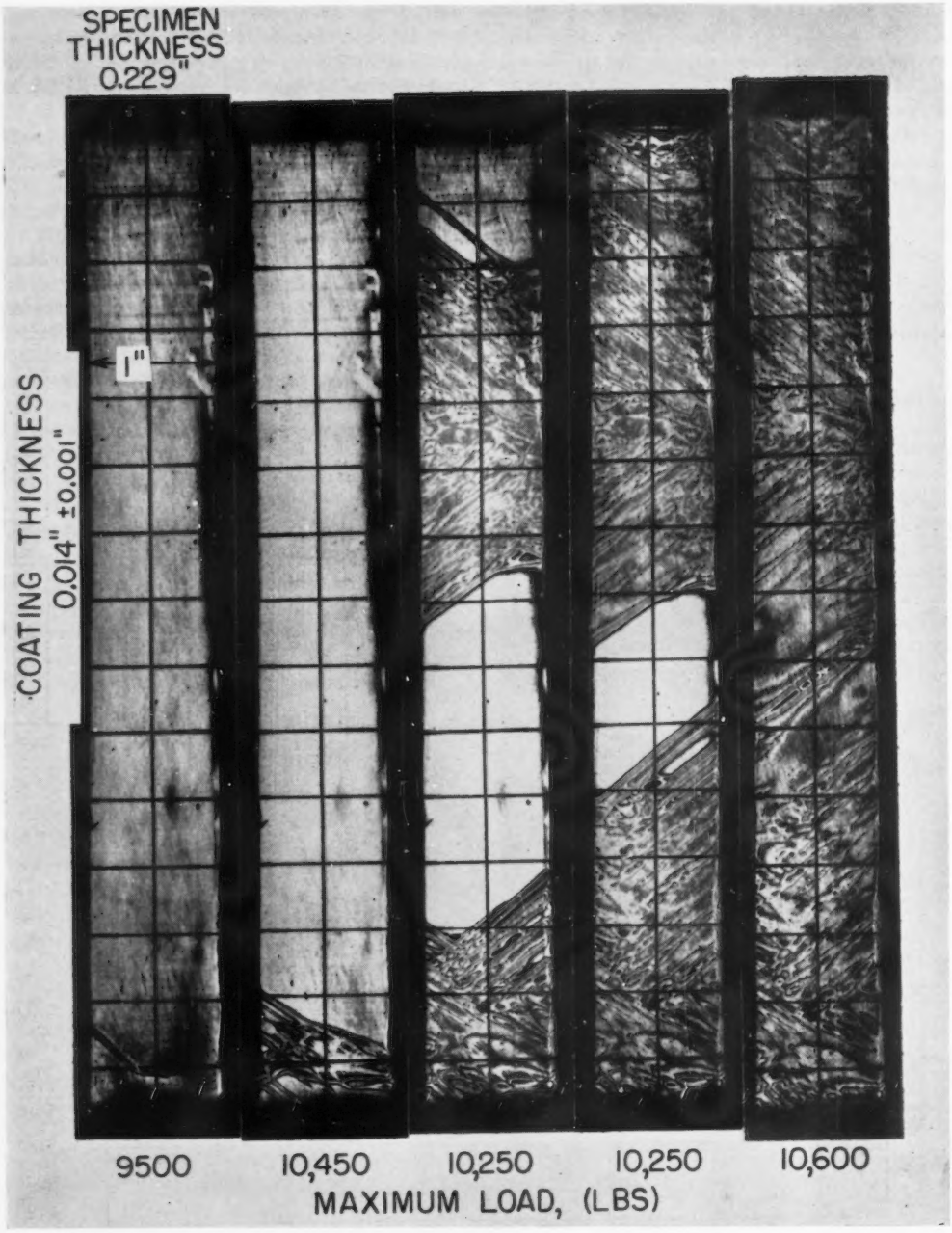

Fig. 3—Propagation of Lueders' lines with increasing loads on a hot-rolled mild-steel tensile specimen (photoelastic-coating pattern). The above photographs are dark-field isochromatic fringe patterns obtained at increasing load increments. One fringe order in this figure corresponds to a maximum shearing strain of 4400 microinch per inch

psi. The specimens were either sprayed with Stresscoat ST1200 and cured under the conditions previously mentioned or coated with liquid Photostress plastic. The tensile specimens were then loaded in increments and the propagation of Lueders' lines recorded. Upon completion of the test, the tensile specimens were unloaded, the coating removed and the lines recorded by using oblique-incident light. Subsequently, the tensile specimens were etched by Fry's etchant and the results recorded.

Figure 1 shows a comparison of the final results obtained by three methods.

Figure 1-a shows the Lueders' lines photographed by oblique-incident light. This method of recording requires great skill. It is hard to distinguish the Lueders' lines in some instances. (Figure 10 shows a better example of the application of this method.)

Figure 1-b shows the lines obtained by applying Fry's etchant to the tensile specimen. The visible horizontal lines in the specimen are parallel to the rolling direction of the material and are believed to be caused by the impurities along the grain boundaries. The thin vertical lines are due to the residual stresses caused by the machining in the preparation of the specimen. The Lueders' lines in this figure are fairly distinguishable since they are inclined with respect to the horizontal and vertical etched lines. If the Lueders' lines should happen to be codirectional with either the vertical or horizontal etched lines they would become hard to detect by this method.

Figure 1-c shows a photograph taken from a sequence of photographs of brittle-coating cracks recording the propagation of Lueders' lines with increasing load.

Figure 2 shows a series of brittle-coating crack patterns obtained by applying successive increments of load to the specimen, without unloading. The load-elongation curve for this experiment is shown on the right side of this figure. Because of the type of testing machine used, a small drop-off at each load increment is noticed in this load-elongation curve. The load and the corresponding strain sensitivity of the coating at each load increment are marked in this figure. This strain sensitivity was obtained by correcting the static strain sensitivity of the coating for creep according to the creep-correction chart published by the Magnaflux Co.[6]

By comparing the photographs and the load-elongation curve in Fig. 2, one can see that the yield point established by the conventional method of testing corresponds to the state when the Lueders' lines have completely propagated across the width of the tensile specimen.

Figure 3 illustrates the propagation of Lueders' lines as recorded by the photoelastic-coating technique. The photographs show dark field isochromatics.

This method shows thin bands of photoelastic fringe patterns running parallel to the Lueders' lines. In Fig. 3-a, a maximum fringe order of two can be counted in the specimen which indicates a maximum shearing strain of approximately 8800 microinch per inch.* The entire specimen in this figure has been strained such that the major portion of the specimen is shown light at the beginning of plastic yielding. The Lueders' lines as shown in Fig. 3-a first started from a small recess which was erroneously machined in the specimen. They then spread across the tensile specimen at the next load. With increasing load, the lines appeared at different locations, and then spread out into plastically yielded regions in the specimens. The method of detecting Lueders' lines by means of photoelastic coatings offers an opportunity of determining the maximum shear-strain distribution within the lines.

The suitability of any of the techniques described for detecting Lueders' lines depends on the objective to be obtained.

The oblique-incident light method has the advantage of being the simplest method but lacks positiveness in detection since much of it depends on the proper illumination of the specimen. The method can be supplemented by painting the Lueders' lines and photographing the painted pattern by normal illumination. This supplemental method had been used by many investigators.[7]

The etching method has the advantage of being applicable for Lueders' lines detection in the interior of the specimen after dissecting it. It is especially suitable for recording the lines after the specimen has been loaded up to its maximum load. Because of the corrosive and toxic nature of the reagents employed, this method is not recommended for recording the propagation of the lines with increasing load on a specimen in a testing machine. Another disadvantage is that, for the application just mentioned, the specimen surface must be repolished after recording the pattern at each load increment. Also, the machining of the specimen must be done with extreme care in order to eliminate the machining stresses which obscure the lines. It is also desirable for the specimen material to be of specially prepared high-nitrogen, low-carbon steel.

The brittle-coating method has the advantage of being simple and positive. The method cannot be used on specimens under dead loading since each load application will require a load duration of about fifteen minutes before a condition of equilibrium is reached between the load and displacement. Under several such prolonged load applications, the coating will creep and eventually lose its sensitivity.

The photoelastic-coating method has the advantage of providing a measure of the maximum shearing strains inside the Lueders' bands. This coating exhibits little creep so that the method can be used on specimens under dead loading.

From the above, it is apparent that brittle coatings and photoelastic coatings are two desirable means of detecting Lueders' lines in mild-steel specimens. In the following, the authors used the brittle-coating method in a series of investigations.

Applications of the Brittle-coating Method

Using the previously described brittle-coating method, a series of investigations were conducted on several simple specimens and the propagation of Lueders' lines were recorded. Some of these tests will be described below.

Beams Under Pure Bending

STRAIGHT BEAM—A mild-steel beam with a cross

* *This value was obtained by assuming that the strain-optical coefficient of the plastic is 0.09 as stated by the distributor.*

section as shown in Fig. 4 was subjected to increasing bending moments after being coated. The successive brittle-coating crack patterns were developed by means of the Statiflux technique (Figs. 4 and 5).

In this pure-bending test, the compression cracks appeared slightly after tension cracks. The compression cracks are parallel to the neutral axis of the beam while the tension cracks are irregular but with an average direction perpendicular to the neutral axis.

Observation of the crack pattern shows that on the tension side of the beam, generally a single crack propagates deep into the unyielded portion of the beam. With increase in load, a series of small cracks form along the first crack thus making a yield band. The stress distribution across the beam cross section (computed assuming that the material is ideally plastic) is drawn in Figs. 4 and 5. The tips of the Lueders' lines in the tensile region of the beam are at a distance from the axis which is approximately the same as the distance of the computed elastic-plastic boundary from the same axis. The complete yield bands are not represented by the brittle-coating cracks in the compression region.

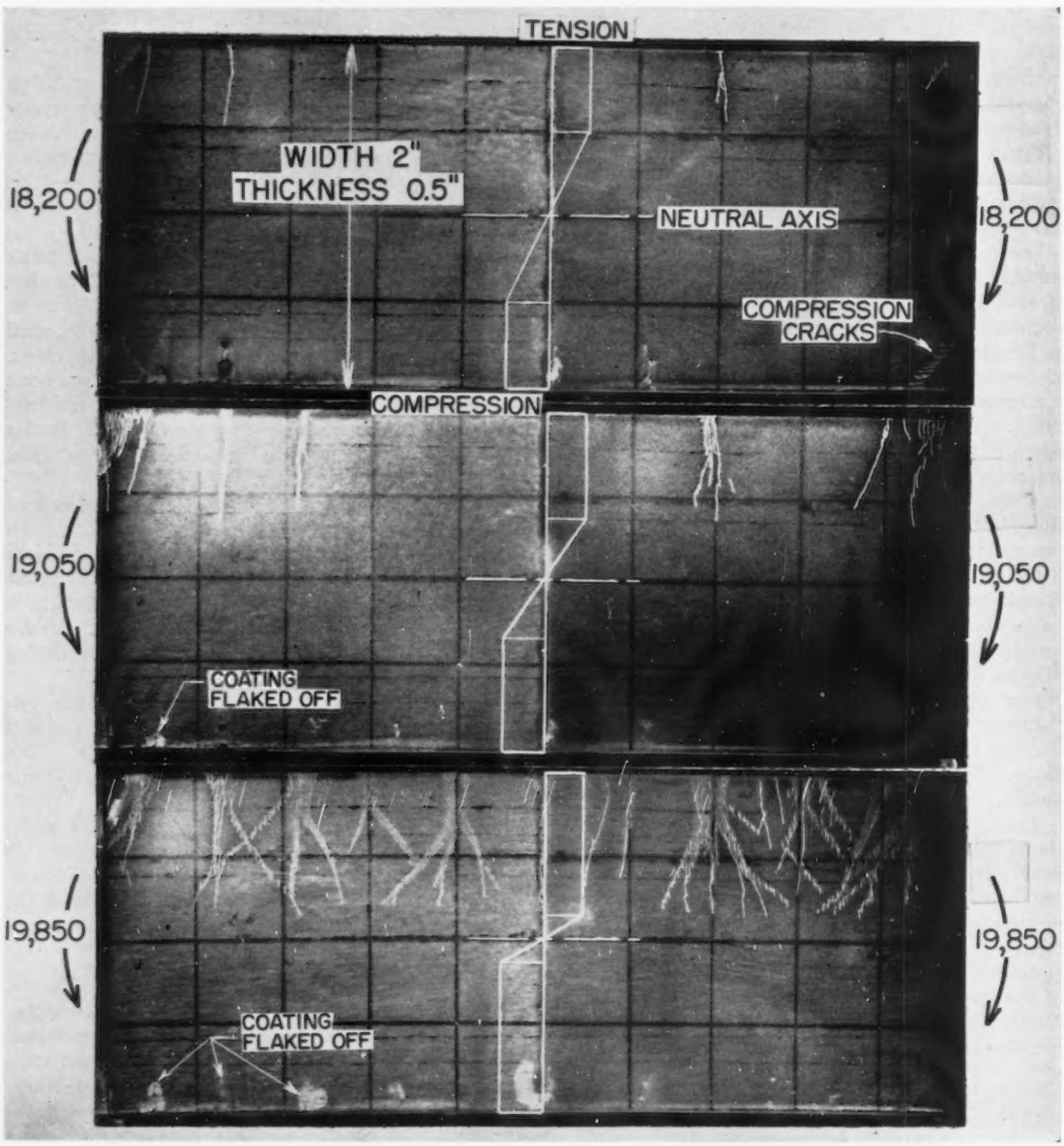

Fig. 4—Lueders' lines propagation with increasing pure-bending moment in a straight mild-steel beam. The Lueders' lines shown by the brittle-coating cracks appear discontinuously in the otherwise elastic region

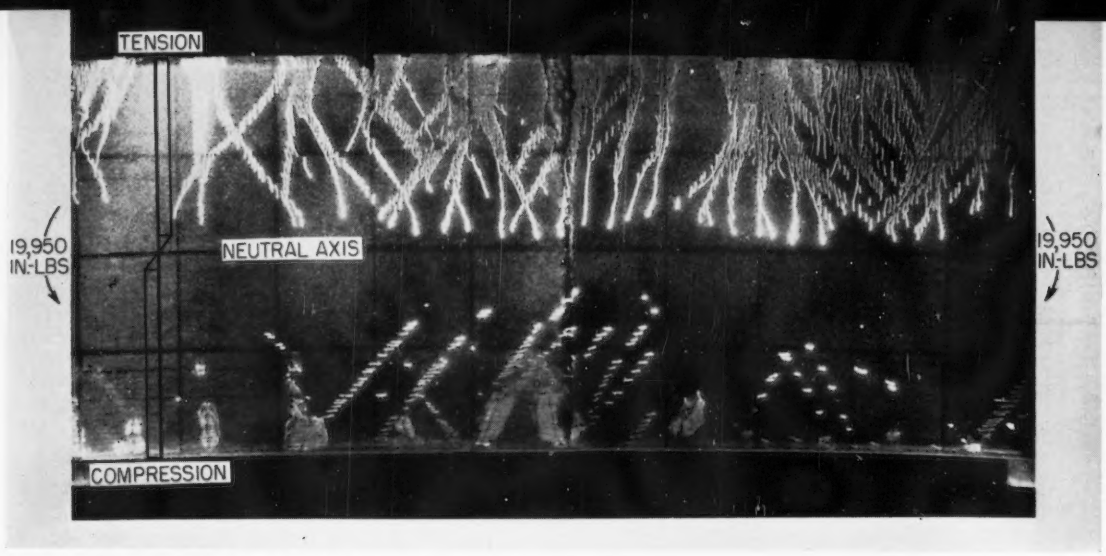

Fig. 5—Lueders' lines in a straight mild-steel beam under pure bending. The Lueders' lines are shown by brittle-coating cracks

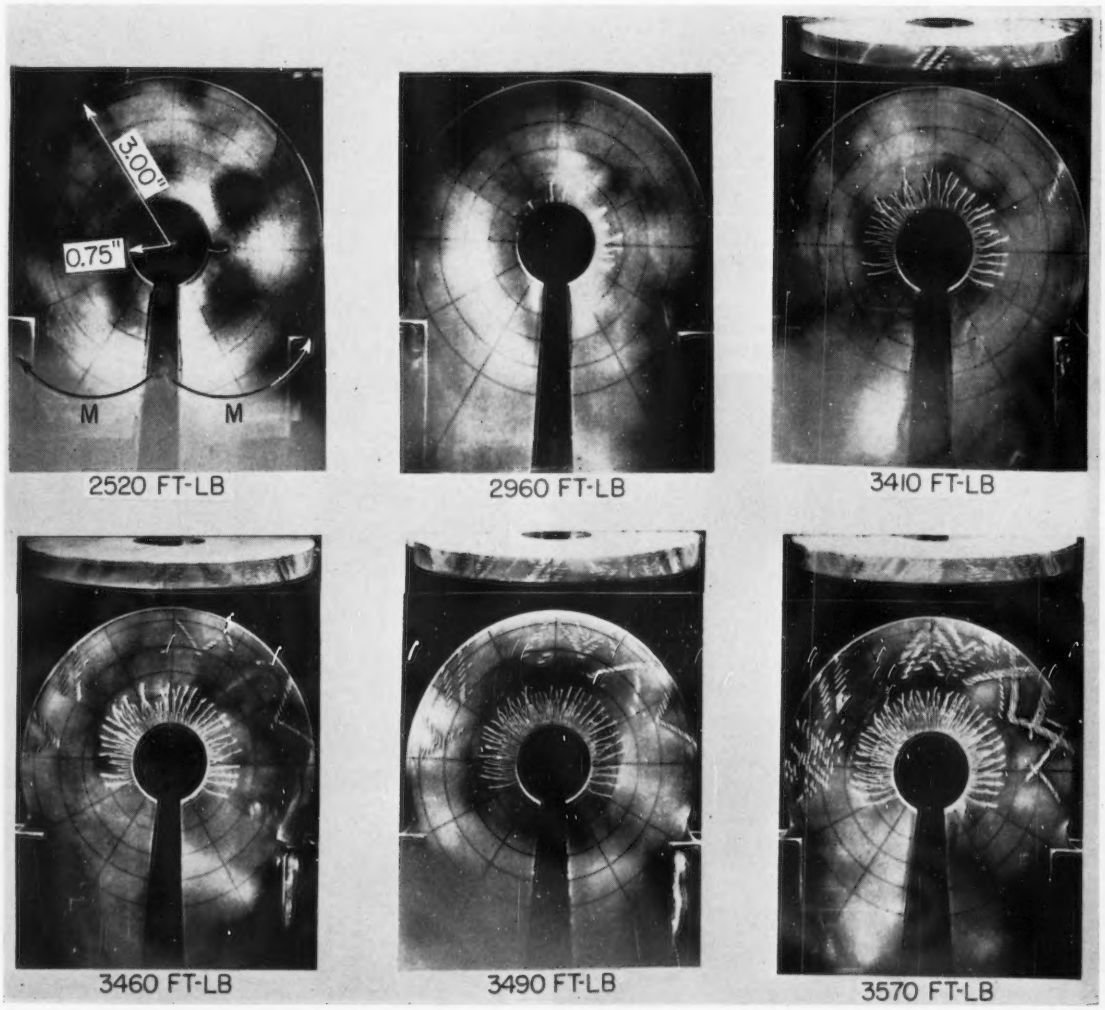

Fig. 6—Propagation of Lueders' lines in a mild-steel curved beam under pure bending (brittle-coating patterns)

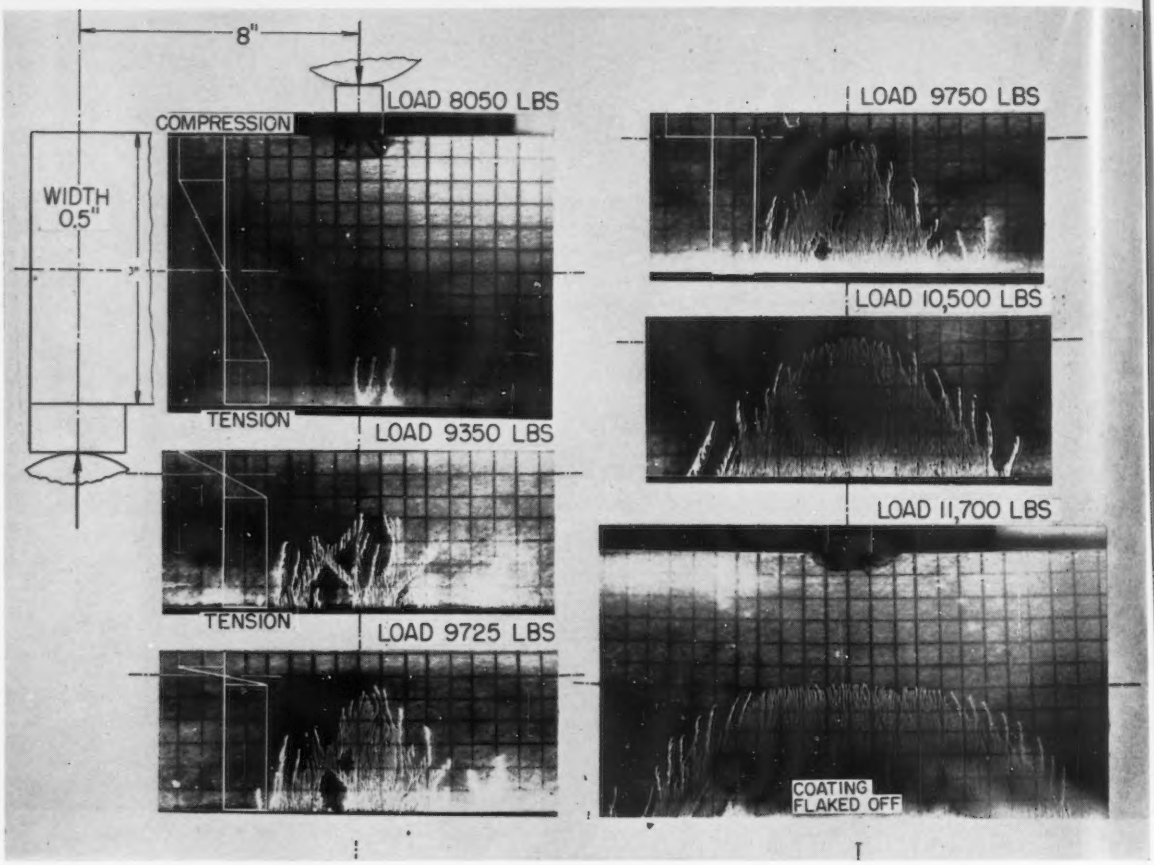

Fig. 7—Propagation of Lueders' lines with increasing load in a straight mild-steel beam under simple bending (brittle-coating patterns)

Fig. 8—Three views in detail of Lueders' lines in a straight mild-steel beam under simple bending (load 8050 lb in Fig. 7)

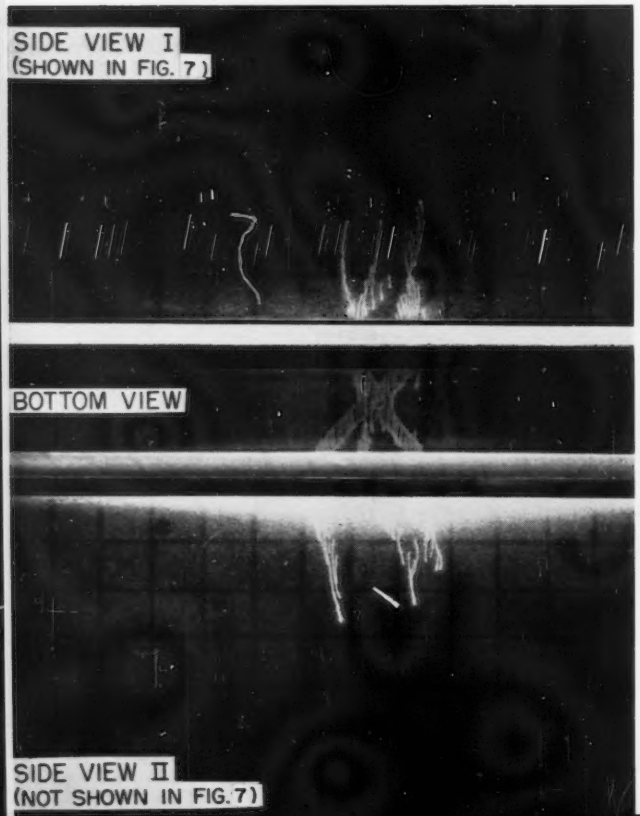

Fig. 9—Three views in detail of Lueders' lines in a straight mild-steel beam under simple bending (load 9350 lb in Fig. 7)

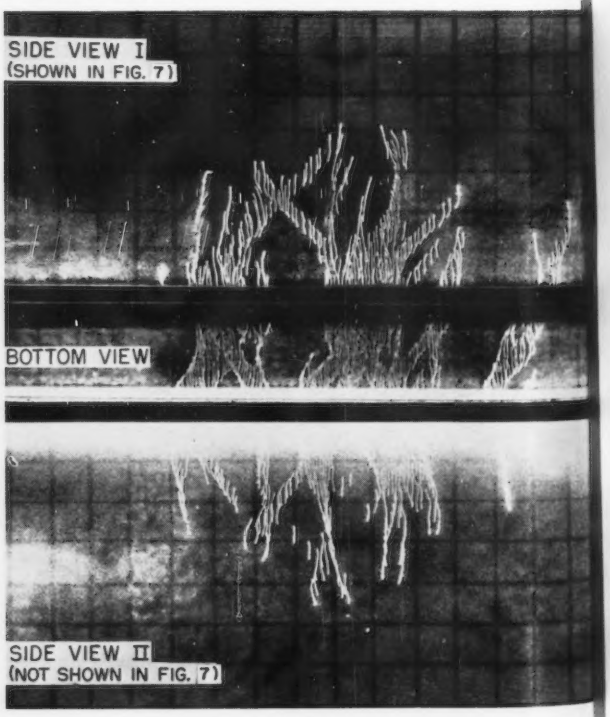

CURVED BEAM—A curved beam was machined from a mild steel similar to that used in the straight-beam experiments, and coated in a similar manner. Figure 6 shows the development of the Lueders' lines with increasing bending moment.

Yielding patterns in the region of circumferential compressive stresses consist of short cracks oriented in the circumferential direction with over-all appearance of curved bands which intersect radial lines at a 45 deg angle. In the region of circumferential tensile stresses, the yielding pattern consists of short cracks which follow approximately the radial direction, with over-all appearance of curved bands which intersect the radial lines often at approximately a 30 deg angle.

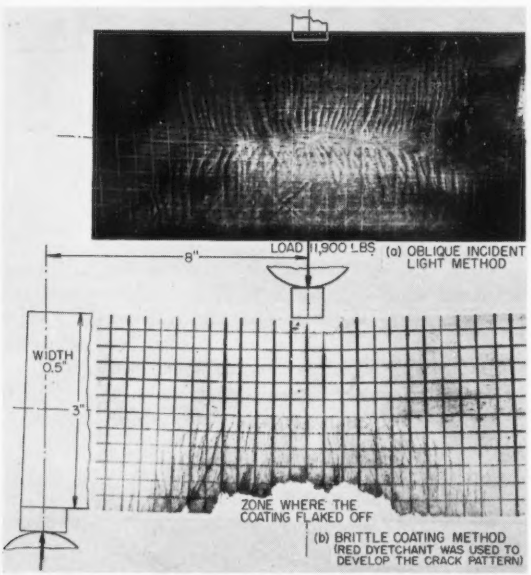
8"
LOAD 1,900 LBS
(a) OBLIQUE INCIDENT LIGHT METHOD
WIDTH 0.5"
3"
ZONE WHERE THE COATING FLAKED OFF
(b) BRITTLE COATING METHOD (RED DYETCHANT WAS USED TO DEVELOP THE CRACK PATTERN)

Fig. 10—Comparison of two methods for recording Lueders' lines. (Mild-steel straight beam under simple bending)

Lueders' lines in the tensile regions appeared before those in the compressive regions in both the straight beam and in the curved beam. This phenomenon is not entirely unexpected. Other authors have noted the same occurrence.[8] The cracks inside the Lueders' band have a direction parallel to the compression, and are probably produced by the difference in Poisson's ratio between the steel (0.5) and the coating (0.42).

Beam Under Simple Bending

Figures 7 to 9 show the development of Lueders' lines in a mild-steel beam under simple bending. The dimensions of the beam and its loading mechanism are shown in Fig. 7. No coating cracks appeared on the compression side of the beam under simple bending. Figures 8 and 9 show two views of the initial stages of loading of the beam. The Lueders' lines generally appear as very narrow bands which consist of short curved cracks adjacent to each other.

Figure 10 shows a comparison of Lueders' lines obtained by the oblique-incident light method and the brittle-coating method. The brittle-coating crack pattern was developed by the use of Red Dyetechant† in this photograph. Once the coating is treated by this etchant it cannot be reused. Therefore, this method cannot be used to develop patterns in the same coating on a specimen under increasing load.

Figure 11 shows the elastic brittle-coating crack pattern and is included here to show the difference between the elastic and plastic pattern in a mild-steel beam under simple bending.

90-deg Doubly Notched Plate Under Tension

Figure 12 shows the propagation of the Lueders' lines in a 90-deg doubly notched plate under tension. The yielding patterns which form at the two notches grow toward each other with increasing load without

† *A product by Magnaflux Corp., Chicago, Ill.*

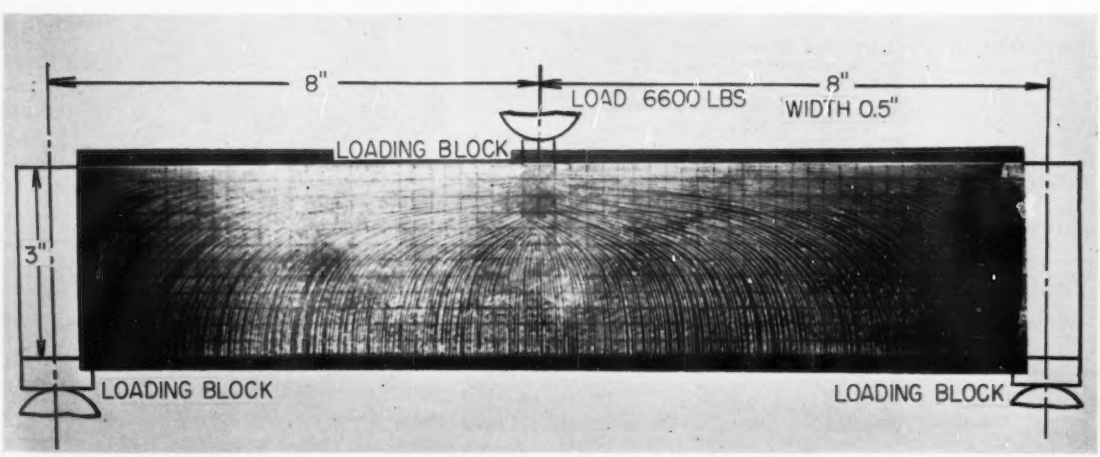

Fig. 11—Elastic pattern obtained by means of brittle coating. Mild-steel straight beam under simple bending. Statiflux penetrant was used to develop crack pattern

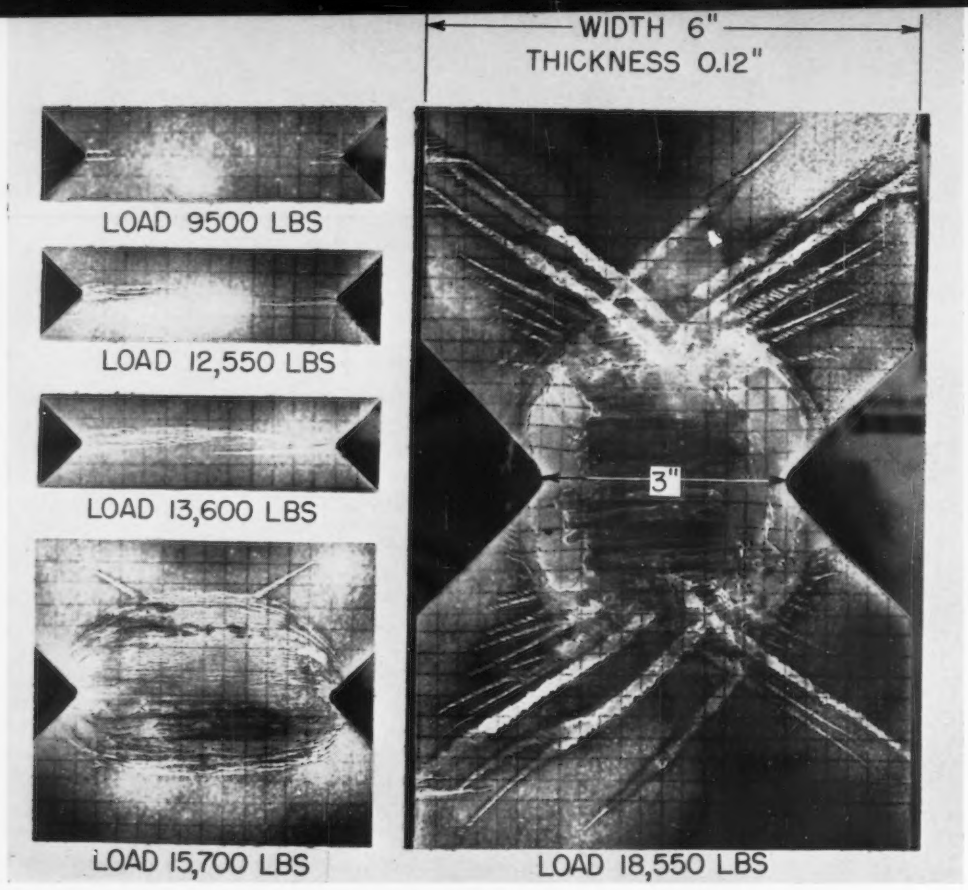

Fig. 12—Propagation of Lueders' lines with increasing load in a 90-deg doubly-notched mild-steel piate under tension

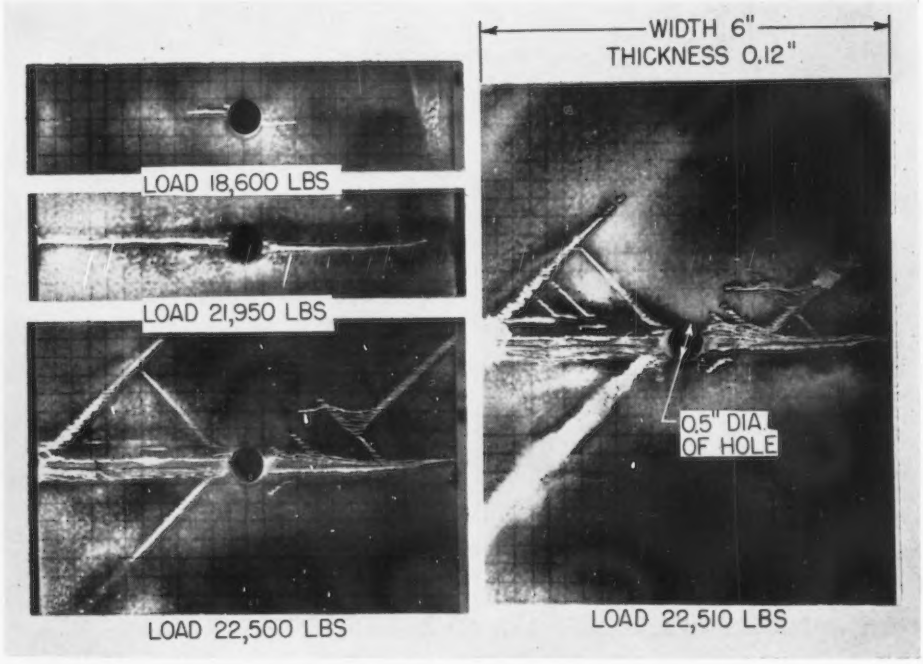

Fig. 13—Propagation of Lueders' lines with increasing load in a mild-steel plate with a $^1/_2$-in. diam hole

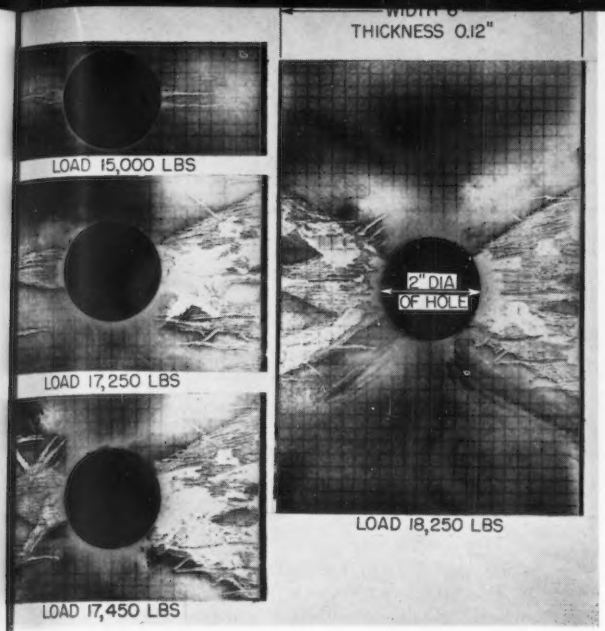

Fig. 14—Propagation of Lueders' lines with increasing load in a mild-steel plate with a 2-in. diam hole

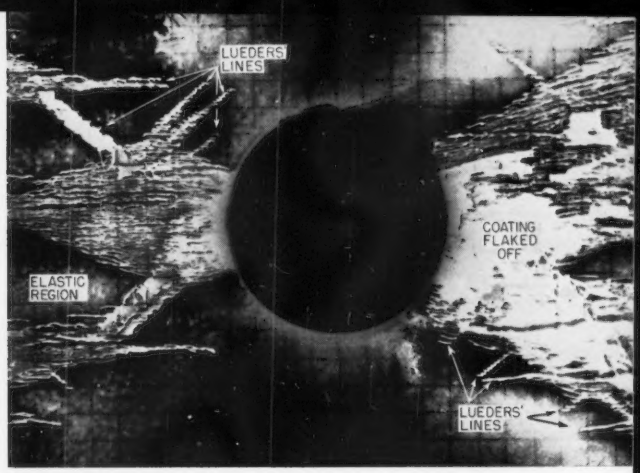

Fig. 15—Enlarged picture of the brittle-coating pattern (load of 17,450 lb in Fig. 14)

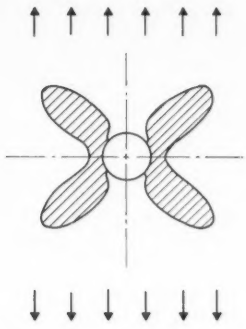

Fig. 16—Spreading of plastic region from hole in a tension member (plane stress). Hatched portion indicates fully plastically yielded region. (From A. Nadai, Theory of Flow and Fracture of Solids, McGraw-Hill, New York, 1950, p. 291)

spreading out appreciably. Eventually, a narrow plastically yielded band is formed across the waist of the plate. This band was judged to be caused by plastic strains because the strain sensitivity of the brittle coating used (somewhat higher than 1100μ-in./in) was greater than the strain at the yield point of the base material (1000μ-in./in.). With increase in load, this plastically yielded region continues to enlarge until suddenly the familiar Lueders' lines begin to reappear and grow in two directions, approximately 60 deg away from the vertical axis. This behavior contradicts some conclusions derived using "ideally plastic" assumptions, such as Southwell's[9] statement that the plastic region does not take a short cut across the waist.

Plate with a Hole Under Simple Tension

Figures 13 to 15 show the growth of the yielding pattern, detected using brittle coating, in plates with different hole diameters under simple tension.

Figure 15 shows an enlarged view of the plate with 2-in. diam hole under a maximum load of 17,450 lb. Here again, the plastic region stretched across the plate in a direction normal to the axis of the load, and starting from the hole boundary. The Lueders' lines appeared later in two directions at an angle of about 45 deg with the axis. It can also be noted that small isolated elastic regions exist within the plastic regions at the intermediate stages of plastic yielding.

Figure 16 shows the spreading of the plastic region from a hole in a tension member as described by Nadai.* Nadai concludes that the yielding tends to progress along two narrow bands, symmetrically situated with respect to the axis of tension and at an angle of about 45 deg with the direction of tension.

Comparison between the pattern of the growth of plastic regions obtained in Figs. 13 to 15 and in Fig. 16 shows some differences with these predictions. In the brittle-coating test, the plastic region propagated from the hole boundary across the width of the specimen first and later began to spread out following the pattern mentioned by Nadai.

* *Nadai, A., "Theory of Flow and Fracture of Solids," McGraw-Hill, New York, 1950, pp. 289–295.*

Acknowledgment

The research work reported in this paper was sponsored by the Office of Ordnance Research.

Bibliography

1. See, for example, Nadai, A., Theory of Flow and Fracture of Solids, Vol. 1, McGraw-Hill Book Co., New York, pp. 275–296 (1950).

2. MacGregor, C. W., "The Plastic Flow of Metals," Am. Inst. Mining and Metallurgy Engrs., Trans., 133, 302–320 (1939).

3. Steele, M. C., "Interferometry and Etching Studies of Non-Homogeneous Yielding," T.&A.M. Rept. No. 98, Department of Theoretical and Applied Mechanics, University of Illinois, June 1956.

4. Miklowitz, J., "Initiation and Propagation of the Plastic Zone in a Tension Bar of Mild Steel as Influenced by the Speed of Stretching and Rigidity of Testing Machine," Jnl. Appl. Mech., 14, No. 1, 31–38 (March 1947).

5. Zandman, M. F., "Analyse des constraintes par vernis photoelastiques," Analyse des Constraintes, 2, No. 6, 3–14 (1956).

6. Principles of Stresscoat, Magnaflux Corp., 1955, p. 69.

7. Clark, M. E., Corten, H. T., and Sidebottom, O. M., Inelastic Behavior of Ductile Members Under Dead Loading, Engineering Experiment Station Bull. No. 426, University of Illinois, Vol. 52, No. 16, October 1954.

8. Boklen, R., "Some Observations on Steels in Pure Static Bending," Z. Metallkunde, 42, No. 6, 170–174 (June 1951).

9. Allen, D. N., and Southwell, R., "Relaxation Methods Applied to Engineering Problems, XIV Plastic Straining in Two-Dimensional Stress-Systems," Philosophical Trans. Royal Soc. London, 242, A, 379–414 (June 1950).

Beam Subjected to Eccentric Longitudinal Impact

Theoretical analysis of the response of a free-free beam subjected to a dynamically applied end moment is undertaken to correlate analytical theories with the results of experimental investigation

by Shan S. Kuo

ABSTRACT—This paper is concerned with an experimental investigation of the bending stresses in a bar subjected to eccentric longitudinal impact. The test beam was a round steel bar, 1 in. in diam and 8 ft long which was suspended by wires at two points. Strains were measured by SR-4 strain gages at 18 stations along the bar. The signals were fed through an amplifier to an oscilloscope and the trace on the screen was photographed for a permanent record. The impact was obtained by means of a striking bar with a conical end. The striking bar was suspended in a pendulum rig and striking height adjusted so as to impact the test bar at any desired eccentricity. The dimensionless impact duration t/T_1 is about 0.02, where T_1 denotes the fundamental period of the beam.

A theoretical analysis of the response of a free-free beam subjected to a dynamically applied end moment is undertaken to correlate analytical theories with the experimental results. The theoretical results based on the Timoshenko theory were found numerically, using the method of characteristics. Good agreement is found for the moment response curves at ten representative beam stations. Comparison is also made with related results from the Bernoulli-Euler theory, using the normal-mode method. The numerical calculations were carried out on both IBM 704 and IBM 650 digital computers.

List of Symbols

The following symbols are used in the paper:

E = modulus of elasticity.
G = modulus of elasticity in shear.
I = cross-sectional moment of inertia.
K = shear-deflection coefficient.
L = length of beam.
M = moment.
M_0 = moment input.
$\overline{M}$ = M/M_0.
Q = dimensionless vertical shear = vertical shear/(EI/L^2).
T_1 = fundamental period of beam.
V = dimensionless velocity of beam deflection/$(G/\rho)^{1/2}$.
c = $(E/\rho)^{1/2}$.
h = mesh size.
r = cross-section radius of gyration.
t = time.
x = axial distance.
β_n = $\omega_n^{1/2}/(EI/\rho)^{1/4}$.
ξ = dimensionless coordinate along beam = x/L.
η = $2/[1 + (KG/E)^{1/2}]$.
ρ = density of beam material.
τ = dimensionless time = ct/L.
τ_0 = dimensionless rise-time of a moment input in the form of a ramp-platform.
$\phi_n(x)$ = eigenfunction, see Reference 4.
$\phi_n'(x)$ = $(1/\beta_n)(d\phi_n(x)/dx)$.
$\phi_n''(x)$ = $(1/\beta_n^2)(d^2\phi_n(x)/dx)$.
ω_n = natural circular frequency of the n-th mode of vibration of a beam.
Ω = dimensionless velocity of rotation = velocity of rotation/(c/L).
$\mathfrak{M}$ = dimensionless bending moment = $(ML)/(EI)$.
$\mathfrak{M}^*$ = dimensionless moment input = moment input/(EI/L).

Shan S. Kuo is Assistant Professor of Civil Engineering, Yale University, New Haven, Conn.

Paper was presented at 1960 SESA Spring Meeting held in Indianapolis on May 18–20.

Introduction

The work reported in this paper is concerned with three related investigations of the propagation of stress waves in an elastic uniform beam. The first is an experimental investigation of the bending stresses in a bar subjected to eccentric longitudinal impact. The second is a theoretical analysis of the response of a free-free beam subjected to a dynamically applied end moment; this was undertaken to correlate analytical theory based on the Timoshenko beam equations with the experimental results of the first investigation. The third investigation is an analytical solution based on the Bernoulli-Euler equation; this was undertaken to check the extent of agreement for the response curves resulting from the two different theories.

For the eccentric longitudinal impact, few experimental data occur in the literature. Davidson and Meier[1] carried out some off-center impact experiments, but their chief interest was the measurement of the energy consumed in the lateral vibration. A rather recent investigation concerning the measurements of bending wave pulses generated from an eccentric impact was reported by Ripperger and Abramson.[2] The impact duration was about 2 microseconds long. While the study of these very short bending pulses is extremely valuable, information concerning the response to a relatively long pulse appears to be lacking. It was to obtain such information that the experimental work reported in this paper was originally initiated. The impact

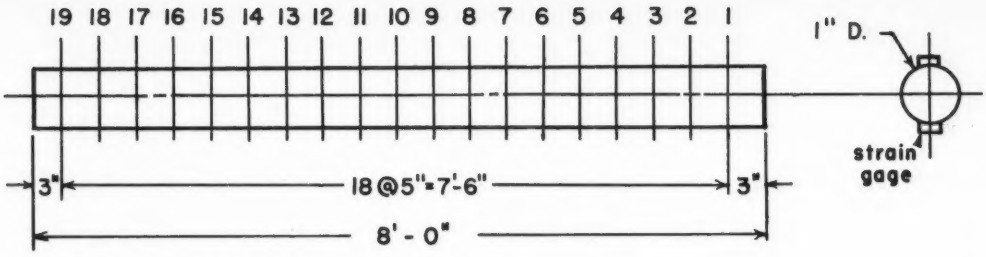

Fig. 1—Struck-bar detail and locations of strain gages

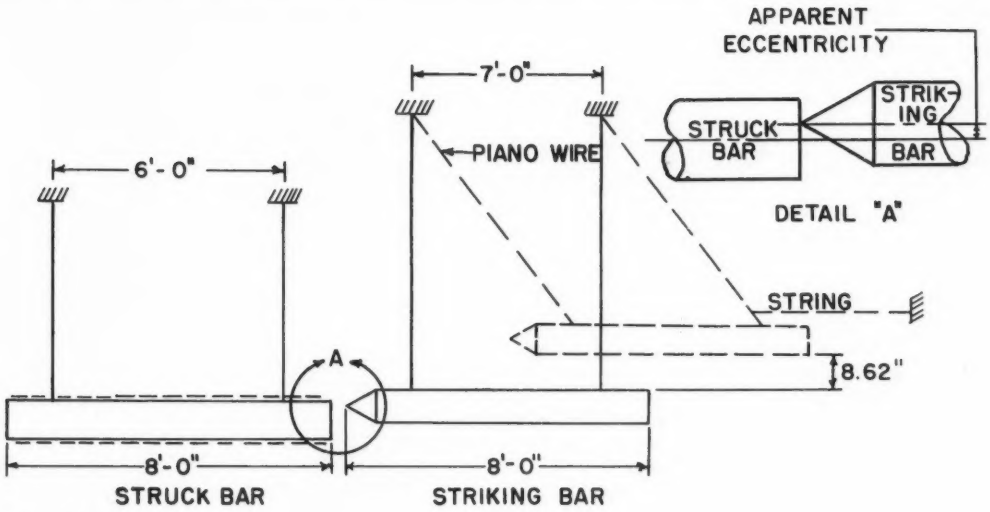

Fig. 2—Bar-suspension detail

duration considered in this paper is about 0.02 in the dimensionless quantity t/T_1 and it is equivalent to 950 microseconds in absolute time.

The theoretical analysis of a free-free beam based on the method of characteristics is described in a previous paper.[3] This is a numerical procedure based on the Timoshenko beam theory. It was programmed for the IBM Type 650 computer and various numerical solutions were carried out and compared with experimental records.

The second theoretical treatment of a free-free beam is based on the Bernoulli-Euler beam theory which neglects the effect of rotatory inertia and shear deformation. This was solved by the normal mode method and use is made of the eigenfunctions which represent the normal mode of vibration of a uniform beam. These functions have been computed up to the fifth mode by Young and Felgar.[4] Recently the tables have been extended to and including the twenty-seventh mode by Kuo.[5]

Experimental Study

Two low-carbon steel bars, 96 in. long by 1 in. in diam each, were used (L/r = 384). One was used as a striking bar, the other as the struck bar. Thirty-eight strain gages were cemented in pairs diametrically opposite each other at nineteen stations along the struck bar (Fig. 1). The gages are SR-4, Type A-5. The impact was obtained by means of a striking bar with a contacting end machined to a $2^1/_2$ deg cone. The striking bar was suspended in a pendulum rig and the striking height adjusted so as to impact the test bar at any desired eccentricity (Fig. 2).

The striking bar is pulled back a given distance and released. At the time of impact, the difference in elevation (or the true eccentricity) would not be the same as the difference in elevations of the two bars in their rest positions (or the apparent eccentricity). The magnitude by which the true eccentricity differs from the apparent eccentricity depends mainly on the amount of stretch of the piano wires during the swing. However, for a given pull-back distance, the apparent eccentricity differs from the true eccentricity by a constant which was determined experimentally at 0.051 in. for our tests. The apparent eccentricity was chosen as 0.305 in. for all tests. Hence, the true eccentricity was equivalent to 0.254 in.

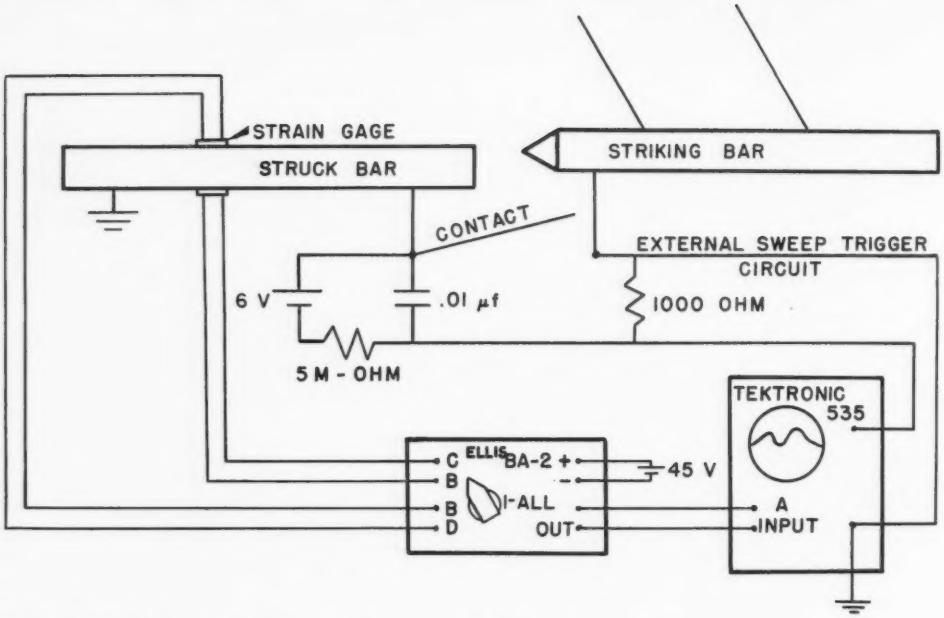

Fig. 3—Circuit arrangement of apparatus for recording bending stress alone

In all tests, the longitudinal wave was eliminated by a proper arrangement in the circuit shown in Fig. 3. When the bars touched, the resulting signal in the strain gages was first amplified, then displayed on oscilloscope screens and photographed for a permanent record.

For the purpose of checking, a minimum of three impact runs were made at each station for three different time-scale settings, namely, one horizontal division = 200, 500 and 1000 microseconds. Thus, three pictures were required at each station. For completeness, the results of all three sets of tests are presented in the form of photographs of the traces shown in Figs. 4 through 6. The ordinate of each record represents the dynamic outer-fiber strain; each vertical division is equivalent to 200 microinches per inch except for the records pertinent to the Station 16 where each vertical division is equivalent to 400 microinches per inch. The abscissa of each record represents the time; each horizontal division is equivalent to a specified time-scale setting which is shown in the last record of each array of pictures. An inspection of these traces indicates that the corresponding strain time curves at any beam station resulting from three impact runs agree very well and that the eccentric impact appears to be reproducible.

Theoretical Study

The response of a free-free beam subjected to a suddenly applied end moment is undertaken to correlate the analyses with the experimental results.

For purposes of comparison both Timoshenko and Bernoulli-Euler beam theories are used. The pertinent equations based on these two theories are summarized here.

Method of Characteristics Applied to Timoshenko Beam Equations

The Timoshenko theory for beam vibration can be represented in the nondimensional form by the following set of four equations:

$$\frac{\partial \mathfrak{M}}{\partial \tau} - \frac{\partial \Omega}{\partial \xi} = 0$$

$$\frac{\partial \mathfrak{M}}{\partial \xi} - \frac{\partial \Omega}{\partial \tau} - Q = 0$$

$$\frac{\partial Q}{\partial \tau} + \frac{L^2}{r^2}\frac{KG}{E}\left(\sqrt{\frac{KG}{E}}\frac{\partial V}{\partial \xi} - \Omega\right) = 0$$

$$\frac{\partial Q}{\partial \xi} + \frac{L^2}{r^2}\frac{KG}{E}\frac{\partial V}{\partial \tau} = 0 \qquad (1)$$

Making use of the method of characteristics[6, 7] eq. (1) can be transformed into eight ordinary differential equations, four giving the characteristic direction (or the principal equations) and four connecting the changes in $\mathfrak{M}$, Ω, V, Q along the corresponding characteristics (or the auxiliary equations). These equations are grouped as follows:

Principal Equations	*Auxiliary Equations*
$\frac{d\xi}{d\tau} = 1$	$d\mathfrak{M} - d\Omega - Q d\tau = 0$
$\frac{d\xi}{d\tau} = -1$	$d\mathfrak{M} + d\Omega + Q d\tau = 0$
$\frac{d\xi}{d\tau} = \sqrt{\frac{KG}{E}}$	$dQ + \frac{L^2}{r^2}\frac{KG}{E}(dV - d\tau \cdot \Omega) = 0$
$\frac{d\xi}{d\tau} = -\sqrt{\frac{KG}{E}}$	$dQ - \frac{L^2}{r^2}\frac{KG}{E}(dV + d\tau \cdot \Omega) = 0$

(2)

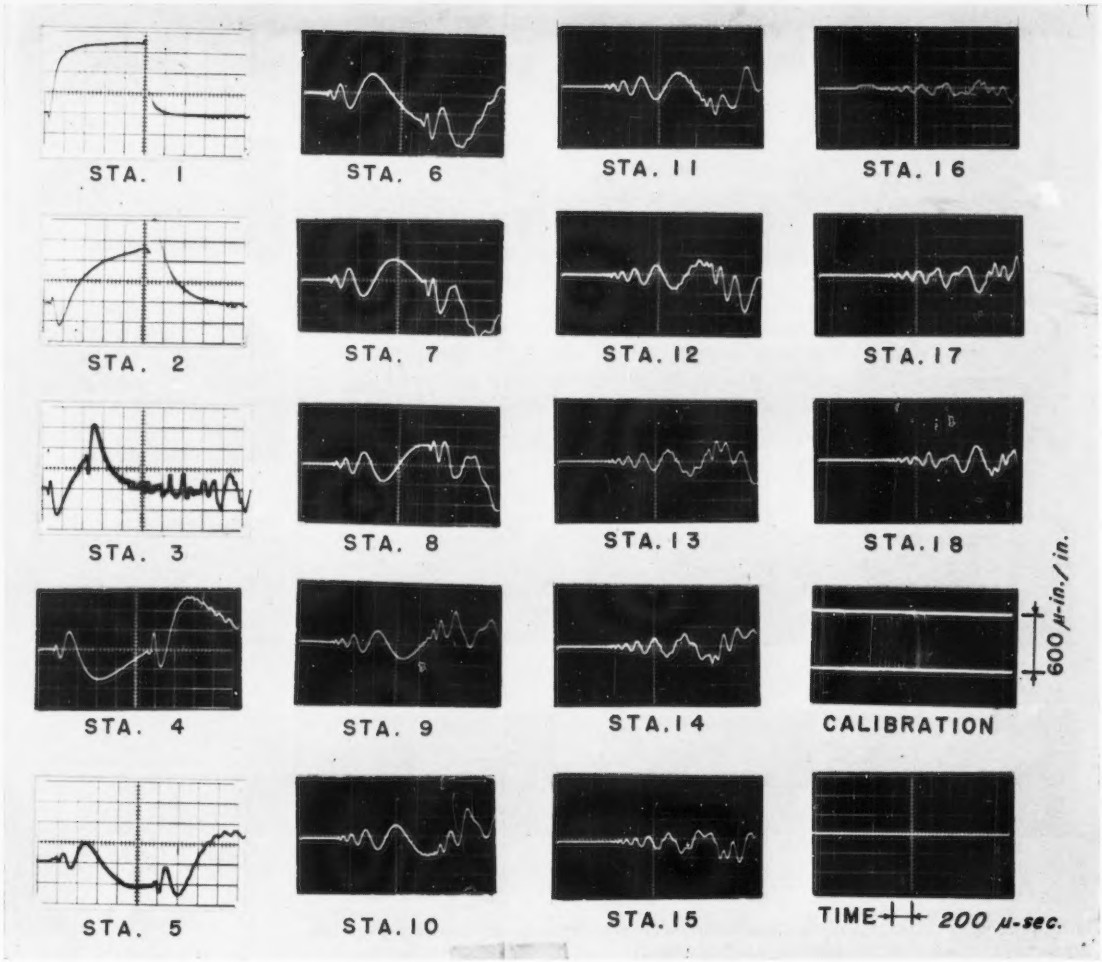

Fig. 4—Photographic records of oscilloscope traces representing outer fiber strain vs. time. (Time scale: one horizontal division = 200 microsec)

In the network shown in Fig. 7, the unknown values Q_N, Ω_N, V_N, and $\mathfrak{M}_N$ at the point N depend on the previously calculated values at the points E, W, S. It can be shown that the step-by-step integration formulas are as follows:[8]

$$\begin{vmatrix} \Omega_N \\ Q_N \end{vmatrix} = \frac{1}{1 + \eta \frac{L^2}{r^2}\frac{KG}{E}\frac{h^2}{4}} \left\{ \begin{bmatrix} 1 & -\frac{h}{2} \\ \frac{L^2}{r^2}\frac{KG}{E}\frac{\eta h}{2} & 1 \end{bmatrix} \begin{vmatrix} \Omega_E + \Omega_W \\ Q_E + Q_W \end{vmatrix} + \begin{bmatrix} \frac{L^2}{r^2}\frac{KG}{E}\frac{\eta h^2}{4} - 1 & h \\ -\frac{L^2}{r^2}\frac{KG}{E}\eta h & \frac{L^2}{r^2}\frac{KG}{E}\frac{\eta h^2}{4} - 1 \end{bmatrix} \begin{vmatrix} \Omega_S \\ Q_S \end{vmatrix} \right\} \quad (3)$$

$$\mathfrak{M}_N = \mathfrak{M}_S + \Omega_E - \Omega_W \quad (4)$$

Equations (3) and (4) are not self-starting. By using the boundary conditions at one end of a free-free beam subjected to a suddenly applied moment $\mathfrak{M}^*$ beginning at $\tau = 0$, it can be shown that the self-starting relation for any half mesh at this end is

$$\Omega_N = 2\Omega_E - \Omega_S + \mathfrak{M}_S^* - \mathfrak{M}_N^* \quad (5)$$

At the other end of a free-free beam, the values of $\mathfrak{M}$ and Q are zero. The relation for any half mesh at this end is

$$\Omega_N = 2\Omega_W - \Omega_S \quad (6)$$

Modal-superposition Method Applied to Bernoulli-Euler Beam Equation

The Bernoulli-Euler equation for vibration of a uniform beam which neglects the effects of rotatory inertia and shear deformation is

$$EI \frac{\partial^4 y}{\partial x^4} + \mu \frac{\partial^2 y}{\partial t^2} = 0 \quad (7)$$

The boundary conditions corresponding to a step moment applied at one end of the free-free beam are

$$\begin{aligned} M(O, t) &= 0 \qquad \text{for } t \leq 0 \\ M(O, t) &= M_0 \qquad \text{for } t > 0 \end{aligned} \quad (8)$$

The application of the Lagrangian method in forced vibration problems is discussed in most books on the subject of vibration, for example, see Reference 9. It is necessary in this method to express the kinetic and potential energies of the vibrating beam as functions of the generalized coordinates.

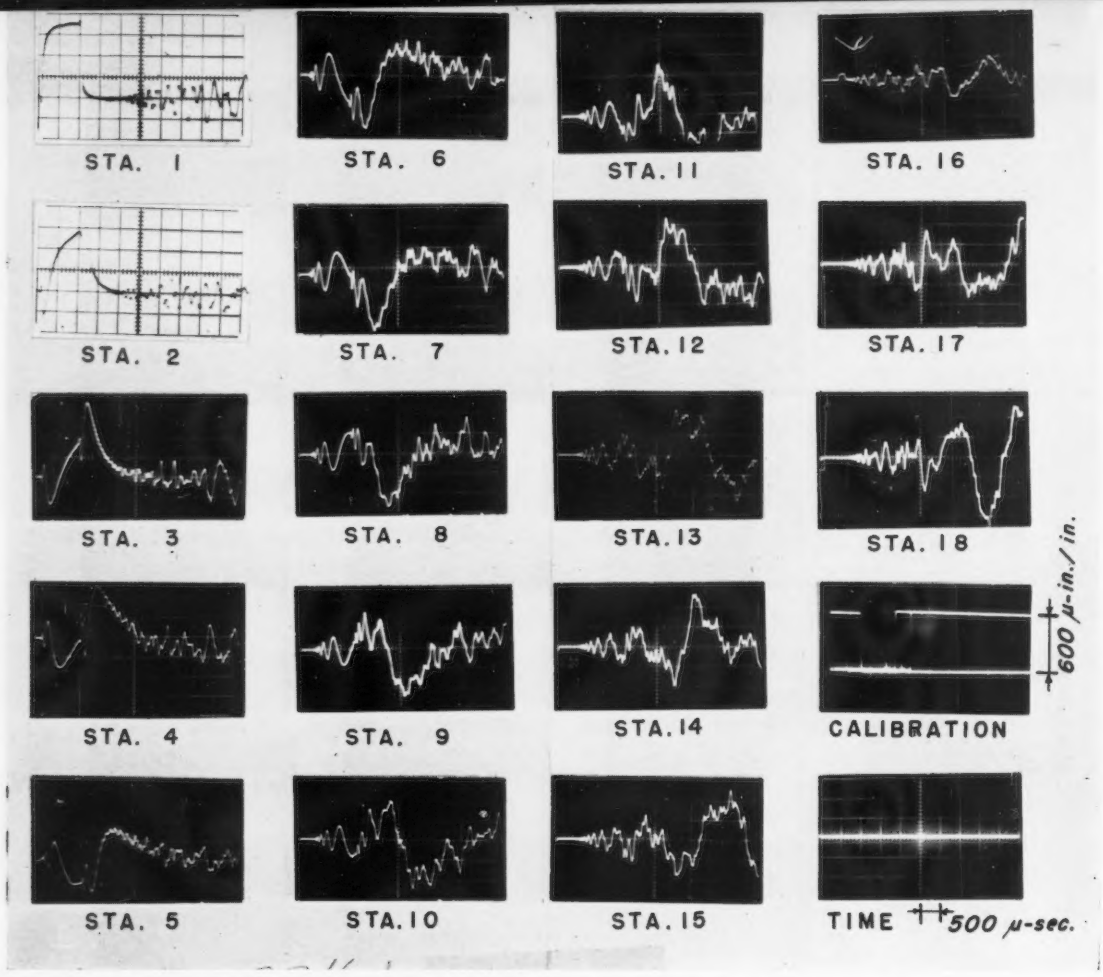

Fig. 5—Photographic records of oscilloscope traces representing outer fiber strain vs. time. (Time scale: one horizontal division = 500 microsec)

By using this method, it can be shown that

$$M = \frac{M_0}{\beta_1 L} \sum_{n=0}^{\infty} \frac{\phi_n'(0) \cdot \phi_n''(x)}{(\beta_n/\beta_1)} \left[1 - \cos 2\pi \frac{\beta_n^2 t}{\beta_1^2 T_1}\right] \quad (9)$$

Theoretical Moment Response

For the characteristic solution, an IBM 650 digital computer was used to perform the numerical integration by the repeated application of eqs. (3) through (6). The following numerical values were used:

$$\begin{aligned} L/r &= 384 \\ KG/E &= 1.0 \\ h &= 1/160 \end{aligned}$$

The moment input was taken to be in the form of a ramp-platform (see the first curve in Fig. 8) with the rise time $\tau_0 = 0.1$. In the numerical integration, the new values depend on previously determined values and, in so doing, numerical results were tabulated at each mesh point. These results can readily be used for plotting $\mathfrak{M} - \tau$ curves at any desired beam station. In Fig. 8 are shown the representative moment-response curves at eight beam stations. They are marked with Timoshenko theory.

In addition, the moment response based on the normal-mode method was readily computed by means of eq (9) which represents an alternating series. The moment input was taken as a step function or $\tau_0 = 0$. The calculations were carried out on an IBM 704 digital computer. It was found that a superposition of 27 modes was sufficient to yield satisfactory and convergent results. The values of $\phi_n'(0)$ and $\phi_n''(x)$ are provided by the extended tables of normal modes.[5] The interval of t/T_1 was taken as 0.0001. The results are shown in Fig. 9.

Conclusions and Comments

Comparison with Theoretical Results: Theory vs. Experiment

On comparing the experimental results with the theoretical curves based on the Timoshenko beam equations shown in Fig. 8, a good agreement is found at each of the eight representative beam stations. The comparison is limited to the initial stress build-up and the discrepancy is most marked in the phase shifting.

In a previous paper[3] it was shown that the phase shifting is sensitive to many parameters, particularly

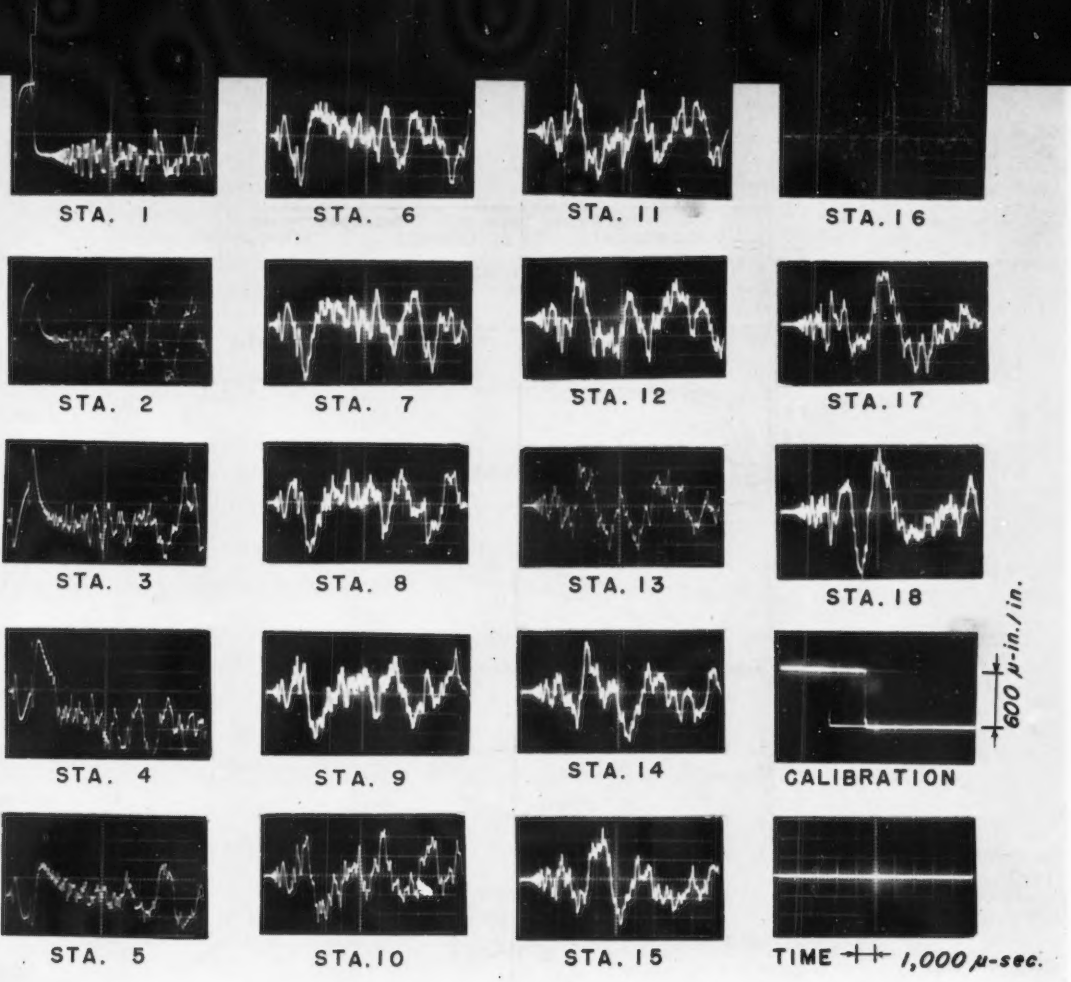

Fig. 6—Photographic records of oscilloscope traces representing outer fiber strain vs. time. (Time scale: one horizontal division = 1000 microsec)

to the quantity KG/E and to the rise time τ_0. As far as the quantity KG/E is concerned, it was found that the curves based on taking a higher value of KG/E invariably lead ahead of those based on taking a lower value. As to the effect of the rise time upon the response curve, it was found that the response curve shifts slightly to the left when a smaller value of τ_0 is assigned. These findings serve to indicate that the numerical values used in the characteristics method may be changed so as to have a much better fit to the experimental records.

However, if these differences in phases are to be disregarded and the general wave pattern and amplitude are to be considered, it seems fitting to state that, for the given impact duration, the Timoshenko theory predicts quite satisfactorily the dynamic response even in the initial stress build-up.

Comparison of Theoretical Results: Timoshenko Theory vs Bernoulli-Euler Theory

The theoretical moment-time relations at three representative beam stations are shown in Fig. 9. Each curve is marked with the corresponding theory. It is seen upon examining these curves that the agreement between the results based on two different theories is fairly good. The most marked discrepancy appears in the starting point of wave propagation. This serves to illustrate the inherent difficulty in Bernoulli-Euler beam theory that the wave travels with infinite speed from the impact end to any other beam station. Discrepancy also appears in the phase. It is apparently a direct result from the difference in the assumed rise times.

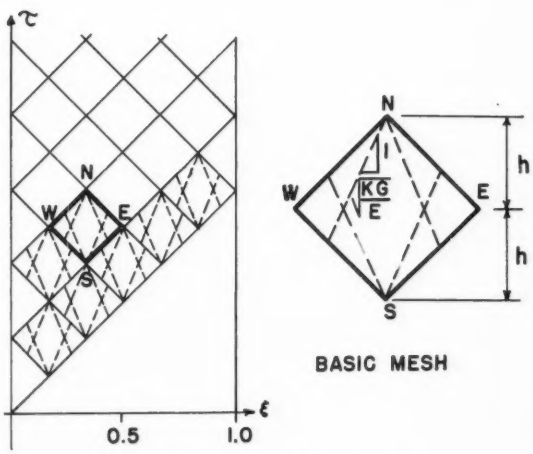

Fig. 7—Network for characteristics solution

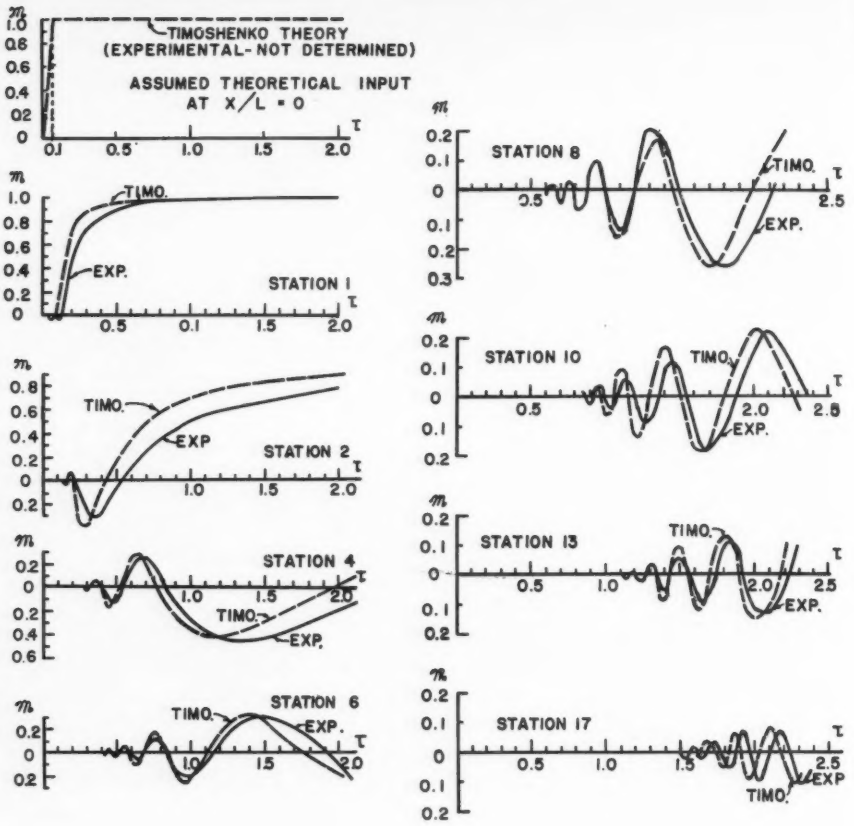

Fig. 8—Response curves at various beam stations. Experimental compared with Timoshenko theory

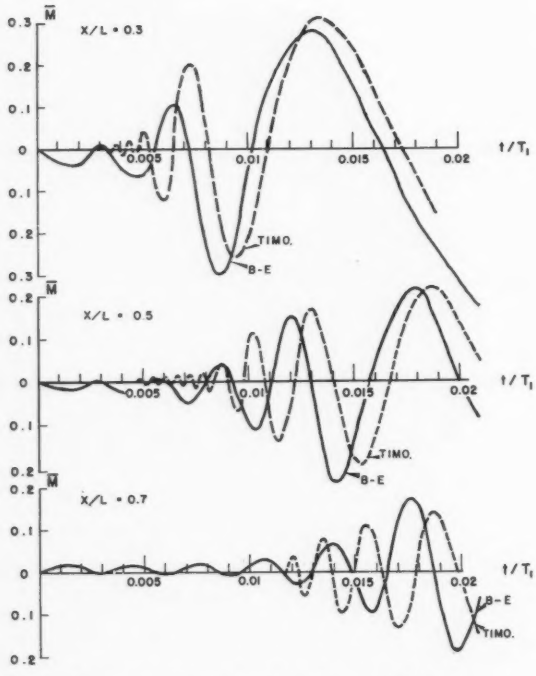

Fig. 9—Response curves at various beam stations. Timoshenko theory compared with Bernoulli-Euler theory

Acknowledgment

The author is grateful to Dana Young, Dean of the School of Engineering, Yale University, who suggested the problem and who provided advice throughout the investigation.

The numerical work in the characterisic solutions was done in both Yale Computation Center and Watson Laboratory, Columbia University. The numerical work for the normal-mode solutions was done at the Massachusetts Institute of Technology, 704 Computation Center.

Bibliography

1. Davidson, T., and Meier, J. H., "Impact on Prismatical Bars," Proc., Experimental Stress Analysis, 4, No. 1, 88–111 (1946).

2. Ripperger, E. A., and Abramson, H. N., "A Study of the Propagation of Flexural Waves in Elastic Beams," Jnl. Appl. Mechanics, 24, 431–434 (1957).

3. Kuo, S. S., "Bending Waves in Free-Free Beams," Proc. Fourth Midwestern Conference of Solid Mechanics, 457–467 (1959).

4. Young, D., and Felgar, R. P., "Tables of Characteristic Functions Representing Normal Modes of Vibration of a Beam," The University of Texas, Publication No. 4913 (July 1949).

5. Kuo, S. S., "Tables of Eigenfunctions Representing Normal Modes of a Free-Free Beam," Civil Engineering Department, Yale University (mimeographed), (July 1959).

6. Courant, R., and Hilbert, D., "Methoden der Mathematischen Physik," 2, Springer, Berlin, 2nd ed., 291–345 (1937).

7. Pfeiffer, F., "Uber die Diffentialgleichung der transversalen Stabschwingungen," Zeitschrift fur angewandte Mathematik and Mechanik, Bd. 25/27, Nr. 3, 83–91 (1947).

8. Kuo, S. S., "Traveling Waves in a Free-Free Beam," Progress Report, Vol. 1, Civil Engineering Department, Yale University (unpublished), (October 1957).

9. Young, Dana, "Vibrations of Multi-degree of Freedom Systems and Continuous Systems," General Engineering Laboratory, Technical Information Series, Schenectady, New York (1955).

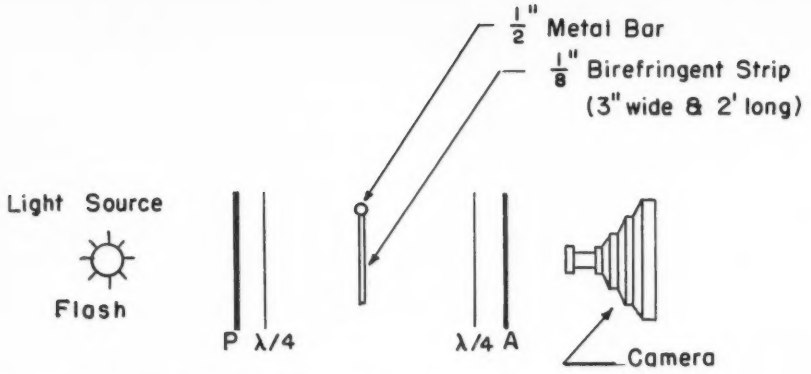

Fig. 1—Cross section showing birefringent strip and metal bar

Measurement of Surface Strain by Means of Bonded Birefringent Strips

Preliminary report contained in this technical note outlines a technique whereby the narrow edge of the birefringent strip, rather than its flat surface, is cemented to the metal surface. Viewing is done through the birefringent strip

by J. Duffy and T. C. Lee

Introduction

The determination of the strain on the surface of an opaque body has received considerable attention on the part of a number of investigators. This interest is due in large measure to the fact that in dynamic problems three-dimensional photoelasticity becomes more difficult. In particular, the "frozen-stress" technique is no longer applicable. Another reason for the interest in surface strain is that in certain applications it is preferable to make measurements on the prototype rather than on a model.

The birefringent-coating technique, originally proposed by Mesnager,[1] and developed by d'Agostino, Drucker, Liu and Mylonas,[2] provides a measure of the strain over the entire surface area in one picture. It has been shown, however, that the fringe pattern obtained with a coating is dependent in general not only on surface strain but on the thickness of the coating as well.[3,4] To put it more precisely, the observed fringe order is proportional to the average strain across the thickness of the coating rather than to the interface strain. This produces considerable difficulties under certain circumstances in interpreting the fringe pattern in terms of surface strain. It is evident also that, in dynamic work, the influence of thickness will produce even greater problems.

As is well known, in the Mesnager technique, the light is reflected from the metal surface. In the technique proposed in the present note, the narrow edge of the birefringent strip rather than its flat surface is cemented to the metal surface, and viewing is through the birefringent strip (Fig. 1). This has the advantage of giving the fringe pattern at any depth in the birefringent strip and, in particular, at the metal surface itself, so that all problems associated with thickness are avoided. In dynamic problems where light intensity must be high, it has a further advantage: the light does not have to be reflected from the metal surface and hence be dispersed and reduced in intensity.

Experimental Technique

As an example of the use of this technique, compressional waves initiated by a small explosion were

J. Duffy and T. C. Lee are Assistant Professor and Research Assistant, respectively, Brown University, Providence, R. I.
Manuscript received by the Society on July 14, 1959.
The results presented in this note were obtained in the course of research sponsored by the Ballistic Research Laboratories of Aberdeen Proving Ground under Contract DA-19-020-ORD-4674.

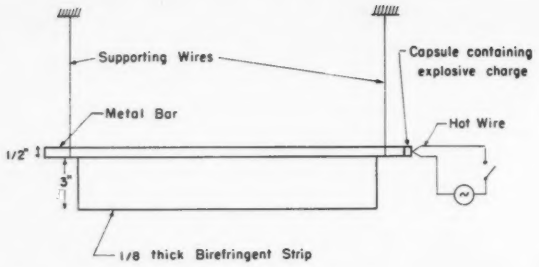

Fig. 2—Test setup of metal bar and bonded birefringent strip

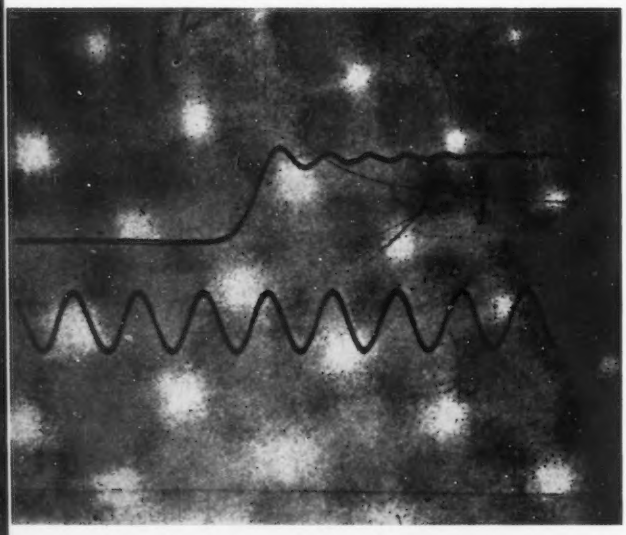

Fig. 3—Oscilloscope trace obtained by Hsieh and Kolsky, of end displacement of steel bar for 0.01 g lead azide charge detonated at other end. Length of bar 22.5 cm. Diameter 0.63 cm. Lower trace: 100 kc/sec timing wave

propagated longitudinally in metal bars and their presence detected by a birefringent strip (Fig. 2). The material used was Hysol 6000-OP, an epoxy resin. The plastic strips were $^1/_8$ in. thick, about 3 in. wide and 2 ft long. They were cemented to $^1/_2$-in. diam metal bars about 3 ft long either of steel or aluminum which were freely suspended by two thin wires. A small charge of lead-azide powder was set off at one end of the bar and the waves in the plastic strip photographed in the polariscope. The light source* provides a flash of high intensity and about $^3/_4$ microsec duration. This is done by the discharge of a large capacitance across two electrodes. A light filter was inserted to produce a reasonable approximation to monochromatic light. Synchronization was achieved by detecting the explosion with a photocell and using a built-in delay to provide a time lag of 5 to 100 microsec between explosion and flash. Since the camera was kept open it had to be shielded from the light produced by the explosion. Fringe order was established by means of colored photographs, the same light source being used but without the filter.

The technique for initiating the wave in the metal was suggested to the authors by S. R. Bodner. A small capsule containing from 0.05 to 0.2 g of lead-azide powder is placed against the end of the bar and the powder ignited by a hot wire. The resulting stress pulse in steel bars is of about 10 microseconds duration. Figure 3 shows the displacement at the other end of the bar as obtained by Hsieh and Kolsky.[5] Since dispersion effects in steel are small, one can assume that, once the pulse has penetrated some distance along the bar, its shape will remain substantially unchanged until, of course, the pulse reaches the other end of the bar. Accordingly, Fig. 3 represents fairly well the shape of the pulse at any point along the bar away from the end. The oscillations in the tail of the pulse should be noted.

Experimental Results

Figure 4 is a set of photographs of the photoelastic pattern induced in the plastic sheet by compressional waves in a steel bar. In each case the bar lies off the picture at the top while the free edge of the plastic is at the bottom. The plastic itself is about $3^1/_4$ in. from top to bottom. (The small black specks are impurities within the plastic.) The wave, of course, is traveling from right to left. In the first picture (Fig. 4a), the disturbance has reached a point about 16 in. from the end of the bar. The delay between detonation and flash was set at 80μ sec. For the next picture (Fig. 4b) the delay was set at 100μ sec. But, for each succeeding photograph, the delay remained at 100μ sec while the specimen was moved about 4 in. within its plane. In addition, in the last picture (Fig. 4e) the camera was brought closer to get a better picture near the end of the disturbance.

A careful interpretation of the photoelastic patterns in Fig. 4 cannot be made without a better knowledge of the dynamic properties of the plastic. It can be expected that visco-elastic effects play an important role. Obviously, the waves in both metal and plastic are influenced by dispersion not only due to the presence of the geometric boundaries but, in addition, and this is true mainly for the plastic, because of the inelasticity of the material. In the discussion presented, these effects are disregarded and computations are made on the crude basis of phase velocities.

The photographs show two families of waves. The slower has a wave front making an angle of about 11.5 deg with the axis of the metal bar and the faster an angle just exceeding 21 deg. (These are the angles when the bar is of steel. With an aluminum bar the angles are very slightly larger.) If the velocity, v_M, of the compressional wave in the bar is computed on the basis of the elementary theory for slender bars, and if $E = 30 \cdot 10^6$ psi and the weight density, $\gamma = \rho g$, is 491 lb/cu ft, one ob-

* *Built by Edgerton, Germeshausen and Grier, Inc.*

tains v_M = 16,860 fps. For the plastic, S. R. Bodner obtained a value of $\sqrt{E/\rho}$ of approximately 5300 fps from resonance tests of a slender bar of Hysol in lateral vibrations at frequencies from 163 to 4100 cps. Since the specific gravity of the material is about 1.21, this corresponds to a value of E = $0.5 \cdot 10^6$ psi which agrees quite closely with results of static tests. Making the further assumption that the static value of Poisson's ratio, $\nu = 0.35$, remains unchanged under dynamic conditions one finds

$$v_D = \sqrt{\frac{\lambda + 2G}{\rho}} \approx 6750 \text{ fps}$$

$$v_C = \sqrt{\frac{E/(1 - \nu^2)}{\rho}} \approx 5700 \text{ fps}$$

$$v_S = \sqrt{\frac{G}{\rho}} = v_C \Big/ \sqrt{\frac{2}{1 - \nu}} \approx 3230 \text{ fps}$$

where v_D is the velocity of dilatational waves in the infinite medium, v_C that of compressional waves in a thin plate and v_S that of shear waves. In these expressions, λ is Lamé's constant and G is the shear modulus of the plastic. Waves traveling with these velocities would make angles of 23.6, 19.8 and 11.1 deg., respectively, with the axis of the metal bar, as compared with the experimental values of 21.2 and 11.5 deg. These angles seem to indicate that the two waves observed are a shear wave and probably a compressional wave. The possibility of a dilatational wave of appreciable intensity existing in the plate seems unlikely. One would expect a dilatational wave to have a decreasing amplitude and a change in shape as a result of the presence of the free surfaces. Actually, the isochromatics are remarkably straight for a long distance from the metal bar, so that the waves in the plate have constant shape. This is brought out very clearly in some pictures taken with color film, which show no change in the width of the bands of the various color tints along the entire wave front as long as there is no interference with other waves, such as the reflections from the free edge evident in Figs. 4 c, d and e.

The fringe orders obtained depend, of course, on the size of the detonation. Figures 4 a–e were made with 0.05 g of lead azide and a steel bar. Color photographs with the same bar and an equivalent charge indicate that the maximum fringe order is about $1^1/_2$ and occurs between the pair of closely spaced fringes at the front of the family of waves traveling at approximately the shear-wave velocity (see Fig. 4a). Following this pair of fringes, there

Fig. 4—Waves in a birefringent strip induced by a compressional wave traveling longitudinally in a metal bar. The metal is steel and the explosive charge weighed about 0.05 g. (The distance given is measured from the end of the bar to the center of the field of view. The time given is the delay between detonation and the flash of light)

(a) Distance = 16 in.; delay = 80 μsec

(b) Distance = 16 in.; delay = 100 μsec

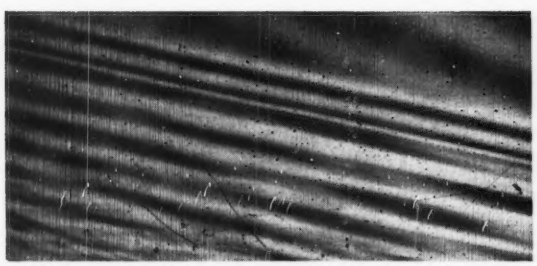

(c) Distance = 12 in.; delay = 100 μsec

(d) Distance = 8 in.; delay = 100 μsec

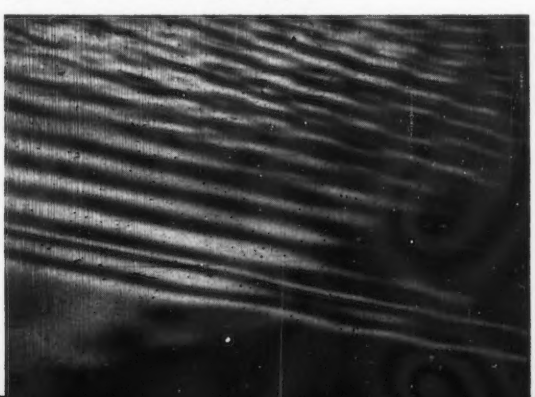

(e) Distance = 4 in.; delay = 100 μsec

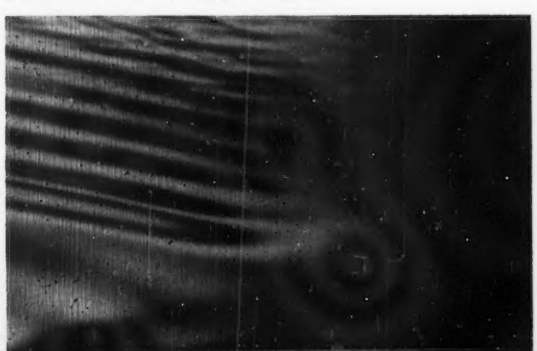

are many fringes lying apparently at the same angle. These represent only fractional fringe orders, being principally black and white with an occasional yellowish tint in the color photographs. They are probably produced by the oscillations in the tail of the disturbance, and their dappled appearance would be a superposition of the faster and slower waves. The fringe order in the faster wave also is only a small fraction of a fringe.

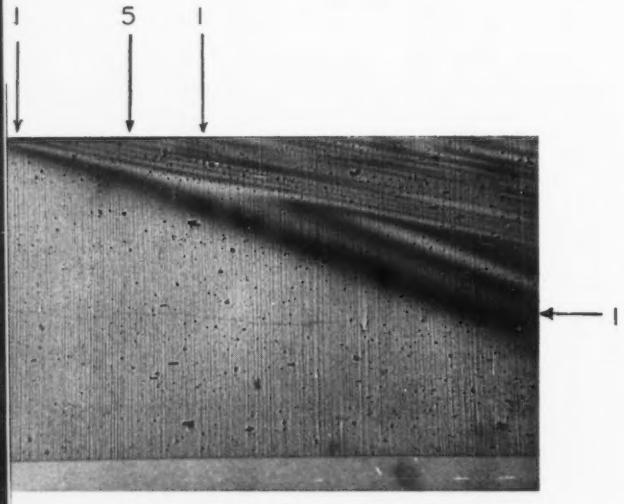

Fig. 5—Waves in birefringent strip induced by a compressional wave traveling longitudinally in the metal bar. The metal is aluminum and the explosive charge weighed about 0.1 g

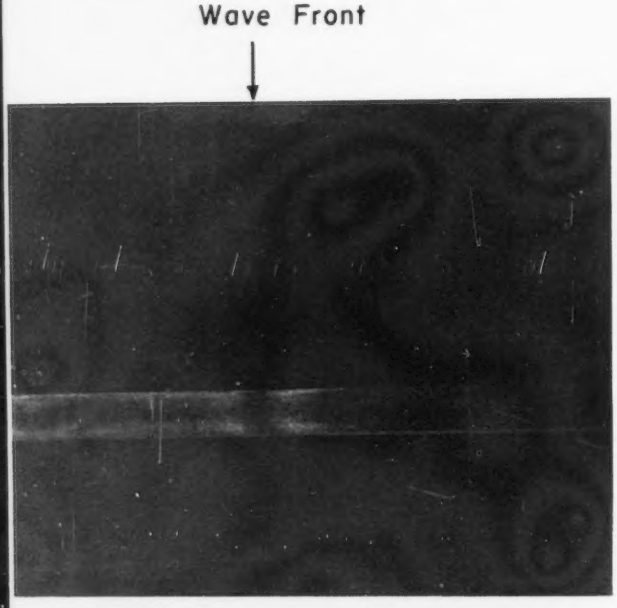

Fig. 6—Birefringent coating on $^3/_8$-in. square steel bar. The disturbance in the metal bar has reached a point about half way across the photograph

If we assume that the value of the strain optical coefficient $C_\epsilon = 0.00018$ in./fringe obtained by static tests with this resin remains unchanged under dynamic conditions, then for a $^1/_8$-in. thick plastic strip the strain difference in the slower wave is about 0.0015.

Figure 5 shows the photoelastic pattern when an aluminum bar is used and the wave is initiated by a 0.1 g charge. The fringe order of the slower wave is 5 representing a strain difference of about 0.007, while the more rapid wave has a fringe order of about 1. A similar pattern is obtained using a steel bar if one goes to a larger charge. Strains of this magnitude indicate that the stress in the metal bar is nearly equal to the yield stress. About the only evident difference between aluminum and steel is in the length of the pulse, which appears slightly longer for aluminum (11μ sec) than for steel (8.5μ sec). In each case, the peak in the pulse occurs at about $^5/_8$ of the distance along its length.

Comparison with Birefringent Coatings

A few pictures were made employing the birefringent-coating technique using a metal bar with the wave initiated as above. Of course, birefringent coatings are not limited to studies of one-dimensional effects, so that it is highly worth while to perfect the technique even though the photograph presented in this note is not particularly revealing.

A $^1/_8$-in. thick birefringent coating was cemented to a $^3/_8$-in. square steel rod. An explosive charge of 0.05 g detonated at one end of the bar was used to initiate the disturbance. The effect produced by the wave can be seen in Fig. 6 in which the approximate position of the wave front is indicated. Obviously numerous improvements must be made to give better photographs by reflection. The pictures taken, however, show that the birefringent strip is more revealing of the behavior of the metal bar. Also it is evident that a quantitative measure of strain at any point is easier to obtain, although a complete interpretation of the pattern has not yet been made either for the coating or the strip.

Acknowledgment

The authors wish to thank S. R. Bodner for his suggestions, the use of some of his equipment, and for measurements of the dynamic properties of the epoxy resin. They are also grateful to D. C. Drucker and C. Mylonas, as well as to R. D. Mindlin of Columbia University, for numerous comments and suggestions.

References

1. *Mesnager, M., "Sur la Determination Optique des Tensions Interieures dans les Solides a Trois Dimensions," Comt. Rend., Paris, 190, 1249 (1930).*
2. *D'Agostino, J., Drucker, D. C., Liu, C. K., and Mylonas, C., "An Analysis of Plastic Behavior of Metals with Bonded Birefringent Plastic," Proc. Soc. Exptl. Stress Anal., XII, No. 2, 115–122 (1955).*
3. *Duffy, J., "Effects of the Thickness of Birefringent Coatings," Tech. Rept. No. 34, Division of Applied Mathematics, Brown University, April 1958.*
4. *Lee, T. C., Mylonas, C., and Duffy, J., "Thickness Effects in Birefringent Coatings with Radial Symmetry," Technical Report of the Division of Applied Mathematics, Brown University, April 1959.*
5. *Hsieh, D. Y., and Kolsky, H., "An Experimental Study of Pulse Propagation in Elastic Cylinders," Proc. Phys. Soc., 71, 608–612 (1958).*

Strain Field Associated with Brittle-fracture Propagation in Wide Steel Plates

Studies indicate that, for the particular specimen geometry used and for the associated test conditions, the strain field surrounding the tip of the advancing fracture remains essentially unchanged after traversing about one-third of the width of a 6-ft wide plate

by S. T. Rolfe and W. J. Hall

ABSTRACT—The results of an experimental investigation concerned with the study of the strain field surrounding a brittle fracture propagating across a wide steel plate are presented in this paper. The data were obtained from tests of 6-ft wide steel plates that were instrumentated to measure surface strain and crack speed. The plates were tested at an average net applied stress of 19,000 psi, a temperature of about −5° F, and with the notch-wedge-impact method for fracture initiation. Several plates were tested under similar conditions and the results were superimposed to give a representative picture of the strain distribution on the surface of a plate in the region of the tip of a propagating fracture. Contours of the maximum principal strain for various lengths of crack are presented. The studies indicate that for this particular specimen geometry and associated test conditions, the strain field surrounding the tip of the advancing fracture remains essentially unchanged after traversing about one-third of the width of a 6-ft wide plate.

Introduction

Little information is available in the literature concerning the magnitude and extent of the strain field associated with a brittle fracture that is propagating across a wide steel plate. Strain–time records from gages located at isolated points near a crack propagating across a steel plate have been obtained and reported earlier as a part of the brittle-fracture mechanics program that has been underway at the University of Illinois for several years.[1–4] Robertson[5] also has reported the results of some strain–time measurements that are similar in nature to those reported herein. The dynamic stress distribution surrounding a running crack in CR-39 as measured by photoelastic methods has been reported by Wells and Post.[6] To obtain a better understanding of the brittle-fracture phenomenon, a more detailed knowledge of both the magnitude and extent of the strain field surrounding a propagating fracture in a wide steel plate is desirable. The studies described in this paper were undertaken to establish the characteristics of the strain field associated with a brittle fracture propagating across a wide steel plate.

S. T. Rolfe and W. J. Hall are associated with University of Illinois, Urbana, Ill.

Paper was presented at 1960 SESA Annual Meeting held in Berkeley, Calif., on October 19–21.

The experimental approach consisted of measuring the surface strain at various points across a 6-ft wide steel plate during fracture propagation with SR-4 strain gages. Because of the limited number of dynamic recording channels available, the results from several similar tests were superimposed to obtain strain contours on the plate surface for certain positions of the fracture. The strain contours thus obtained were found to be representative of all surface-strain measurements made on plates tested in the earlier stages of this program.

Method of Investigation

Description of Specimens and Test Procedure

The test specimens were $^3/_4$-in. thick semikilled steel plates, 6 by 10 ft in plan dimension. Representative mechanical, chemical and Charpy V-notch impact properties of the plate material are given in Table 1. The specimens were welded to pull-plates in a 3,000,000-lb hydraulic testing machine. The test procedure consisted of cooling the plate to approximately −5° F by means of

TABLE I—REPRESENTATIVE MATERIAL PROPERTIES

Check Analysis							
C	Mn	P	S	Si	Cu	Ni	Al
0.20	0.76	0.019	0.03	0.05	0.025	Trace	0.02

Tensile Data				
	Yield stress, ksi	Maximum stress, ksi	Percent elongation in 2-in.	Percent reduction in area
Longitudinal	34.6	63.5	39	66
Transverse	34.7	63.6	38	60

Charpy V-notch Data	
Temperature, °F	Absorbed energy, ft-lb
−25	7
−10	9
0	11
10	13
15	14
20	17
30	22
40	30

crushed dry ice placed in boxes along each side of the specimen, loading the specimen to an average net stress of about 19,000 psi, and initiating the fracture by driving a tapered hardened-steel wedge into a prepared notch $1^1/_8$-in. long cut into an edge of the plate. A picture of the testing machine with the cooling tanks covering a specimen is shown in Fig. 1.

Instrumentation

To arrive at a picture of the strain field associated with the propagating fracture, it was desired to have continuous strain–time records from gages located on the plate surface while the fracture propagated across the plate. Also, it was desired to have independent measurements of the average fracture speed.

The strain data were obtained in each test from eleven rectangular SR-4 Type A-7 strain rosettes mounted on the plate surface. The data from the individual component gages were recorded with 33 channels of oscilloscope equipment utilizing 35 mm moving-film cameras.

The average surface-crack speed was measured with a system of six crack detectors (SR-4 Type A-9 single-wire strain gages) which were broken as the fracture traversed the plate. The breaking of a crack detector opened an electrical circuit and caused a stepped change in voltage that was recorded by a single oscilloscope unit. From a knowledge of the time of breaking and the distance between crack detectors, it was possible to compute the average surface-crack speed.

A more complete description of recording instrumentation and testing techniques used may be found elsewhere.[1,3,4]

Data Reduction

Reduction of the strain data recorded on 35 mm strip film was facilitated with a decimal converter and the University of Illinois high-speed digital computer, the "Illiac." Briefly, the procedure consisted of enlarging the 35 mm film strips on which the strain–time traces, and calibration and timing marks were recorded. With the aid of a reader and decimal converter, values of component gage strain vs. time were simultaneously punched on IBM cards, plotted on an X-Y plotter and typed in tabular form. The times at which strain values

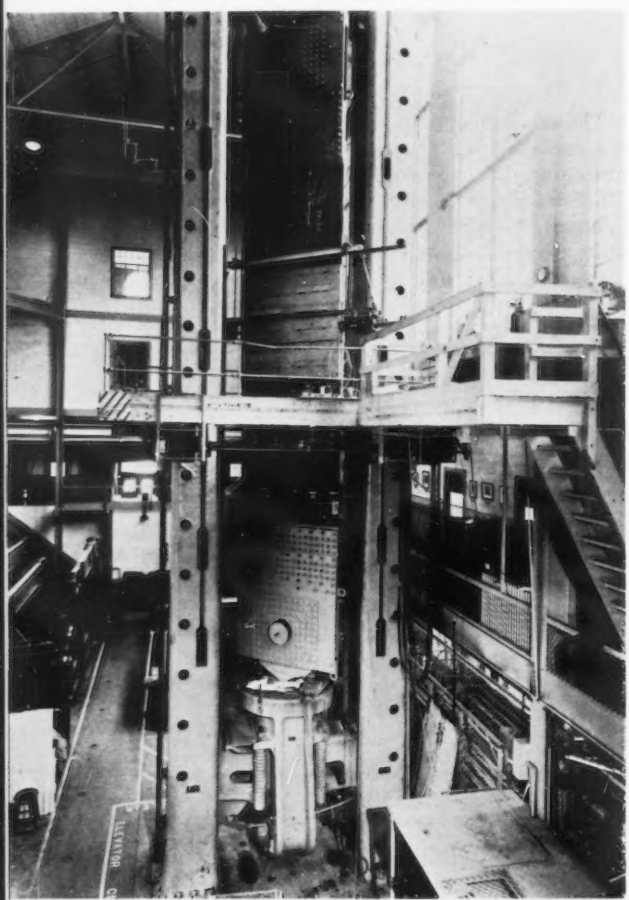

Fig. 1—Specimen mounted in 3,000,000-lb testing machine

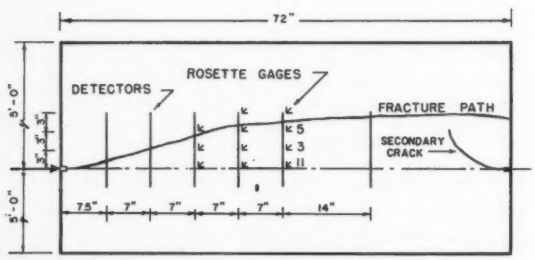

Fig. 2—Typical instrumentation layout and fracture path

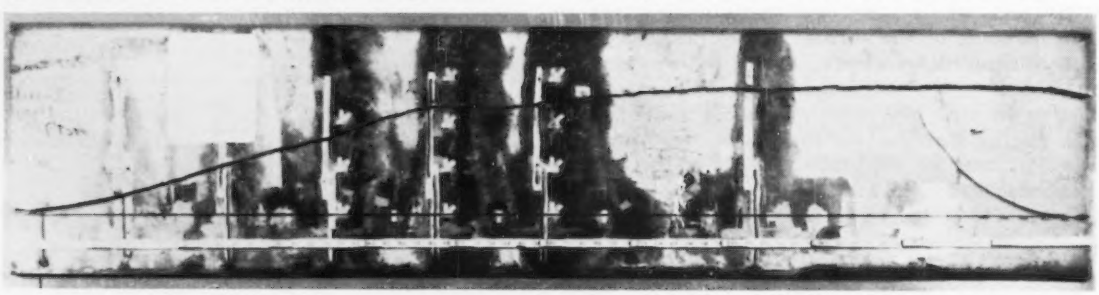

Fig. 3—Typical fracture path

were read were selected arbitrarily but judiciously at points corresponding to changes in strain in the component gage traces. The strain–time values were then transferred from IBM cards to punched paper tape, and processed through the "Illiac" to compute values of the principal strains. The "Illiac" results consisted of tabulated principal-strain data, as well as scaled oscilloscope displays of component gage and principal-strain traces which were photographed for later enlargement and use.

Analysis of Test Results

Test Results

The purpose of this investigation was to obtain sufficient data to establish the characteristics of the strain field surrounding a brittle fracture that is propagating across a wide steel plate. Because of the limited number of recording channels and because the exact location of the fracture path was unknown prior to each test, it was decided to concentrate the strain rosettes in general areas with respect to width on the plate specimens, and thereafter superimpose the data to obtain a picture of the strain distribution associated with the propagating crack. The results presented are based primarily on five wide-plate tests which were instrumentated to obtain measurements of surface strain and crack speed.

A typical instrumentation layout and crack path for one specimen is shown in Fig. 2 and a photograph of the fractured portion of this same specimen is presented in Fig. 3. In general, the fracture paths in each test curved upward from the initiation edge and then remained essentially straight while traversing the rest of the plate; rarely did the fractures rise above the notch line (an imaginary horizontal line connecting notches on opposite edges of the plate) as much as the fracture shown in Fig. 3. Often a secondary fracture initiated from the notch at the far edge of the plate and propagated toward the main fracture as may be seen in Fig. 3.

Strain–time traces for three rosettes of the specimen shown in Figs. 2 and 3 are presented in Fig. 4. In this figure, zero time corresponds approximately to the time of fracture initiation. The initial strain values correspond to the strain resulting from the applied test load. The vertical and diagonal component gage traces of each rosette exhibit a general shape characterized by a slight decrease and then a fairly steady and rapid increase in strain to a maximum value as the fracture propagates past the gage. The peak is followed by a decrease to a strain level associated with the removal of external load. As may be seen in Fig. 4, the pulse is very sharp for gages located close to the fracture; for gages located away from the fracture, the peak strain is of a lower magnitude and the pulse extends over a longer time.

The horizontal-gage traces are characterized by three major changes in strain. The strain trace first exhibits an initial relaxation of compressive strain followed by a compressive pulse corresponding to the tensile peak of the vertical gage. Finally, the trace exhibits another relaxation of compressive strain before leveling off at the final strain value. The strain–time traces shown in Fig. 4 are representative of all the strain records obtained as a part of this investigation.[1–4]

The crack speed detectors were used to measure

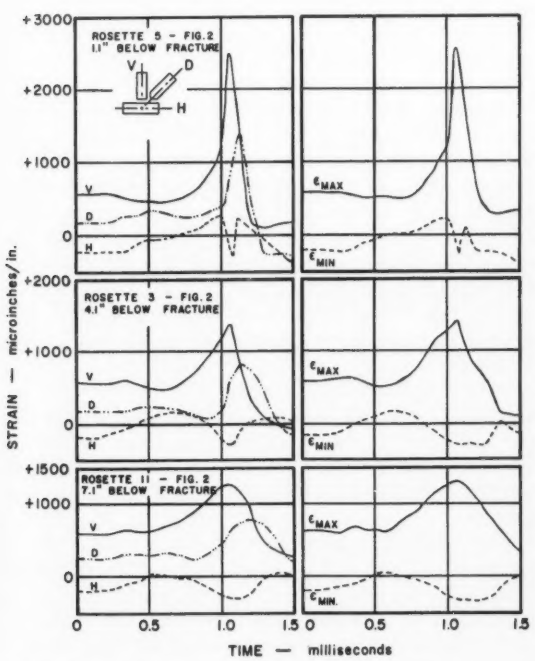

Fig. 4—Typical strain traces and computed principal strains for rosettes located at various distances from the fracture

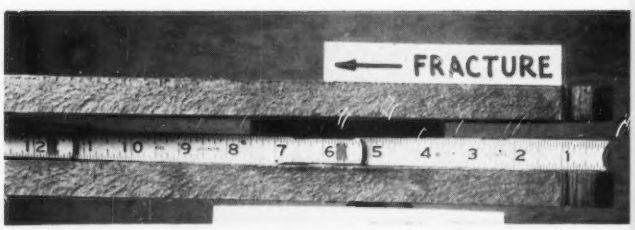

Fig. 5—Typical smooth fracture surface near fracture source

Fig. 6—Typical coarse fracture surface in central region of plate

the approximate surface-fracture speed and to aid in determining the location of the surface fracture at any time. For the five major tests, the recorded fracture speeds ranged from 1850 to 4750 fps, with an average fracture speed of 2700 fps in the region where the rosettes were located.

As may be seen in Figs. 5 and 6, which are views of typical fracture surfaces, the fracture textures were usually smoother in the initiation region than in the central region of the plates. Although speed measurements were not obtained for the first 6 in. of crack propagation, more recent studies of low-velocity brittle fractures[7] indicate that smooth crack textures occur in regions of low crack speed. Thus it is probable that the relatively smooth crack texture near the point of initiation of a crack (Fig. 5) indicates a low fracture speed. All plates had only a very slight reduction in thickness in the region of the fracture surface, always less than 2%.

Principal Strains

Typical principal-strain curves for three rosettes are presented in Fig. 4. In general, the maximum principal-strain trace for each rosette is of essentially the same shape and magnitude as the vertical-component gage trace shown in the same figure; this merely indicates that the strain in the vertical direction is dominant. Almost all peak strain values fall in a range between 800 and 3000 microinches/in. The minimum principal-strain traces are of much lower magnitude and resemble the horizontal-gage-strain traces.

For rosettes located close to the fracture path, the magnitude of the strain peak is relatively large. As the vertical distance between a rosette and the fracture increases, the peak principal-strain magnitude decreases rapidly up to a distance of about 2 in. This may be seen clearly in Fig. 4, and in Fig. 7 in which the peak maximum principal strains are plotted against vertical distance between the rosette and the fracture. It should be noted that in all cases, even in the case of very high vertical-component gage strains, the exhibited response was elastic with negligible permanent set remaining after fracture.

The maximum strain rates, as measured by the slope of the strain–time trace of a gage during peaking, were computed for all vertically oriented gages. Strain rates ranged from 1 to 109 in./in./sec, and as would be expected, the highest strain rates were obtained for gages closest to the fracture. Although the scatter was fairly large, typical strain rates were 20 and 5 in./in./sec for gages 1 and 3 in. from the fracture, respectively.

Strain Contours

In order to portray the strain distribution on a plate surface during the time a crack is propagating, contours of maximum principal strain for various surface-crack lengths were plotted. The procedure used in superimposing the results from several tests may be summarized as follows. It was first necessary to establish from the original strain–time curves the times corresponding to various selected crack lengths and to establish the position of the gages with respect to the fracture path. Then, at any particular time corresponding to a given crack length, strain values were obtained from the test data and were used in plotting the contours. The contour lines of surface strain for various crack lengths were drawn in regions where data were available. No contours were drawn in regions where there were no data, although it is obvious that strain contours do exist in these regions.

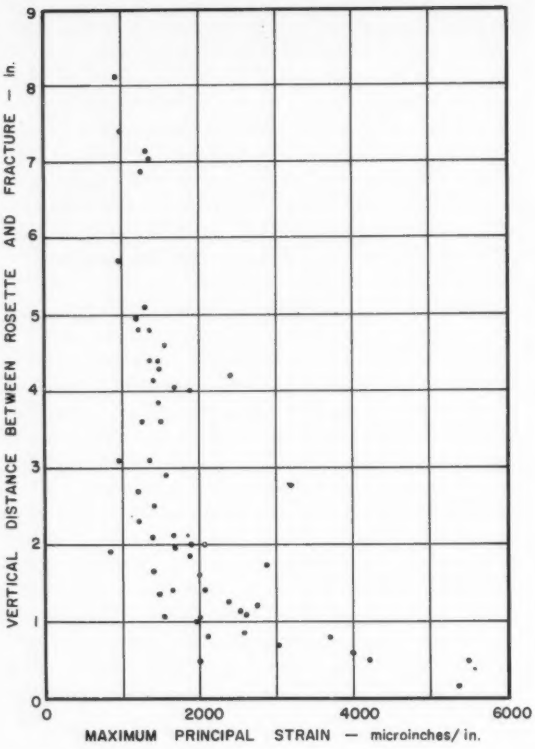

Fig. 7—Maximum principal strain versus vertical distance between rosette gage and fracture

The respective times that corresponded to the desired surface-crack length in each test were determined from a knowledge of the breaking times of the crack detectors and the peaking times of the vertically oriented strain gages located closest to the fracture. It was assumed that the peak strain of a gage close to the fracture occurred when the surface fracture was directly above or below the gage.

The horizontal projection of the actual fracture path on the notch line was used as the common fracture path for all tests for purposes of superposition. In general, the fracture followed a horizontal path as it passed through the region where rosettes were placed so that little error was introduced in the contours by using this assumption.

Maximum principal-strain contours for various

crack lengths are presented in Fig. 8. In the contour for a 22-in. crack, the magnitudes and directions (shown as short straight lines) of the maximum principal strains are shown at their respective locations on the plate layout. The individual strain values are not shown for the other crack lengths in order to simplify the drawings. The contour interval selected for the plots was 200 to 400 microinches/in., and the strain contours are plotted in terms of absolute strain, that is, with respect to the as-rolled condition. Thus, the 600 contour for maximum principal strain corresponds approximately to the initial applied stress of 19,000 psi. The data shown in Fig. 8 (c) for the 22-in. crack were obtained from strain data similar to those of Fig. 4, and are presented elsewhere.[4]

Since strain–time traces for vertical and maximum principal strains are similar, as noted earlier, it was possible to use the results of all earlier tests conducted as a part of this investigation in developing the strain contour patterns. Thus, in spite of the limitations imposed by the procedure of superimposing data from similar tests and the variations in strain data as may be noted in Fig. 8 (c), based on the large amount of data available it is believed that the strain contours presented are representative of the strain distribution surrounding the tip of a brittle crack propagating in a wide steel plate.

For the majority of the rosettes, as the fracture approaches the rosette, the direction of the maximum principal strain rotates slightly so that it points

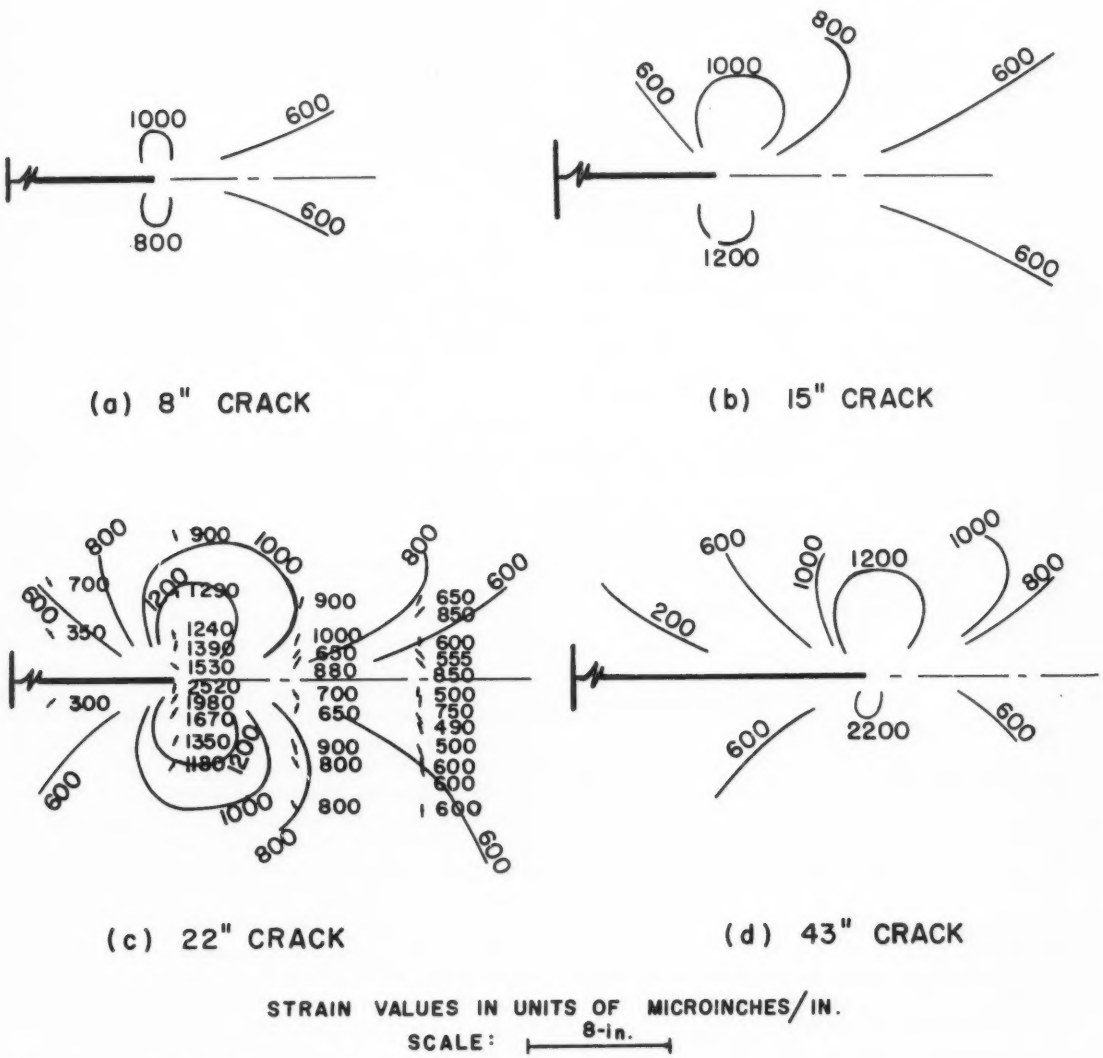

Fig. 8—Maximum principal-strain contours for various crack lengths

toward the approaching fracture, and follows the fracture for a short time as it goes by the gage position. The direction of the maximum principal strain more or less retains a vertical orientation. Values of θ for ϵ_{max} as indicated by the slope of the short straight lines in Fig. 8 (c) illustrate this general trend.

For an 8-in. crack (Fig. 8), the shortest crack length for which contours have been plotted, it will be noted that the increase in strain directly above and below the fracture tip is small in comparison with strain changes for longer crack lengths. The small changes in strain exhibited by the rosettes located only 8 in. from the initiation edge attest to the fact that the notch-wedge-impact method of fracture initiation has little effect on the strain distribution in a wide plate in regions away from the notch.

The change in strain distribution as the crack length increases may be seen clearly by comparing the contours for crack lengths of 8, 15 and 22 in. As the crack length increases, it will be noted that the magnitude and extent of the strain field associated with the crack tip likewise increases. For crack lengths in excess of 22 in., the extent of the strain contour ahead of the fracture increases only slightly with increasing crack length and the strain field surrounding the advancing crack tip remains essentially unchanged. Strain contours for crack lengths between 22 and 43 in. are not shown but are essentially the same as the contours for either the 22 or 43 in. crack length. Thus, for this particular specimen geometry, apparently the propagating brittle fracture reaches a more or less "steady-state" condition after it has traversed a distance of about 22 in.

The major portion of the strain field associated with the propagating brittle fracture extends only about 8 to 10 in. directly ahead of the fracture. The main changes in strain occur above and below the fracture tip and slightly ahead of it; behind the fracture front, the strains decrease rapidly. All strain contours appear to converge toward the fracture front. Although extensive strain measurements were not obtained at distances far above and below the fracture, the available data indicate that the contours are symmetrical about the fracture path.

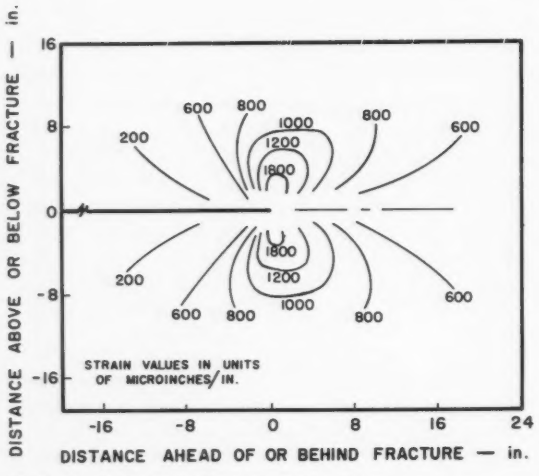

Fig. 9—Typical set of principal-strain contours for 22- to 50-in. crack length

A set of typical maximum principal-strain contours for a crack length of 22 to 50 in. is presented in Fig. 9; these contours are based on the results presented in Fig. 8 for a 22-in. crack and a 43-in. crack, and for strain contours for other crack lengths between 22 and 50 in. as presented in Reference 4. For the geometry and test conditions used herein, these strain contours are considered to be representative of the strain field associated with the surface-crack tip for crack lengths of 22 to 50 in.

Contours for vertical strain and maximum shear strain also were plotted as a part of this study but are not presented. The variation in maximum shear strain with distance from the crack path is less clearly defined than the variation for the maximum principal strain because the maximum shear strain is more dependent upon the somewhat erratic horizontal-strain readings than is the maximum principal strain. However, in spite of the slightly nonuniform nature of the shear-strain contours, they are similar in shape to the maximum principal-strain contours, and likewise similar to those observed in photoelastic studies.[6] As would be expected, the vertical-strain contours are quite similar to the maximum principal-strain contours.

Summary

This paper describes a study made for the purpose of determining the characteristics of the strain field surrounding a brittle fracture propagating across a wide steel plate. The specimens from which the data were obtained consisted of $^3/_4$ in. by 6-ft wide steel plates tested with an average net stress of about 19,000 psi, at a temperature of about $-5°$ F, and with the notch-wedge-impact method for fracture initiation. The instrumentation was arranged to provide a record of the strain–time response at various points on the plate surface as the fracture propagated across the plate, as well as to provide an indication of the average crack speed. Of particular interest is the fact that, for gages near the fracture oriented perpendicular to the crack path, the recorded strains remained elastic even though the peak magnitudes were in excess of 5000 microinches/in.

From the strain–time data of the component gages of each rosette, principal strains were computed for each gage during fracture propagation. Since the plate tests were conducted under similar conditions of stress, temperature and initiation, it was possible to superimpose the data to obtain a comprehensive picture of the surface-strain distribution

associated with a moving crack and to derive contours of maximum principal strain for various crack lengths. The crack speed was essentially constant in the regions where the rosettes were located and had an average value of 2700 fps.

Initially, for a crack length less than about 22 in., the magnitude and extent of the strain field associated with the surface crack tip was found to increase with increasing crack length. For crack lengths in excess of about 22 in. it was observed that the extent, magnitude and nature of the strain field associated with the advancing tip of the fracture remained essentially unchanged. A study of the strain contours reveals that the major portion of the strain field associated with the surface tip of the propagating brittle fracture extends only about 8 to 10 in. ahead of the fracture, the most highly strained regions being those above and below the fracture tip and slightly ahead of it. Although extensive strain measurements were not obtained at distances far above and below the fracture, the recorded strain data indicate that the contours are symmetrical about the fracture path. The contours also support the assumption that a "steady-state" condition may be attained for a fracture propagating under more or less uniform conditions.

Acknowledgment

The work described in this paper was conducted in the Structural Research Laboratory of the Department of Civil Engineering, University of Illinois, under sponsorship of the Ship Structure Committee through the Bureau of Ships, U. S. Navy, Contract NObs 65790. The authors gratefully acknowledge the assistance of the many persons who have contributed to the various phases of the program and particularly T. M. Lynam, formerly research assistant in civil engineering. The opinions expressed in this paper are those of the authors and do not necessarily represent those of the Ship Structure Committee or its member agencies. The members of the Brittle Fracture Mechanics Advisory Committee under the cognizance of the Committee on Ship Structural Design of the National Academy of Sciences—National Research Council, have acted in an advisory capacity for this program.

Bibliography

1. Hall, W. J., Mosborg, R. J., and McDonald, V. J., "Brittle Fracture Propagation in Wide Steel Plates," The Welding Jnl., 36 (1), Research Suppl., 1-s to 8-s (1957).

2. Hall, W. J., Godden, W. G., and Fettahlioglu, O. A., "Preliminary Studies of Brittle Fracture Propagation in Structural Steel," Ship Structures Committee Report Serial No. SSC-111, Washington: National Academy of Sciences—National Research Council (May 15, 1958).

3. Lazar, R., and Hall, W. J., "Studies of Brittle Fracture Propagation in Six-Foot Wide Structural Steel Plates," Ship Structure Committee Report Serial No. SCC-112, Washington: National Academy of Sciences—National Research Council (Sept. 17, 1959).

4. Rolfe, S. T., Lynam, T. M., and Hall, W. J., "Studies of the Strain Distribution in Wide Plates During Brittle Fracture Propagation," Ship Structures Committee Report Serial No. SSC-118, Washington: National Academy of Sciences—National Research Council (Dec. 31, 1959).

5. Robertson, T. S., "Experimental Techniques Developed in Investigations into High-Speed Yield in Brittle Fracture," Proceedings of the Conference on, "The Properties of Materials at High Rates of Strain," The Institution of Mechanical Engineers, London, 22-30 (Apr. 30, 1957).

6. Wells, A. A., and Post, D., "The Dynamic Stress Distribution Surrounding A Running Crack—A Photoelastic Analysis," Proc. Soc. Exp. Stress Analysis, XVI, No. 1, 69-92 (1958).

7. Barton, F. W., and Hall, W. J., "Studies of Brittle Fracture Propagation in Six-Foot Wide Steel Plates with a Residual Strain Field," Ship Structure Committee Report Serial No. SCC-130, Washington: National Academy of Sciences—National Research Council (April 3, 1961).

On Saint Venant's Principle Under Dynamic Conditions

Paper by P. D. Flynn and M. M. Frocht was published in January 1961, issue of EXPERIMENTAL MECHANICS, pages 16-20

Discussion

by S. F. Borg

The paper by Flynn and Frocht discusses an interesting problem in dynamic analysis. The following discussion deals with a theoretical treatment of a rather closely related phenomenon and may be of interest.

It is well known that the elementary Bernoulli-Euler beam vibration equation

$$EI \frac{\partial^4 w}{\partial x^4} + \rho A \frac{\partial^2 w}{\partial t^2} = 0 \qquad (1)$$

(in which EI is the beam stiffness, ρA is the mass per unit length of beam, w is the deflection and x, t are the space, time coordinates) will not adequately describe the effect of impact loadings during the time period immediately after contact, when the wave transmission characteristics of the beam predominate.

Timoshenko introduced a refinement by including shear and rotary inertia effects. His equation is given in Reference 1 as

$$\frac{\partial^4 w}{\partial x^4} - \left(\frac{1}{C_1^2} + \frac{1}{C_2^2}\right) \frac{\partial^4 w}{\partial x^2 \partial t^2} + \frac{1}{C_1^2 C_2^2} \frac{\partial^4 w}{\partial t^4} + \frac{K}{\partial t^2} \frac{\partial^2 w}{\partial t^2} = 0 \qquad (2)$$

S. F. Borg is Professor and Head, Civil Engineering, Stevens Institute of Technology, Hoboken, N. J.

In this equation K is a constant dependent upon the cross section and physical properties of the beam, and[2] (*a*) C_1 is the velocity of moment discontinuities; (*b*) C_2 is the velocity of shear discontinuities. C_1 and C_2 are not, in general, equal. Indeed, C_1, the bending discontinuity velocity may be twice (or more) C_2, the shear discontinuity velocity for ordinary engineering type structures.

The physical significance of C_1 and C_2 appear to be clearly brought out in Reference 1, which solves analytically the problem of a semi-infinite beam (hinged at its left end, right end to infinity) subjected to a step-function bending moment, M, applied at its left end. The solution (eqs 12 b, c of Reference 1) consists of two-parts, the first (apparently being directly due to the moment) extending a distance C_1t down the beam and the second (although not so stated, but apparently being due to the shear-reaction induced at the hinge by the moment) extending a distance C_2t down the beam.

Although the Timoshenko equation represents a considerable improvement over the Bernoulli-Euler equation in so far as the early-time-history effects of impact loadings are concerned, it does introduce an effect which is very closely related to the dynamic Saint Venant principle. Thus, going back to the problem solved in Reference 1, we now state this problem in the following two, physically equivalent, ways:

(I) The applied load is a step function pure moment, M, as considered in Reference 1. This moment is applied at the hinge, $x = 0$, and may be assumed as applied by means of the usual $\sigma = My/I$ distribution across the cross section of the beam.

(II) The applied load is a step function pair of equal concentrated loads, Q, one applied at the hinge and the second at a distance δ to the right of the hinge, such that

$$M = Q\delta, \delta \to 0 \qquad (3)$$

Now, as pointed out in Reference 1, the response due to (I) is felt at a distance C_1t down the beam and at this point the moment is just equal to M, the applied moment. Between 0 and C_1t the moment is continuous.

On the other hand, since the loading of (II) may be represented by a superposition of shear-discontinuity effects, it follows that the discontinuous response due to (II) is felt at a distance C_2t down the beam—and this distance may very easily be only half the distance C_1t. The moment at $x = C_1t$ will be zero. It is not clear whether there will be a large change in moment near this point, since the theory indicates only that discontinuities in moment, M, propagate with velocities C_1 and the pair of shear forces, for any finite δ, do not give a discontinuous moment.

Thus, in the case considered, the solution of the Timoshenko equation for the same (physical) loading will indicate effects at large distances from the point of application of the load, which differ considerably because of the different representations of this loading.

Otherwise stated—*a dynamic Saint Venant Principle does not exist (in the form considered herein, which most closely parallels the static formulation) for the Timoshenko representation of the vibrating beam.*

References

1. Flügge, W., and Zajac, E. E., "Bending Impact Waves in Beams," Ingenieur-Archiv, Band 28 (June 1959).

2. Leonard, Robert W., and Budiansky, Bernard, "On Traveling Waves in Beams," NACA-TN 2874 (January 1953).

Authors' Closure

Dr. Borg compares the response of two beams subjected to equivalent dynamic loads by using the Timoshenko beam equation, and he concludes that a conventional dynamic Saint Venant principle does not exist in the problem considered. This result is in agreement with the analytical work of Boley[1] who stated that conventional formulations of Saint Venant's principle do not hold under dynamic conditions and that deviations from this principle are greatest for rapidly applied loads.

The authors have recognized the inadequacy of conventional formulations and have compared states of stress not under equivalent force systems but under conditions of impact with equal mass and velocity. The results showed that, under such conditions, uniform stress distributions are developed in regions sufficiently removed from the load or discontinuity, and the maximum stresses and the duration of impact are not affected significantly by the area of contact or by the presence of a hole. However, the shape of the wave front is disturbed by a concentrated load. Davies[2] also observed experimentally that uniform stress distributions are obtained in a bar subjected to longitudinal impact by a central, concentrated load in regions removed from the load.

The authors believe that considerably more theoretical and experimental work is required to permit the formulation of a general dynamic Saint Venant principle, assuming that one exists.

References

1 (a) Boley, B. A., "Application of Saint Venant's Principle in Dynamical Problems," J. Appl. Mech., 22, 204–206 (1955).

(b) Boley, B. A., "Some Observations on Saint Venant's Principle" Proc. 3rd U. S. Nat'l. Cong. Appl. Mech., pp. 259–264 (1958).

(c) Boley, B. A., "On a Dynamical Saint Venant Principle," J. Appl. Mech., 27, 74–78 (1960).

2. Davies, R. M., "A Critical Study of the Hopkinson Pressure Bar," Phil. Trans. Roy. Soc. London, Series A, 240, 375–457 (1948).

sesa news

Egon Orowan to Present Murray Lecture at International Congress

Recent Experiments on Crystal Structure Form Basis For New Point of View

The noted scientist and educator, Egon Orowan, who has made the study of plastic deformation and fracture his life's work, will present the annual William M. Murray Lecture on Friday, November 3, at the First International Congress for Experimental Mechanics at the Hotel New Yorker, New York City.

An outstanding event of the three-day Congress, the Murray Lecture is given each year by an eminent engineer or scientist who has been invited by a special committee of the SESA to present a paper of significant import. The occasion also pays tribute to William M. Murray, a founder and, for many years, the voluntary Secretary-Treasurer of the Society.

The 1961 Murray Lecture

This year the title of the lecture will be "The Structure of the Cold-worked Crystal." The physical properties of materials relating to strength characteristics are presently the subject of intensive research. Both the engineer and the scientist are deeply interested in an accurate theoretical basis for evaluating materials. In the words of Dr. Orowan, "Until a few years ago the arrangement of dislocations in a plastically deformed crystalline material was a matter of theoretical speculation alone. Recently, however, remarkable developments in observing dislocation arrangements by electron-microscopic, X-ray, and etch-pit methods have unfolded detailed pictures of the architecture of dislocation arrays both before and after deformation, and after annealing. To say that these observations have reversed the dominating trends of thought during the last two decades would be wrong since perhaps most of the observed features have been anticipated theoretically. Nevertheless, it cannot be denied that the most popular concepts of this period have proved less important in the cases so far investigated. The experimental results are too scanty to permit general conclusions; in particular, the thin foils on which electron-microscopic work has been carried out may not reflect the behavior of bulk material. However, certain general lines can be recognized, and in the lecture an attempt will be made to synthesize from the available observations what seems at present the most likely picture of strain hardening, thermal softening, recrystallization, and the formation of cracks by plastic deformation."

The lecture will immediately follow a noontime luncheon at which Dr. Orowan will be guest of honor. In order to give all members and guests an opportunity to hear the address, no other events have been scheduled for this part of Friday afternoon.

Egon Orowan, George Westinghouse Professor of Mechanical Engineering at Massachusetts Institute of Technology, has spent most of his working life on the study of plastic deformation and fracture. Born in Budapest, Hungary, in 1902, he studied physics and chemistry at the University of Vienna from 1920 to 1922. He received his Diploma in engineering and physics at the Technical University of Berlin, Charlottenburg, in 1929. An assistant professor at Berlin-Charlottenburg from 1928 to 1932, he received his Doctorate in the latter year. Dr. Orowan was engaged in industrial work in Budapest until 1937 when he became research associate at the University of Birmingham, England. From 1939 to 1950 he was first research associate and later reader in the physics of metals at Cambridge University. Coming to this country in 1950, Dr. Orowan joined the faculty of Massachusetts Institute of Technology as professor of mechanical engineering and subsequently accepted the chair of the George Westinghouse Professor of Mechanical Engineering.

Egon Orowan

Principal Events of the Congress

Principal events of the First International Congress will also include five regular technical papers sessions, a manufacturers equipment exposition and two special educational lectures. About 23 technical papers have been scheduled tentatively in the arrangement shown in the Tentative Program appearing in the pages immediately following. A number of well-known investigators from six different countries abroad have accepted invitations to present papers. Two of the foreign speakers will present surveys of the work being done at national laboratories in Scotland and the Netherlands, respectively. Five others will present investigations of timely nature on

several subjects of paramount interest to workers in the field. Another foreign paper will be by title only. About 15 additional papers from authors in this country and abroad will make up the balance of the program. In scope and variety these presentations represent a good cross section of the field of experimental mechanics.

Exposition

The manufacturers' exposition will be a display of representative equipment and instrumentation used in the research and industrial laboratories of the country. All but a small area of the mezzanine lounge will be given over to exposition displays. Both foreign and domestic manufacturers will be represented. Among the attractive features of the arrangements is the fact that all principal activities are at present scheduled to take place on the one floor—displays, technical sessions, banquet and other social activities. Educational exhibits will also appear on this floor in a section separately reserved for this type of display.

Educational Lectures

A specially arranged program for Wednesday evening is titled "Educational Lectures in Experimental Stress Analysis." Consisting of two simultaneous lecture sessions, one will be presented by C. C. Perry, associate professor of engineering mechanics at Wayne State University. Professor Perry will describe the basic principles of operation of strain gages, photoelasticity and stresscoat. He will also briefly cover their fields of application, instrumentation and techniques. This session is designed primarily for undergraduate and graduate students at colleges in the New York Metropolitan area who have had little or no exposure to the methods of experimental mechanics.

The other session will treat the electric wire resistance strain gage and the photoelastic technique in some depth, especially in connection with thermal problems. Burton Erickson, assistant professor of mechanics at the Polytechnic Institute of Brooklyn will give a short talk on recent measurements he has made of transient strains at elevated temperatures. Dr. Herbert Becker of New York University will also make a presentation in connection with photoelasticity, including thermal effects: photothermoelasticity.

Other Events of Interest

An attractive ladies' program will feature visits to various points of interest in New York City including the United Nations Building, as well as fashion shows in some of the well-known stores.

For the banquet to be held on Thursday evening, an unusually interesting speaker has been promised in addition to a first-rate dinner menu. Final program details, including other activities of interest, will appear in October. Arrangements for the 1961 Congress are under the direction of the Metropolitan New York Section.

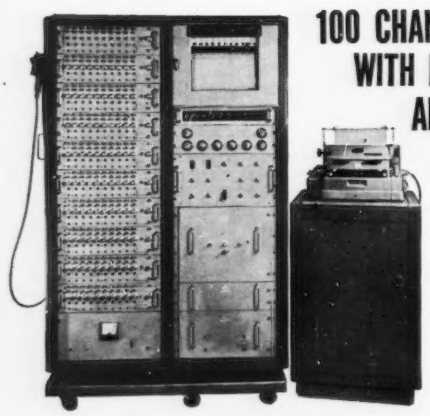

100 CHANNEL STRAIN GAGE SYSTEM WITH BOTH ANALOG RECORDING AND DIGITAL READOUT

- direct strain readout on typewriter, paper tape punch, digital lamp bank and recorder simultaneously
- inherent flexibility to adapt plotter, summary punch, or other end equipments
- sophisticated system controls
- modular construction offers ability to expand both input and output of system
- designed by strain gagers for strain gagers
- B & F's answer to the problem of documenting strain information with maximum accuracy and ultimate ease.

Visit us at Booth 322 1961 I.S.A. Show

B&F instruments, Inc.
3644 N. Lawrence St.
Philadelphia 40, Pa.

Input Conditioners, Torque Meter Systems, Accelerometers and other equipment for data acquisition

For details, circle No. 10 on Reader Information Card

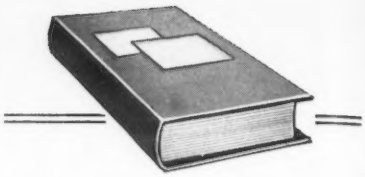

THEORY OF ELASTICITY

For engineers interested in calculating stresses in engineering structures and machine parts—here is the essential knowledge of the theory of elasticity, together with the solution of engineering problems of practical importance. The book discusses approximate and experimental methods of solving elastic problems which have proved useful in the study of complicated cases of stress distribution. **By S. Timoshenko and J. N. Goodier, Stanford Univ. 2nd Ed., 506 pp., 266 illus., $11.50**

THEORY OF PLATES AND SHELLS

Covers the general theory of bending of plates under lateral load, with applications to circular and rectangular plates, and with numerous tables simplifying the calculation of deflections and stresses in plates. The book provides a treatment of combined bending and tension or compression of plates, with applications to thin plates. Also dealt with is the theory of bending of shells, including applications to cylindrical and spherical shells. **By S. Timoshenko, Stanford Univ., and S. E. Woinowsky-Krieger, Université Laval, Quebec, Canada. 2nd Ed., 580 pp., 280 illus., $15.00**

FORMULAS FOR STRESS AND STRAIN

A compact and readily usable summary of important formulas, facts, and principles pertaining to strength of materials. This book is a reliable handbook for engineers concerned with machine and structural design which provides valuable formulas for stress analysis and elasticity. All such experimental data and empirical formulas are in line with current information. New material has been added, ensuring complete coverage of stress and strain. **By Raymond J. Roark, Univ. of Wisconsin. 3rd Ed., 381 pp., $8.25**

THE STRAIN GAGE PRIMER

What the bonded wire resistance strain gage can do in solving problems in experimental stress analysis is explained in this practical book. All phases are covered—from selecting the proper commercial gage through preparing surface of the test member, cementing, damage-proofing, and wiring the gage—to selecting the proper instrument to record the strain gage data, and interpreting readings in terms of significant stresses. **By C. C. Perry and H. R. Lissner, Wayne Univ. 280 pp., 180 illus., $6.00**

SEE THESE BOOKS 10 DAYS FREE

McGraw-Hill Book Co., Dept. EXM-9
327 W. 41st St., New York 36, N. Y.

Send me book(s) checked below for 10 days' examination on approval. In 10 days I will remit for book(s) I keep plus few cents for delivery costs, and return unwanted book(s) postpaid. (We pay delivery cost if you remit with this coupon—same return privilege.)

☐ Timoshenko & Goodier—**Theory of Elasticity**, $11.50

☐ Timoshenko & Woinowsky-Krieger—**Theory of Plates and Shells**, $15.00

☐ Roark—**Formulas For Stress & Strain**, $8.25

☐ Perry & Lissner—**Strain Gage Primer**, $6.00

Name.....

Address.....

City..... Zone..... State.....

Company.....

Position.....

For price and terms outside U. S. write McGraw-Hill Intl., N. Y. C. 36 EXM-9

TENTATIVE PROGRAM

FIRST INTERNATIONAL CONGRESS ON EXPERIMENTAL MECHANICS

NOVEMBER 1-3, 1961

HOTEL NEW YORKER, NEW YORK CITY

NOVEMBER 1—WEDNESDAY MORNING

8:00 A.M. Author's Breakfast

8:30 A.M. Registration
Mezzanine Floor

9:30 A.M. Words of Welcome
Grand Ballroom

10:00 A.M. Exposition Opens
Mezzanine Floor

Technical Papers Session
9:30 A.M. *Grand Ballroom*

Transient Behavior of Rocket Sleds
by D. P. Ankeney and W. Goldsmith, University of California, Berkeley, Calif.

Experimental Investigation of Eccentric Longitudinal Impact of Bars
by S. S. Kuo, Yale University, New Haven, Connecticut

Experimental Mechanics at T. N. O.
by R. Boiten, Technische Hogeschool, Delft, Holland

NOVEMBER 1—WEDNESDAY AFTERNOON

4:00 P.M. Meetings of Standing Committees

6:30 P.M. Committees Dinner

7:30 P.M. Educational Lectures in Experimental Stress Analysis

8:00 P.M. Executive Committee Meeting

Technical Papers Session
1:45 P.M. *Grand Ballroom*

Model Studies of a Radome Shell Under Simulated Wind Loading
by E. Sevin and J. L. MacDonald, Armour Research Foundation, Chicago, Illinois

Experimental Studies on Structures Beyond the Elastic, Limit
by G. Oberti, Istituto Sperimentale Modelli E Strutture, Bergamo, Italy

Experimental Investigation of Wave Propagation in Isotropic Elastic Plates
by M. A. Medick and J. R. Steele, Avco Corp. Wilmington, Massachusetts

Large Deformation of Circular Membranes Under Static and Dynamic Loading
by J. Griffith and H. Vanzant, University of Florida, Gainsville, Florida

Brittle Fracture in Low-carbon Steel Under Tensile and Torsion Test
by T. Yokobori, Tohoku Univ., Sendai, and A. Otsuka, Hiroshima Univ., Hiroshima, Japan

NOVEMBER 2—THURSDAY MORNING

8:00 A.M. Authors' Breakfast

8:00 A.M. Registration
Mezzanine Lounge

8:30 A.M. Exposition Opens
Mezzanine Floor

Technical Papers Session
9:00 A.M. *Grand Ballroom*

Experimental Analysis on the Strength of Cylindrical Shell Under External Pressure
by T. Yamaguchi and J. Imamasa, Kobe Shipyard, Mitsubishi Heavy Industries, Reorganized, Ltd.

The Overstrain of High-strength Open-end Cylinders of Intermediate Diameter Ratio
by T. E. Davidson, A. N. Reiner, D. P. Kendall, Watervliet Arsenal, Watervliet, N.Y., and C. S. Barton, Brigham Young Univ., Provo, Utah

Measuring Creep at Small Strains
by A. Mellgren, Industrial Reactor Division, Aktiebolaget Atomenergi, Stockholm, Sweden

The Micro-Sensor—A New Tool for Experimental Stress Analysis
by J. C. Sanchez, Micro Systems, Inc., San Gabriel, California

Special Techniques in Experimental Stress Analysis
by V. M. Hickson, Ministry of Aviation, Royal Aircraft Est., Farnborough, Hants, England

NOVEMBER 2—THURSDAY AFTERNOON

6:00 P.M. Social Hour
Mezzanine Lounge

7:00 P.M. Banquet
Grand Ballroom

Technical Papers Session
1:45 P.M. *Grand Ballroom*

Experimental Mechanics at the National Engineering Laboratory
by D. G. Sopwith, National Engineering Laboratory, East Kilbride, Glasgow, Scotland

A Pressure Technique for Determining Residual Stresses in Circular Tubes
by R. E. Weigle and J. Purtell, Watervliet Arsenal, Watervliet, New York

Experimental Mechanics in the Development of a New Miniature Pressure Transducer
by C. W. Bert and N. A. Crites, Battelle Memorial Inst., Columbus, Ohio

Frictional-type Wire Resistance Strain Gage
by Kōshirō Ōi, University of Tokyo, Theba City, Japan

NOVEMBER 3—FRIDAY MORNING

8:00 A.M. Authors' Breakfast

8:30 A.M. Registration
Mezzanine Lounge

8:30 A.M. Exposition Opens
Mezzanine Floor

Technical Papers Session
9:00 A.M. *Grand Ballroom*

A New Method for Determining the Elastic Compliances of Stiffened Plates
by R. E. Beckett, State Univ. of Iowa, Iowa City, and R. J. Dohrmann, K. D. Ives, The Babcock & Wilcox Co., Alliance, Ohio

Determination of Slope Contours in Flexed Elastic Plates by the Salet-Ikeda Technique
by J. P. Duncan, Univ. of Sheffield and C. J. E. Brown, Imperial Chemical Industries, Billingham, Division

Experimental Study of Rock-stress Problems in Deep-level Mining
by E. Hoek, South African Council for Scientific & Industrial Research, Pretoria, S. A.

Analysis of Two-Dimensional Stress Problems by the Moiré Method
by J. G. Bouwkamp, University of California

Moiré Effects at High Temperatures
by P. Dantu, Laboratoire Central des Ponts et Chausses, Paris, France

An Experimental Self-temperature Compensated Strain-gage System (*By Title Only*)
by L. G. Randell, Aerodynamics Division, Aeronautical Research Laboratories, Melbourne, Australia

NOVEMBER 3—FRIDAY AFTERNOON

3:00 P.M. SESA Annual Business Meeting

William M. Murray Lecture

Luncheon
12:30 P.M. *Grand Ballroom*

Lecture
1:30 P.M. *Grand Ballroom*

Structure of the Cold-worked Crystal
by Egon Orowan, George Westinghouse Professor of Mechanical Engineering, Massachusetts Institute of Technology, Cambridge, Mass.

NEW SESA MEMBERS

ALABAMA

Parr, Charles H.
Huntsville

CALIFORNIA

Dharmarajan, Sangiah
San Diego

Doering, Frederick J., Jr.
Los Angeles

Matievich, William
Huntington Park

Nelson W. D.
El Segundo

Troke, Robert W.
Rolling Hills

Willis, W. Ernest
Oakland

Winkler, J. E.
Los Angeles

COLORADO

Bishop, Floyd Lewis
Denver

DISTRICT OF COLUMBIA

Kroll, Wilhelmina D.
Washington

FLORIDA

Ekstrom, Ralph E.
Gainesville

ILLINOIS

Davies, James A.
Carpentersville

Fleming, John F.
Evanston

Janicke, Marion Joseph
Argonne

Millan, John F.
Peoria

Potocki, Richard J.
Chicago

Waterfall, Frank E.
Chicago

Zienkiewicz, O. C.
Evanston

INDIANA

Cervelli, Renato V.
South Bend

MARYLAND

Dickinson, Charles W.
Frostburg

MASSACHUSETTS

Davis, Phillip
Melrose

Shapiro, Bernard H.
Cambridge

MICHIGAN

Duckor, Lewis M.
Detroit

Graafsma, Richard S.
St. Joseph

Peterson, Frederick J.
Detroit

MINNESOTA

Johnson, Herbert C.
Minneapolis

Maass, Charles A. J.
Minneapolis

NEW JERSEY

Kuchkuda, Roman W.
Cranford

NEW YORK

Krebs, Neil Ernest
Bellerose

NORTH CAROLINA

Schwantes, Robert O.
Charlotte

OHIO

Gerdeen, James C.
Columbus

Wang, H.
Toledo

PENNSYLVANIA

Cimorelli, Salvatore A.
Philadelphia

Fenton, David H.
West Chester

Hesler, William H.
Philadelphia

Schill, George V.
Pittsburgh

Steimer, John F.
Phoenixville

Unger, William S., Jr.
Pittsburgh

TENNESSEE

Talley, Drayton H.
Chattanooga

UTAH

Brown, Wayne S.
Salt Lake City

Christiansen, Vance T.
Logan

Coombs, D'Monte W.
Provo

Erickson, Carl H.
Brigham City

Jepson, Winston F.
Brigham City

McClure, Samuel R.
Brigham City

Mayhew, Donald J.
Salt Lake City

Rollins, Ralph L.
Provo

Veibell, C. Floyd
Logan

Watkins, Reynold King
North Logan

Wilson, Arnold
Provo

WASHINGTON

Flodin, Len O.
Bellevue

Goldstein, Norton H.
Seattle

Seehorn, L. E.
Seattle

WEST VIRGINIA

Hendershot, H. F.
Huntington

WISCONSIN

Archer, Fred Curtis
Milwaukee

Costin, Robert W.
Milwaukee

OTHER NATIONS

Ethiraj, R.
Trichy Dt, Madras State, India

Hastrup, Ole F.
Copenhagen, Denmark

Lee, Michael Boon Peng
Manchester, Lancashire, England

Oroviogoicoechea, D. A.
Bilbao, Spain

Quarter Ending on June 30, 1961

Members	2182
Honorary Members	3
Corporate Members	85
TOTAL MEMBERSHIP	2270

section reports

Northern Ohio

Testing Laboratory Toured

One hundred fifty members turned out for the May 25 meeting at the Dana Corp., Toledo Division, where *Northern Ohio* held its first joint meeting with the *Detroit* Section. An excellent dinner at the company cafeteria featuring standing rib roasts of beef got the evening's activities off to a good start.

Following dinner, the members broke up into small groups for conducted tours through the Dana Corp.'s testing facilities. Type of equipment tested here included power-transfer equipment, transmissions, power take-offs, universal joints and other components manufactured by the company.

After the tour, a panel presentation was given by members of the laboratory engineering staff, followed by a question-and-answer period. Staff members described four principal areas of interest in the testing of the products manufactured by Dana. They discussed static and fatigue testing, road testing, dynamometer testing and instrumentation. Both the tour and the panel discussion turned out to be highly interesting and informative. The meeting was thoroughly enjoyed by all—thanks to the generous cooperation of the Dana Corp.

(Reported by H. Calvert for the Northern Ohio Section)

Washington Area

Plastic Submarines?

The great oceans cover 70% of the earth's surface, and 70% of these oceans are between two and four miles deep. In man's quest to explore, utilize and understand the seas around him, he is developing high-strength hull structures which can withstand deep-submergence pressures and still be sufficiently light in weight to carry a practical payload of crew and equipment.

In an address at the May 24 meeting, John E. Buhl, Jr., of the David Taylor Model Basin, presented background information on the use of glass-reinforced plastics (GRP) for the construction of deep-submergence pressure hulls. His paper, "Reinforced Plastics for Hydrospace Vehicles," described the characteristics of an ideal material for deep-depth operating hulls. Available information on structural response to static loading of cylindrical hulls made of glass-filament reinforced plastics was summarized to show the potential advantages over metals. Mr. Buhl indicated that collapse pressures obtained from a limited number of tests with structural models fabricated with commercially available GRP materials agree well with the values computed from thin-shell theory for isotropic materials. Plans for future research were reviewed.

The following officers were elected to serve for the 1961–62 term: Roland E. Seely, president; Leonard Mordfin, vice-president; Miss Wilhelmina D. Kroll, secretary-treasurer; and E. R. Hitchcock, Presley A. Wedding and Edward Wenk, directors.

(Reported by L. Mordfin for the Washington Area Section, Photograph by N. Halsey)

GRP SHELLS DISCUSSED

Speaker John Buhl (right) looks on as President Myron Lunchick opens the discussion on "Reinforced Plastics for Hydrospace Vehicles," at the Washington Area Section's May 24 meeting.

NORTHERN OHIO AND DETROIT SECTIONS TOUR DANA LAB

One hundred fifty members (count 'em) attended the first joint meeting of the Northern Ohio and Detroit Sections at the Dana Corp., Toledo, Ohio, on May 25

Following tour of laboratory test equipment. Dana test engineers presented topics of major interest in their field.

from the campus

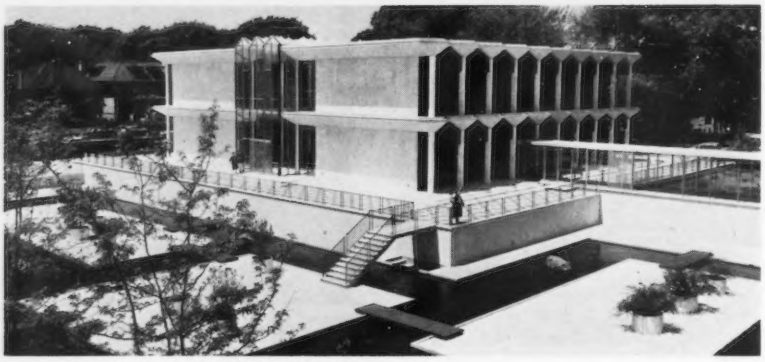

Community Service Building, Wayne State University

MEASUREMENT-ENGINEERING COURSE AT ARIZONA STATE

A short course on measurement engineering will be given at Arizona State University, Tempe, Ariz., from January 29–February 2, 1962. The purpose is to present the science of measurement in a logical and orderly manner. The lecture program will consist of a presentation of basic concepts—transducer physical principles, measurement-engineering theory, experimental planning, data analysis—along with a series of special lectures covering: acoustic measurements, biological measurements, flexures in measuring devices, rotating parts, strain measurement, temperature measurement and vibration measurement.

The experimental program available to a limited number of registrants during 3-hr scheduled laboratory periods includes the following: the cantilever beam as a transducing element, impact-created stress waves, steady-state mechanical vibrations, frequency analysis, amplitude modulation and noise-elimination methods, pressure transients, amplifier characteristics, bridge-circuit computers, characteristics of commercial measuring systems and accelerometer calibration and frequency response.

The lecturers have been selected for their complete familiarity with both the theoretical and practical aspects of their special fields and for their contributions in the advance of the state of their own art.

BIOMEDICAL ENGINEERING AT JOHNS HOPKINS

A new graduate curriculum which integrates the engineering and medical sciences will be initiated by The Johns Hopkins University this September, it was announced by Milton S. Eisenhower, University president.

The program in biomedical engineering leading to the doctoral degree is the first of its kind in the country. Two other institutions, the University of Pennsylvania and the University of Rochester, are cooperating with Johns Hopkins in instituting similar programs.

Students enrolled will take course work both in the School of Medicine in East Baltimore and at the Homewood Campus. At least four years of study and research will be required to fulfill the requirements for the degrees, with an additional year of post-doctoral study in biomedical research recommended.

The purpose of the new program is to train students in advanced engineering subjects of particular pertinence to research in biological systems and to offer systematic study in how the principles of physical and engineering science apply to biological systems.

NEWMARK AMONG WINNERS OF ASEE AWARDS

Nathan M. Newmark, head of the civil engineering department at the University of Illinois, was among the winners of four of the nation's highest awards in engineering education given by the American Society for Engineering Education. Dr. Newmark, who received the Vincent Bendix Award for outstanding research contributions by an engineering educator, has been an active SESA member for some years.

Other recipients include Olof A. Hougen, professor of chemical engineering at the University of Wisconsin, who was awarded the Lamme gold medal; David C. White, professor of electrical engineering at Massachusetts Institute of Technology, who won the George Westinghouse Award; and William A. Nash, professor of engineering mechanics at the University of Florida, who was given the Curtis W. McGraw Research Award.

CENTRALIZED ENGINEERING AT CASE INSTITUTE

The fact that when an engineer embarks upon his professional career he will not find his problems arbitrarily split between specialized and narrowly defined engineering fields is one reason given for a recent centralization move at Case Institute of Technology.

By creating a new Engineering Division to include the departments of civil, electrical, mechanical and chemical engineering, greater flexibility will also be possible, according to T. Keith Glennan, president.

Resulting flexibility will enable the Institute to anticipate swiftly changing engineering educational requirements and will also help to accommodate the interests of the student.

YOUNG STUDENT WINS PRIZE WITH STRAIN-GAGE DISPLAY

Fourteen-year-old William Brockett, a ninth-grade student at Edison Junior High School in Champaign, Ill., became curious about strain gages and, as a result, won a first prize at the district Junior Academy of Science fair at Bloomington, Ill. He then went on to win a first at the state fair held at the University of Illinois.

It all began when young Brockett's curiosity led him to write Professor W. M. Murray at MIT. Armed with his own zeal and some high-level academic advice, he set about on his own. He wrote to manufacturers and users of strain gages, and he studied up on the subject. Getting good cooperation, he managed to assemble material for an interesting display on the SR-4 strain gage.

As William describes it in a recent letter, "along with my display, I wrote a scientific paper. This was about the history, theory, and uses of gages, and was a complete paper."

William Brockett proudly displays his prize-winning entry at Illinois State science fair

New from VIBRASONICS...

low-cost, precision
BENCH-TYPE SHAKER

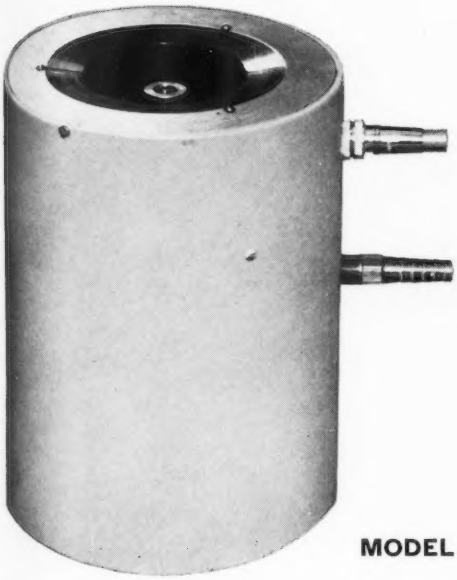

MODEL V-10

A unique vibration test instrument representing the ultimate in engineering design and quality at a surprisingly low price. New, but not experimental; tested and proved in use.

- Frequency Range: 20 c/s to 27 kc/s at full thrust with useful power to 100 kc/s
- Harmonic Distortion: better than 0.1% up to 5 kc/s
- Compressional Resonance: 17 kc/s—First Anti-resonance: 27 kc/s
- Frequency Response with a 2 oz. load is flat to within 10% from 50 c/s to 10 kc/s with no feedback
- Nominal Force Output: 20 lbs.—Force Factor: 5 lbs./amp

Send for catalog #601

For details, circle No. 9 on Reader Information Card

reliable, inexpensive
ULTRASONIC PROBE

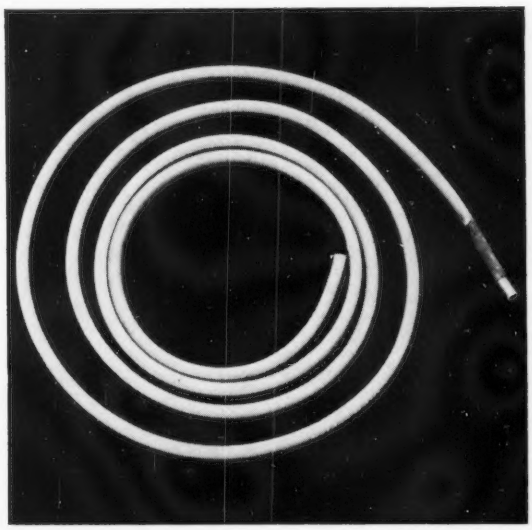

MODEL VP-10

This highly accurate probe obsoletes costly and, too often, inaccurate microphone equipment used for measuring ultrasonic levels.

Has a wide variety of applications in ultrasonic cleaning and processing; For displaying sound levels; For comparing sound levels at different times or in different tanks; For locating optimum position and power level; For setting similar sound levels with different amounts and types of liquids.

Will stand a static pressure of 100 lbs./sq. in. Unaffected by high temperatures; can be sterilized at up to 125 °C.

Send for catalog #611

For details, circle No. 11 on Reader Information Card

VIBRASONICS INCORPORATED

10 High Street Boston 10, Massachusetts

telephone: HAncock 6-7866

2-Channel Recording as you want it—

- **IN CARRYING CASE OR CART, OR RACK MOUNTED**
- **WITH BUILT-IN AMPLIFIERS, OR THE ADDED VERSATILITY OF INTERCHANGEABLE PREAMPS**

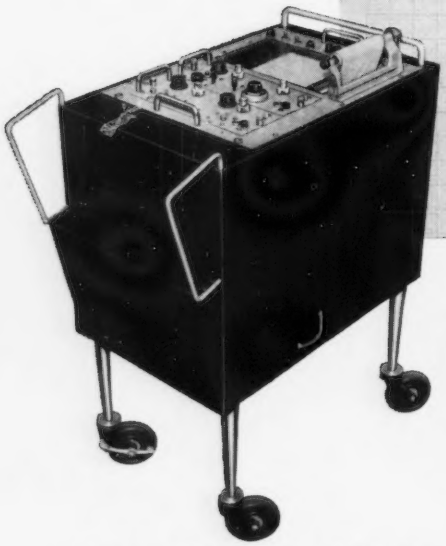

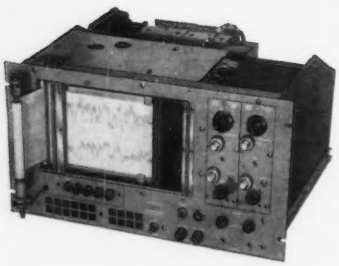

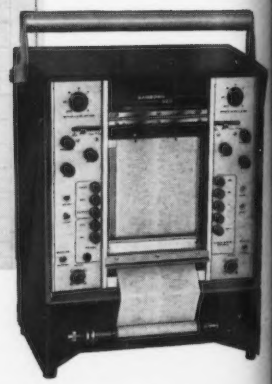

Systems with flexibility of interchangeable preamps – 50 mm channels, 4 speeds; available in 35″-high metal cart, in carrying case, or for rack mounting.

With highly developed, versatile preamps: Model 296 sensitivities from uv to hundreds of volts; transistorized electronics; versatile "350" preamps include Carrier, DC Coupling, Differential DC, Phase Sensitive Demodulator, Logarithmic, Frequency Deviation and Low Level types; Low Level preamp available with plug-ins for general purpose DC with or without zero suppression, and for DC strain gage work; system occupies 14″ in rack.

With simplified, miniaturized preamps: Model 297 sensitivities from uv to hundreds of volts; transistorized electronics; "850" preamps include Phase Sensitive Demodulator, DC Coupling, Carrier, Low Level types, plus MOPA for chopper and carrier excitation; system occupies 10½″ in rack.

Portables for DC coupling, AC transducer work, general purpose DC — 3 models with 50 mm channels, 4 speeds; identical except for transistorized electronics:

New Model 322 DC Coupling: 10 sensitivities 10 mv to 10 v/mm; calibrated zero suppression ±2.5 v max (Model 322A without zero suppression); push-pull input, 5 megohms to ground each side.

New Model 321 Carrier for AC transducer work: maximum sensitivity 10 uv rms/mm; excitation 5 volts; transducer impedance 100 ohms min; uncalibrated zero suppression.

Model 320 General Purpose DC (illustrated): 12 sensitivities 0.5 to 20 mv/mm and v/cm; input impedance ½ megohm (mv/mm ranges) and 1 megohm (v/cm ranges); floating and guarded inputs.

All models occupy approx. 1 cubic foot, can be placed horizontally, vertically, or resting on handle at 20° angle; all accept optional paper take-up (shown).

SANBORN COMPANY

INDUSTRIAL DIVISION 175 Wyman St., Waltham 54, Massachusetts

For details, circle No. 7 on Reader Information Card

C trans-
DC—3
4 speeds;
storized

) sensi-
m; cali-
±2.5 v
ut zero
nput, 5
h side.
trans-
sitivity
5 volts;
) ohms
ression.
(illus-
0.5 to
ut im-
nv/mm
(v/cm
uarded

bic foot,
cally, or
ll accept